Ionic separation of the IEX spent regenerant using Nanofiltration

Dionysia Diamantidou

Technische Universiteit Delft

TU Delft Delft University of Technology

Challenge the future

Ionic separation of the IEX spent regenerant using Nanofiltration

by

Dionysia Diamantidou

in partial fulfillment of the requirements for the degree of

Master of Science

in Civil Engineering

at the Delft University of Technology,

to be defended publicly on Thursday November 15, 2018 at 15:00

Thesis committee:		
	Dr. ir. H. Spanjers (chair)	TU Delft
	Dr. ir. S.G.J Heijman	TU Delft
	Dr. ir. A.H Haidari	TU Delft
	Prof. dr. E. J. R. Sudholter	TU Delft

TU Delft

LENNTECH

Front cover: Photo of water drop. Downloaded from' https://dumielauxepices.net/water-drops-clipart/water-drops-clipart-three-water''

Της παιδείας οι ρίζες είναι πικρές, μα οι καρποί γλυκοί

"The roots of education are bitter, but the fruit is sweet"

Aristotle

Preface

This report concludes my Master of Science program in Water Management at the Faculty of Civil Engineering and Geosciences of TU Delft, the Netherlands. The study has been carried out at TU Delft, in collaboration with Lenntech.

I would like to sincerely express my gratitude to Lenntech for giving me the opportunity to get involved in this project. I would like to thank for their guidance and the technical support that was very helpful for the completion of this research. Thank you all for your advices, your trust and our discussions.

I would also like to thank all the committee members for providing constructive feedback and recommendations during our meetings. Your contribution to this project, your experience, your critical approach and your insightful comments were always valuable for the progress of my project.

I owe many thanks to all the people that I met in the water lab and they helped me with my experiments. A special thank goes to Irene Caltran, David de Ridder and Armand Middeldorp for their support and their tireless assistance.

Furthermore, I would like to express my unreserved gratitude to my parents and my sister, the people who inspire me most in my life and are always there for me. Thank you very much for supporting me during these years. Last but not least, I would like to thank my friends for encouraging me all this period.

D. Diamantidou

Delft, October 2018

Abstract

The need to treat waste streams produced during the water treatment processes is becoming a challenge nowadays due to the industries' disposal expenditures, the limitations imposed by laws and the environmental impacts. The spent regenerant from ion exchange (IEX) processes is an example of such streams. This study investigated the use of Nano-filtration technique for separation as a part of the treatment step for IEX spent regenerant. This research is focused on the parameters such as membrane characteristics, ionic composition and operating conditions that affect the ion rejection of the IEX spent regenerant. This research aims to select a membrane that contributes to a maximum separation of monovalent and divalent ions of the IEX spent regenerant.

During this research six nanofiltration membranes and two reverse osmosis membranes were tested, of which the molecular weight cut-off (MWCO) was measured. Each membrane was placed at a flow Cell unit and fed with artificial water.

The MWCO of the nanofiltration membranes was varied from 115 to 508 Da. The purpose of testing different membranes was to assess how the pore size of the membrane influences the ion rejection of the IEX spent regenerant. In addition, the ion rejection was evaluated in different ionic strengths and different molar ratios. The aim was to investigate how the ionic composition influences the ion rejection. Finally, operating parameters such as permeate flux and temperature were tested to research their impact on the ion rejection of the IEX spent regenerant.

Results showed that the ion rejection of the IEX spent regenerant was strongly affected by the pore size of the membrane as the charge effect was insignificant due to the high ionic strength of the feed solution (1 M). The main exclusion mechanisms were the steric and the dielectric exclusion. Loose membranes with MWCO greater than 500 Da rejected less than 10% of both monovalent and divalent ions. Membranes with pore size from 200 Da to 300 Da rejected 30-60% of Ca^{2+} and contributed to negative rejections of Na^{+}. NF membranes with MWCO of approximately 150 Da, rejected 90% of Ca^{2+} and 40% of Na^{+}. Tighter NF membrane and RO membranes rejected more than 95% of divalent ions and more than 70% of monovalent ions.

It was also observed that the ionic composition did not influence the rejection of divalent cations as it remained almost constant in different ionic strengths and molar ratio of the solution. Contrary, the rejection of monovalent cations was greatly influenced by the molar ratio of the solution due to the presence of predominant amounts of ion of higher charge and the need of the ions to maintain electroneutrality. Higher molar ratio resulted in lower rejection of monovalent cations.

The permeate flux affected the ion rejections. Higher fluxes resulted in higher ion rejection and different ion separation. To keep high rejection of bivalent and low rejection of monovalent ions a compromise would be desired. Temperature had a great influence on the ion rejection of the IEX spent regenerant as a 5^{o}C increase in the temperature cased 19% decrease in divalent cation rejection.

TS80, one of the nanofiltration membranes, performed better than other membranes as it rejected 90% of Ca^{2+} and 40% of Na^{+}. Double Pass NF with TS80 membrane was proposed as the first treatment step of the IEX spent regenerant stream as it resulted in 97% Ca^{2+} and 45% Na^{+} rejection.

Nomenclature

Roman symbols	Description
$c_{i,p}$	Ion concentration in the permeate stream (mg/L)
ci,f	Ion concentration in the feed stream (mg/L)
ci,pore	Concentration of the species I at the pore (mol/m^3)
ci,m	Feed concentration at the membrane-feed solution interface (mol/m^3)
d_{pore}	Diameter of the pores (m)
$D_{i,pore}$	Intra-pore diffusion coefficient of the species i (m^2/s)
I	Ionic strength (mol/L)
$j_{i,pore}$	Solute flux of the species i (mol/m^2s)
J_w	Water flux (L/m^2/h)
K_w	Membrane permeability coefficient (m)
K_{ick}	Convection hindrance factor (-)
$K_{i,d}$	Diffusion hindrance factor (-)
l	Thickness of the membrane (m)
N	Number of species in the mixture (-)
P_f	Pressure of feed (Pa)
P_P	Pressure of permeate (Pa)
p	Porosity of the membrane (-)
R	Ion rejection (%)
TMP	Transmembrane pressure (Pa)
z_i	Ion valence

Greek symbols	Description
$\gamma_{i,pore}$	Solute i activity within the pore entrance (-)
$\gamma_{i,m}$	Solute i activity at the membrane-feed interface (-)
Δπ	Osmotic pressure difference (Pa)
γ	Recovery (-)
ΔP_{hydr}	Hydraulic pressure loss (Pa)
μ	dynamic viscosity of water (Ns/m^2)
$\pi_{membrane}$	Osmotic pressure at the membrane surface at the feed side (Pa)
$\pi_{permeate}$	Osmotic pressure of the permeate (Pa)
π_{feed}	Osmotic pressure at the feed side (Pa)
τ	Tortuosity of the pores (-)
Φ_i	Steric partitioning factor (-)
Φ_B	Born solvation partitioning factor (-)
Ψ	Membrane potential (V)
$\Psi_{D,m}$	Donnan potential at the feed-membrane interface (V)
$\Psi_{D,p}$	Donnan potential difference on the membrane-permeate interface (V)

Table of contents

List of Figures

List of Tables

List of equations

1 *Introduction*

1.1 General Introduction

Ion exchange (IEX) process has many applications in water treatment such as water softening, demineralization/deionization and organic or nitrate removal. There are two types of IEX process; the cationic IEX and anionic IEX. The work done during this master thesis is related to cationic IEX and therefore IEX in the rest of this report refers to cationic IEX. The regeneration of the IEX is typically done with highly concentrated NaCl solutions. The stream produced during regeneration (spent regenerant) contains high percentage of salts (brine). The conventional options to dispose the IEX spent regenerant are discharging to sea or other surface water bodies, discharging to sewers, land application, evaporation ponds or deep well injection [1]. However, the disposal cost and the limitations imposed by local laws and regulations made it an ongoing challenge to find an economic solution for the minimization or elimination of the volume of brine streams and the recovery of valuable minerals. Nowadays, this challenge becomes a topic of research for many scientists as it also reduces the environmental impact of industries.

NaCl recovery from brine is very beneficial in case of ion exchange plants that require large quantities of salt for resin regeneration [1]. IEX spent regenerant is a mixture of salts with concentration not high enough to be economically utilized in industry. Therefore, separation and concentration are necessary to treat the IEX spent regenerant and recover salts that can be used in industry. Closing the loop of salt use in the ion exchange will reduce energy demands linked to salt production and transportation as well as reduce chemical and disposal expenditures [1]. In addition, magnesium hydroxide recovery can be very profitable as metallic magnesium is a crucial raw material to Europe's economy and essential to maintaining and improving human life [2].

Currently, attempts are being made by the ZERO BRINE project, 2017, to demonstrate ion separation as the first stage of the IEX spent regenerant treatment. Nanofiltration (NF) membranes can be used for the ion separation to make a multivalent-rich ion stream (concentrate) that includes ions such as calcium and magnesium, and a sodium chloride rich stream (permeate). NF membranes typically reject 75-99% of divalent ions and 30-50% of monovalent ions [3]. The permeate of the NF membranes can be further treated to reach high NaCl concentrations that can be recycled and used for the resin regeneration step of IEX. Magnesium and calcium ions in the NF concentrate steam can be separated selectively and be used in a cost-effective fashion within a variety water/wastewater treatment process [4], or within different industrial uses.

Nanofiltration is used in many areas including water and wastewater treatment but also in other industries such as pharmaceutical, biotechnology or food industries. Despite the variety of applications, predictive modeling for new NF processes and optimization of the existing membrane applications is still a challenge especially for mixed feeds containing mono-and divalent ions [5]. Additionally, effects of the solution chemistry further complicate the prediction of NF processes. Ionic electrical exclusion, sieve mechanisms, dielectric effects and permeate flux along with the need of ions to maintain electroneutrality influence the ion selective rejection [6].

Partitioning and transport mechanisms have already been researched and widely applied to the membrane applications. Depending on the feed water composition and the membrane type, different

rejection mechanisms participate in the ion rejection. However, predictive description for different salts and salt mixtures has failed to define the accurate ion permeability [5]. Ion rejections by nanofiltration using $CaCl_2$ and NaCl are predicted by Deon et al [7]. However, the authors proposed that a larger range of common ion concentration is important to be investigated. There are very few studies that target multi-ionic mixtures such as artificial seawater [8].

1.2 Problem definition

Achieving a clear (total) separation of monovalent and multivalent ions contributes to a better downstream treatment of the IEX spent regenerant. For example, the permeate of a NF process can lead to an evaporator or to a membrane distillation reactor to increase the concentration of NaCl in order to be used as the primary material for regeneration of IEX. Poor separation of NaCl from multivalent ions can cause impurities in the NaCl-solution produced by evaporator or membrane distillation reactor and thus lower regeneration of the IEX. High permeation of multivalent ions to permeate will end to the downstream steps and increase the scaling risk. On the other hand, high rejection of monovalent ions may deteriorate the purity of recovered magnesium and calcium hydroxide. Zero or negative rejection of monovalent ions is also advantageous since the osmotic pressure on the permeate side increases resulting in a lower driving force requirement and consequently lower energy demand [8].

Therefore, a research on different NF membranes treating the IEX spent regenerant is necessary to be conducted. It is important to be able to predict the ion rejection of multi-ionic mixtures when specific NF membranes are used. The aim of this thesis is to compare a range of NF membranes and propose the most appropriate membrane that separates the ions found in the IEX spent regenerant. As it is very crucial to minimize the presence of divalent ions in the permeate due to their competition with Na^+ during the regeneration of the IEX resin, a membrane that highly rejects the divalent ions (more than 90%) and as low as possible rejects the monovalent ions, will be preferred.

1.3 Research Question

The objective of this thesis is to define the ion rejection of highly concentrated multi-ionic mixtures by nanofiltration and select the most suitable nanofiltration membrane contributing to an optimal separation of monovalent (Na, K and Cl) from divalent ions (Mg, Ca, Ba, and Sr) in the spent regenerant of IEX columns.

The problem can be addressed by answering the following main research question:

> How is the separation of monovalent and multivalent ions of the IEX spent regenerant affected by different polyamide NF membranes and by different ionic compositions?

To answer the main research question, the following sub-questions are formulated:

- What are the rejection and transport mechanisms dominantly influencing the NF selectivity of the IEX spent regenerant, based on literature review?
- What is the influence of the parameters related to the membrane characteristics (pore size of the membrane) in the NF selectivity of the IEX spent regenerant?
- How does the ion composition of the IEX spent regenerant influence the ion rejection?

- How do the operating parameters such as permeate flux and temperature influence the ion rejection of the IEX spent regenerant?

2 *Theory*

2.1 Nanofiltration Principles

2.1.1 Introduction

Nanofiltration is a separation process that its performance is intermediate between reverse osmosis (RO) and ultrafiltration (UF) [8]. The pore size of a nanofiltration membrane is in the order of nanometers, and the corresponding molecular weight cut-off (MWCO) is in the range of 100-1000 Da. Water transport is promoted through NF membranes while TDS is rejected.

The nanofiltration membrane is regarded as a charged porous layer and is described by three parameters; average pore radius, volumetric charge density and effective membrane thickness [9]. The rejection mechanisms are described through steric effect (sieve mechanism), Donnan equilibrium (electrical exclusion) and dielectric exclusion. Donnan Steric Pore Model with dielectric exclusion (DSPM-DE) is widely used to describe nanofiltration as it has successfully used in literature for modelling experimental membrane performance [10]. This model also includes the dielectric exclusion that can better predict the nanofiltration performance in presence of multivalent counter-ions [11]. Similarly, the transport mechanisms are explained through convection, diffusion and electrokinetic effects [12] and they are described by the extended Nernst-Planck equation [9].

There are several commercial membranes with different surface materials such as polyamide (PA), polysulfone (PS), cellulose acetate (CA), polyvinyl alcohol (PVA) and polyethersulfone (PES) [13]. These polymer chains are hydrophilic and tend to be hydrated and ionized in an aqueous solution. Their conformation and ionization are transformed under different surrounding conditions and especially at different pH and ionic strength [13]. It is proved that a minor change in the pore size or charge pattern can have an important influence on NF performance due to the nanoscale pore dimensions and the electrical charged materials of NF membranes. It is therefore concluded that salt concentrations and pH influence the NF performance and cause significant effects on ion rejection [13].

2.1.2 Transport through membranes

As it is already mentioned, the nanofiltration transport mechanisms are described through convection, diffusion and electro-migration, Figure 1. Diffusion occurs due to the concentration gradient of each ion within the membrane. Convection is a result of the solute being carried by the solvent through the membrane pores. Electro-migration occurs due to the membrane potential gradient that is developed to balance ionic fluxes and maintain electroneutrality within the membrane [11].

2.1.2.1 *Solute transport equation*

The solute flux $j_{i,pore}$ is a result of the above transport mechanisms and is described by the Extended Nernst-Planck equation (ENP), Equation 1.

Equation 1: Extended Nernst-Planck equation [15]

$$j_{i,pore} = -D_{i,pore}\frac{dC_{i,\mathrm{pore}}}{dx} - \frac{z_i C_{i,pore} D_{i,pore}}{RT} F \frac{d\psi}{dx} + K_{i,c} C_{i,pore} J_w$$

and $D_{i,pore} = K_{i,d} D_i$

The solute flux consists of the diffusive, electromigrative and the convective terms that appear in Equation 1, in this order. Due to the small size of the membrane Nano-pores, the hindrance factor $K_{i,d}$ is being taken into account to give the diffusivity in the pore. The diffusive term is described by the intra-pore diffusion coefficient $D_{i,pore}$ and the concentration gradient of the species, $\frac{dC_{i,pore}}{dx}$, inside the membrane. The electromigrative transport mechanisms is caused by the membrane potential gradient $\frac{d\psi}{dx}$. Finally, the transport through convection occurs because of the porous nature of NF membranes [9] and it is described by the convective hindrance factor $K_{i,c}$, the water flux J_w and the concentration of the species $C_{i,pore}$ at the pore.

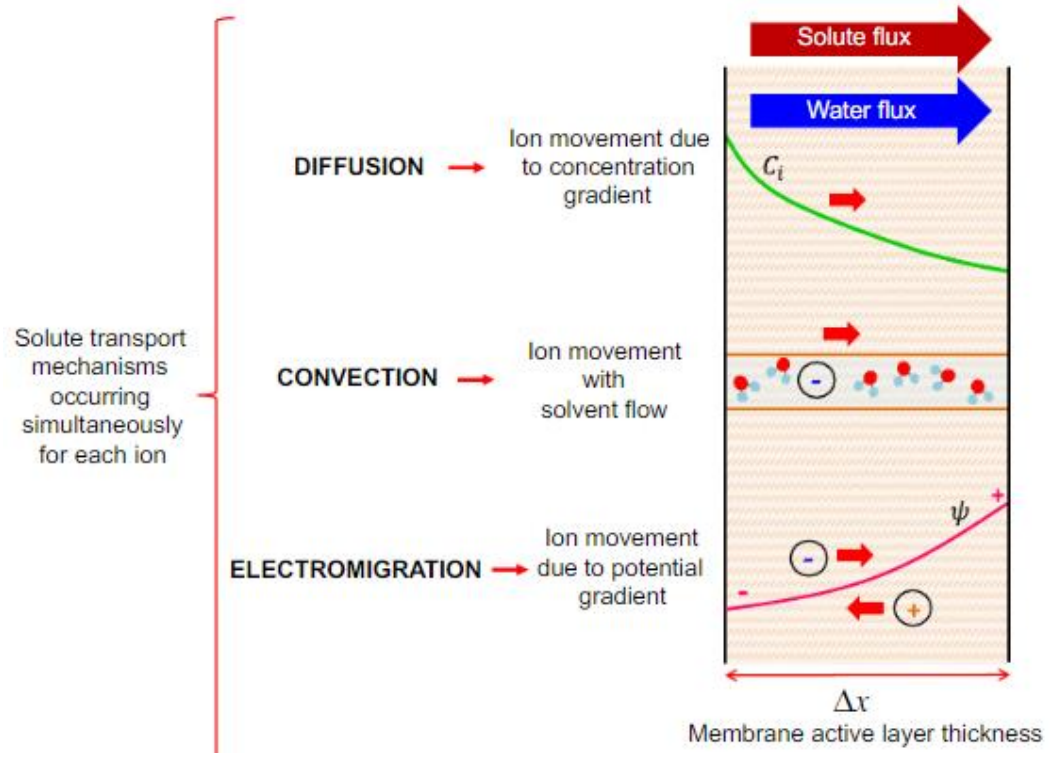

Figure 1: NF Transport mechanisms [14]

2.1.3 Rejection Mechanisms

The three exclusion mechanisms of the nanofiltration that are also described by the DSPM-DE model are the steric exclusion, dielectric exclusion and Donnan exclusion, Figure 2. The ion rejection is defined by Equation 2.

Equation 2: Ion rejection

$$R = 1 - \frac{c_{i,p}}{c_{i,f}}$$

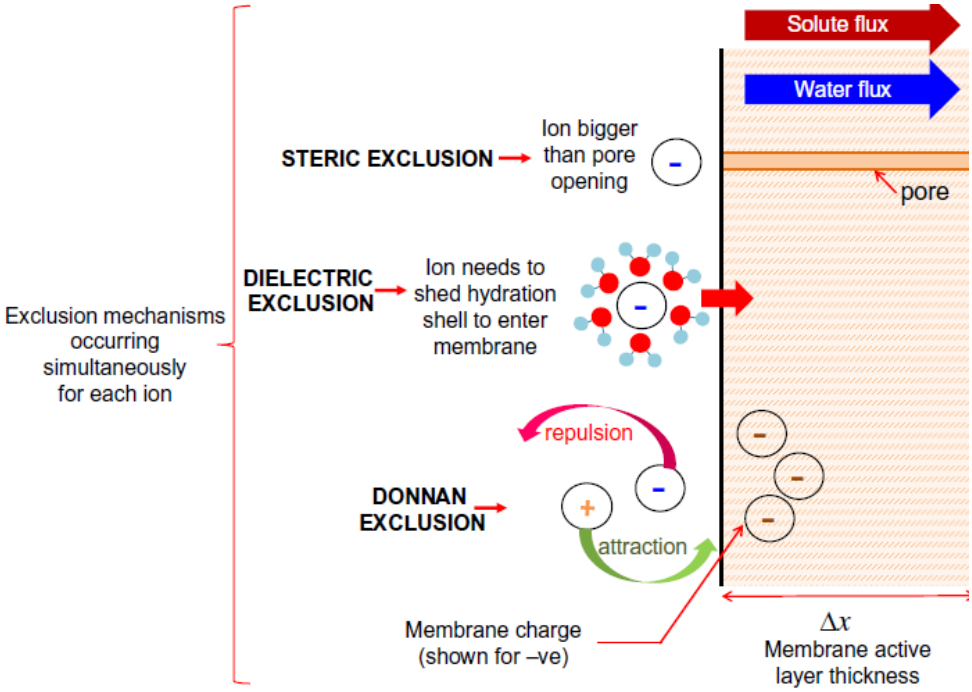

Figure 2: NF solute exclusion mechanisms [15]

2.1.3.1 *Steric Exclusion Mechanism*

This mechanism is size-based exclusion at the pore opening. Nanofiltration membranes have different pore sizes that correspond on different molecular weight cut-off (Da). Ions attract water molecules around, which are polar, and form hydration shells. Cations attract negative ends (oxygen) of the water molecules and anions attract the positive ends (hydrogen) [16]. The hydrated radius of the different ions differs significantly. Monovalent ions have smaller hydrated radius than multivalent ions and can pass easier though the nanofiltration membrane.

2.1.3.2 *Dielectric Exclusion Mechanism*

Except for the hydrated size of the ions, the strength of the hydration shell and the ability of ions to rearrange or lose the water molecules within the hydration shell under shear forces significantly influence the ability of the ions to pass through the thin film membrane. Monovalent ions have week hydration shells and under high pressures can easier lose their hydration shell than divalent ions, enabling them to pass through the membrane.

The dielectric exclusion mechanism is caused by changes in the solvent dielectric constant due to the confinement of water molecules within the nanopore of the membrane. Electrochemical studies suggest that a decrease in the dielectric constant in the membrane's confining pores relative to the bulk is put into evidence [10]. This decrease in dielectric constant presents a barrier to ion solvation into the pores [15]. It is described by the Born model and leads to higher ion rejections. This exclusion mechanism becomes more significant with increasing ion valence [8].

2.1.3.3 *Donnan Exclusion Mechanism*

Membrane charge along the surface and through the pores is an important parameter in the transport process [17] and is based on Donnan exclusion mechanism. When membrane surface effects are

present, variations in ion rejection between the membranes are observed. Co-ions are repulsed, and counter-ions are attracted.

pH protonate and deprotonate the functional groups of the membranes and of the molecules in solution, over its range resulting in changing the membrane charge. The salt rejection increases with membrane charge and is the lowest at the isoelectric point (IEP) of the membrane at which the membrane is uncharged [8].

2.1.3.4 *Equillibrium and electroneutrality conditions*

The two-equilibrium boundary conditions on the membrane-feed and the membrane-permeate interface are described by Equation 3 and Equation 4. The steric and the Born solvation partitioning factor are described by the terms Φ_i and Φ_B, respectively. These two partitioning factors are numbers smaller than unity. According to Equation 3, a smaller value indicates higher rejection because the ratio between the solute concentration in pore entrance and the membrane-feed interface is decreased. The Donnan potential between the feed side and the pore entrance is described by the term $\Psi_{D,m}$. The Donnan potential between the membrane-permeate interface is describe by the term $\Psi_{D,p}$ [15].

Equation 3: Equilibrium boundary condition on membrane-feed interface [15]

$$\frac{\gamma_{i,pore}C_{i,pore}}{\gamma_{i,\mathrm{m}}C_{i,\mathrm{m}}} = \Phi_i\Phi_{\mathrm{B}}\exp\left(-\frac{z_iF}{RT}\psi_{D,\mathrm{m}}\right)$$

Equation 4: Equilibrium boundary on the membrane-permeate interface [15]

$$\frac{\gamma_{i,pore}C_{i,pore}}{\gamma_{i,\mathrm{p}}C_{i,\mathrm{p}}} = \Phi_i\Phi_{\mathrm{B}}\exp\left(-\frac{z_iF}{RT}\psi_{D,\mathrm{p}}\right)$$

Two electroneutrality conditions apply in the feed-membrane and permeate-membrane interface and they are described by the Equation 5. The volumetric charge density is zero, since there is no net charge at any point of the membrane [15].

Equation 5: Electroneutrality conditions [8]

$$\sum_{i=1}^{N} z_i C_{i,w} = 0$$

$$\sum_{i=1}^{N} z_i C_{i,\mathrm{p}} = 0$$

2.2 Nanofiltration of spent IEX regeneration stream

2.2.1 Introduction

Before choosing the NF membrane that performs better than other NF membranes and achieves a good separation of monovalent and divalent ions, it is important to understand the NF rejection mechanisms of the IEX spent regenerant and predict how the operating parameters such as permeate flux, temperature and pH will influence the ion rejection of this stream. For this reason, a characterization of the IEX spent regenerant needs to be done and evaluated.

2.2.2 Characterization of the IEX spent regenerant

During IEX regeneration, a highly concentrated stream is produced, and it is composed of Na^+, Ca^{2+}, Mg^{2+}, K^+, Cl^- ions, Table 1. As it is explained before, a change in salt concentration can have a significant effect on ion rejection [13]. Ionic strength and molar ratio are used to express the variations in ion compositions. The ionic strength of this solution is close to 0.94 M and it is calculated by equation 6. Molar ratio is the ratio between the monovalent anions and the monovalent cations and is given in Equation 7. Table 2 summarizes these values. The total dissolved solids (TDS) are also calculated and depicted in Table 2.

Table 1: Concentration of the IEX spent regenerant

Ion	Concentration (mg/L)
Na^+	3266
Ca^{2+}	7590
Mg^{2+}	1700
K^+	520
Cl^-	23950

Equation 6: Ionic strength

$$I = \frac{1}{2}\sum_{i=1}^{n} c_i z_i^{\,2}$$

Equation 7: Molar ratio

$$Molar\ ratio = \frac{monovalent\ anions\ (-)}{monovalent\ cations\ (+)}$$

Table 2: Characterization of IEX brine

TDS (mg/L)	Ionic strength (M)	Molar ratio
37026	0.94	4.3

2.2.3 Nano-filtration of the IEX spent regenerant

2.2.3.1 *Ion rejection*

The ions do not have fixed radii when they are in an aqueous solution, but they change their shape under pressure. Ionic structure, concentration and environmental factors such as temperature, pH and ionic strength influence the strength of the hydration shell [16]. The smaller ions have stronger hydration shell [18]. Figure 3 represents the hydration shell around a large ion and around a small ion.

Table 3 shows the hydrate radius of the ions found in the IEX spent regenerant. Monovalent ions have smaller hydrated radius than divalent cations and it is therefore predicted that they can easier pass through the nanofiltration membrane based on the steric effect. As it is mentioned before, divalent cations need higher energy to lose the water molecules under shear forces because they have a higher hydration free energy. The hydration free energy of the ions found in the IEX spent regenerant is depicted in Table 3. Monovalent ions that have weaker hydration bonds can lose some or all the water

hydration shell and fit through the membrane pores. It is expected that the order that the ions will pass through the membrane is:

ASSUMPTION 1: Ion permeation: K>Na>Ca>Mg

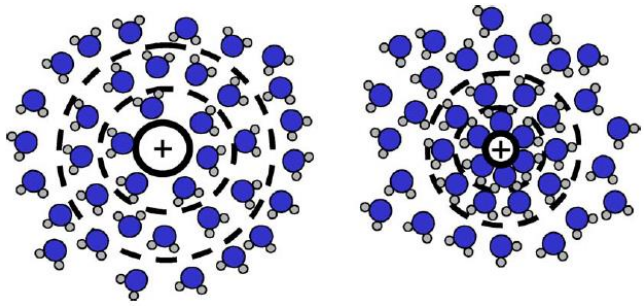

Figure 3: Schematic representation of hydration shells around a large (left) and a small (right) ion [16]

Table 3: Ion Hydrated radius and hydration free energy [19], [20]

Ion	Hydrated radius (nm)	Hydration free energy (kJ/mol)
K^+	0.331	295
Na^+	0.358	365
Ca^{2+}	0.412	1504
Mg^{2+}	0.428	1828
Cl^-	0.332	340

Donnan exclusion mechanism

Donnan mechanism is not sufficient to explain the high rejection rates observed in some NF membranes in case of ionic solutions containing divalent counter-ions [21]. Lower salinity of a solution leads to a higher Donnan potential [22]. Escoda et al proved that the diffusion potential in the case of high concentrated multi-ionic solutions depends on the pore size and the dielectric constant inside the pores [21]. In this study, the ionic strength of the IEX spent regenerant is high; close to 1M. The negative ζ potential of the NF membranes decreases and approximates zero with increasing ionic strength of the solution, which can be explained by the electrical double layer compaction theory, Figure 4. This is because the surface charge gets fully compensated by counter ion accumulation in the membrane layer and thus the potential approaches zero, assumption 2. Because the zeta potential of the membrane surface is close to zero, it is assumed that the pore size of the NF membrane determines the ion rejection of the IEX spent regenerant, assumption 3.

ASSUMPTION 2: Donnan exclusion mechanism does not have an important influence on the ion rejection of the IEX spent regenerant

ASSUMPTION 3: Ion rejection of the IEX spent regenerant is determined by the pore size of the NF membrane

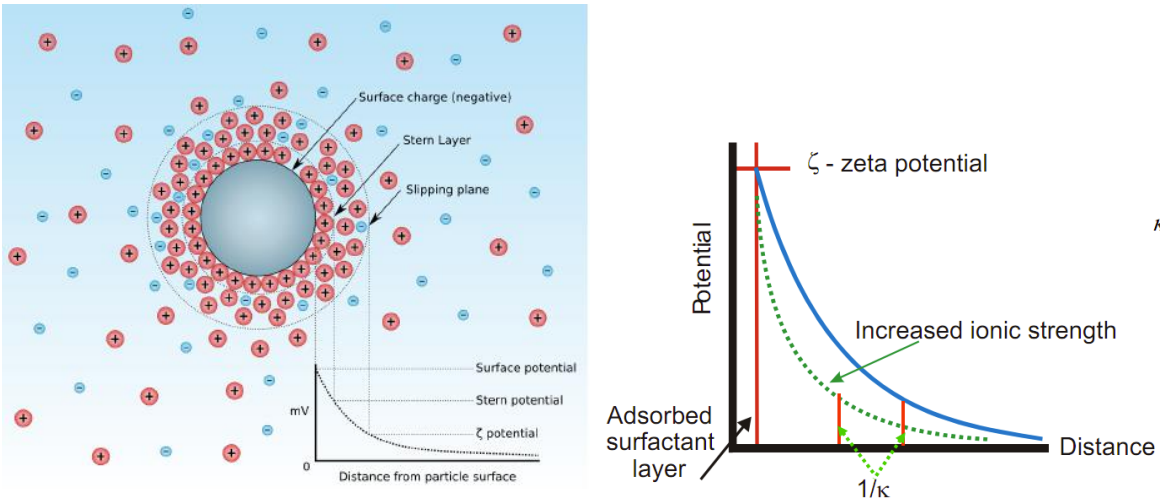

Figure 4: Schematic of double layer in a liquid at contact with a negatively-charged solid and influence of the increased ionic strength [23]

2.2.3.2 *pH influence*

As it is already mentioned, the zeta potential decays to zero within the membrane layer at high ionic strength. As it is depicted in Figure 5, pH does not have significant effect on the zeta potential of the membrane layer in case of highly concentrated solutions.

ASSUMPTION 4: pH does not influence the ion rejection in case of IEX spent regenerant

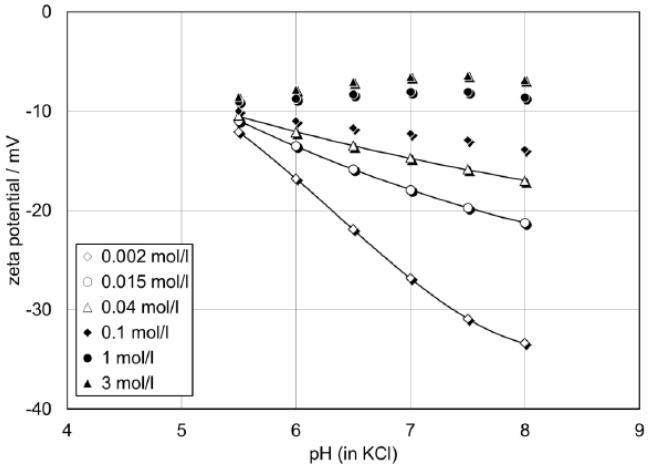

Figure 5: Zeta potential as a function of pH in different ionic strengths [24]

2.2.3.3 *Temperature influence*

Temperature changes the structural properties of the membrane (pore radius and membrane thickness) and it influences the ion diffusivity and solvent viscosity. It is proved that the solute transport increases with temperature due to the effect on the membrane properties. Changes in ion diffusivity and solvent viscosity due to higher temperatures increase the solute transport only to a small extend (up to 5%) [15]. An increase in the pore size of the NF polyamide membrane (desal DK) with the increase of the temperature has been reported by Amar et al. 2006, (Table 4). As it is assumed that the pore size of the membrane determines the ion rejection of the IEX spent regenerant, it is concluded that temperature also has a great influence on the ion transport.

ASSUMPTION 5: Temperature has a great influence on the ion rejection of the IEX spent regenerant

Table 4: Effect of temperature on NF pore size [25]

T°C	r_{pore}(nm)
22	0.58
30	0.60
40	0.63

2.2.3.4 *Flux influence*

Flux is the amount of fluid that passes the membrane per unit area of membrane per unit of time. It depends on the fluid and the membrane characteristics. Labban et al 2017 found that ion rejection is increased with increasing permeate flux as convection becomes more dominant, Equation 1, and the permeate becomes less concentrated [8].

2.2.3.5 *Ion pair-clusters formation*

In addition to hydrated individual ions, the presence of hydration ion pairs, Figure 6, or ion clusters has been observed, especially in highly concentrated solutions [26], where there is less available water to separate the ions. Ion pairs are formed when the ions come close enough to be separated by a specific distance. The ion cluster is composed of three or more ions. Particularly, the mole fraction of individual Na^+ ion decreased from 0.95 to 0.84, when the NaCl concentration increased from 0.1 mol/L to 1 mol/L. In addition, the mole fraction of individual Ca^{2+} ion decreased from 0.71 to 0.24 when $CaCl_2$ concentration increased from 0.1 mol/L to 1 mol/L [26]. That means that NaCl and $CaCl_2$ ion pairs were formed. As the IEX spent regenerant stream is highly concentrated, it is expected that individual ions will form ion pairs and will be better rejected by the NF membrane.

In addition, inside the confined nanopore, it is more difficult for the water molecular dipoles to reorient and apply an electric field as they are forced be aligned [27]. This ordered water appear small polarizability and makes it more difficult for the ions to remain fully solvated. This causes an additional salt rejection of the IEX spent regenerant by NF membrane.

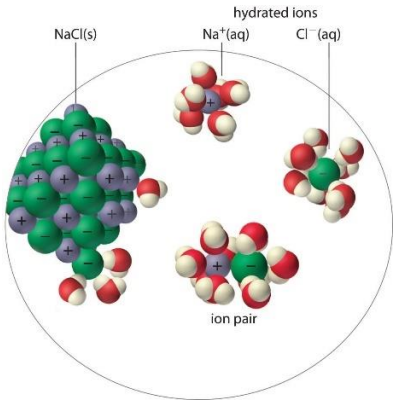

Figure 6: Ion pair formation [28]

3 *Materials and Methods*

3.1 Introduction

Nano-filtration experiments were performed in a lab scale setup with the use of a flow cell (Sepa Cell unit). In addition, two RO membranes were also tested to investigate how ion separation of the IEX spent regenerant is influenced by RO filtration.

3.2 Description of the Sepa Cell experiment

3.2.1 Sepa Cell unit

A GE Sepa Cell unit was used. This contains a membrane housing with the capacity for an active membrane area of 142 cm^2 (9.7 cm × 14.7 cm). The unit consists of a 316 SS steel housing, Figure 7, that can be pressurized up to 69 bars and is able to withstand operational temperatures of 177 °C. The setup contains a piston pump with a constant flow of 420-430 liters per hour, pressure indicators on the feed and the concentrate side and a regulation valve on the concentrate side. The Sepa Cell setup is depicted in Figure 8.

Figure 7: GE Sepa Cell unit

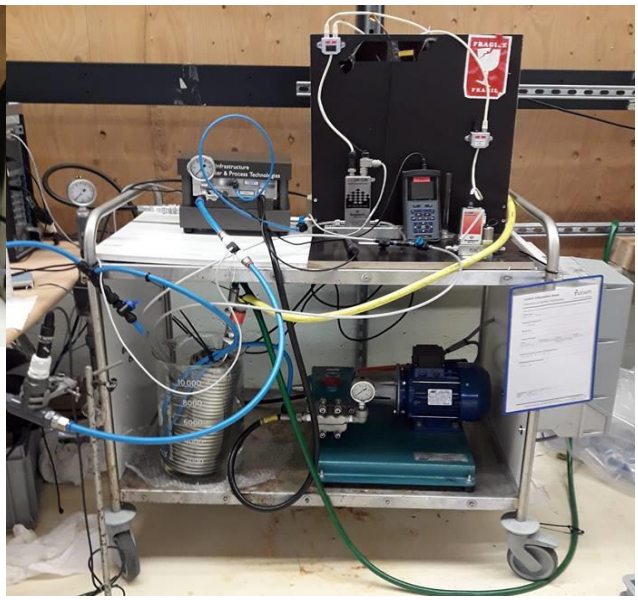

Figure 8: Sepa Cell setup

3.2.2 Description of the lab test

The SEPA Cell unit was used to separate the feed solution into a concentrate stream and a permeate stream over a flat sheet NF or RO membrane that was positioned in the membrane housing. To generate permeate flow through the membrane, feed pressure was applied by means of the positive displacement pump and by adjusting the concentrate valve. The permeate stream through the membrane was collected in a glass cylinder, while concentrate stream was continuously recirculated back to the container with the feed solution. The formula used to calculate the concentration factor (CF) is explained in Equation 8, where γ is the recovery.

Equation 8: Concentration factor

$$CF = \frac{1}{1-\gamma}$$

The permeate flow was being recorded by a mass flow instrument (mini cori-flow) and the concentrate flow by a flow meter (Gems sensors). The flux through the membrane is calculated based on the known effective membrane area of 0.014 m^2. The flux through the membrane was maintained constant by manually adjusting the feed pressure. Furthermore, the temperature of the feed solution was measured by a thermometer and it was controlled by a cooling spiral (on tap water).

Before each test, the dry flat sheet membranes were wetted and rinsed with demineralized water. In addition, the membranes were tested with deionized water at 20°C under step-wise increasing feed pressures. This was done to confirm the proper preparation of the experimental set-up and to compare the measured water flux before and after the membranes were exposed to the brine stream.

3.2.3 Sample procedure

Samples were taken from the permeate and the feed solution with a deviation of ±1min. Two types of permeate samples were taken for different CF. The first sample was taken from the total permeate stream and it was describing the average permeate quality produced in each CF. The second sample was taken directly from the permeate production. When specific CF were reached in order to maintain constant conditions before sampling, the permeate stream was also recirculated to the feed solution for a time period until the permeate water composition was constant. It was researched what is the actual ion rejection of the membrane in different CF.

3.2.4 Operating conditions

The operating conditions during the lab tests were the same for every experiment to derive comparable results and conclusions. These conditions are summarized in Table 5. The permeate flux was 30 LMH. The feed pressure during the tests was manually adjusted to keep the permeate flux constant. The initial feed volume was 8 liters for all the experiments and the pH was 8. In the beginning of each experiment (CF=1), permeate fluxes of 15, 30 and 45 LMH were tested and compared.

Table 5: Operating conditions

	Units	Value
Feed flow	L/h	430
Permeate flux	L/(m^2·h)	30
Operating temperature	°C	20
Initial feed Volume	L	8
pH		8

3.2.5 P&ID

The P&ID of the Sepa Cell unit is depicted in Figure 9.

3.3 Type of tested membranes

Different NF membranes and RO membranes were tested. An overview of the main specifications and the most important operation limits are presented in Table 6.

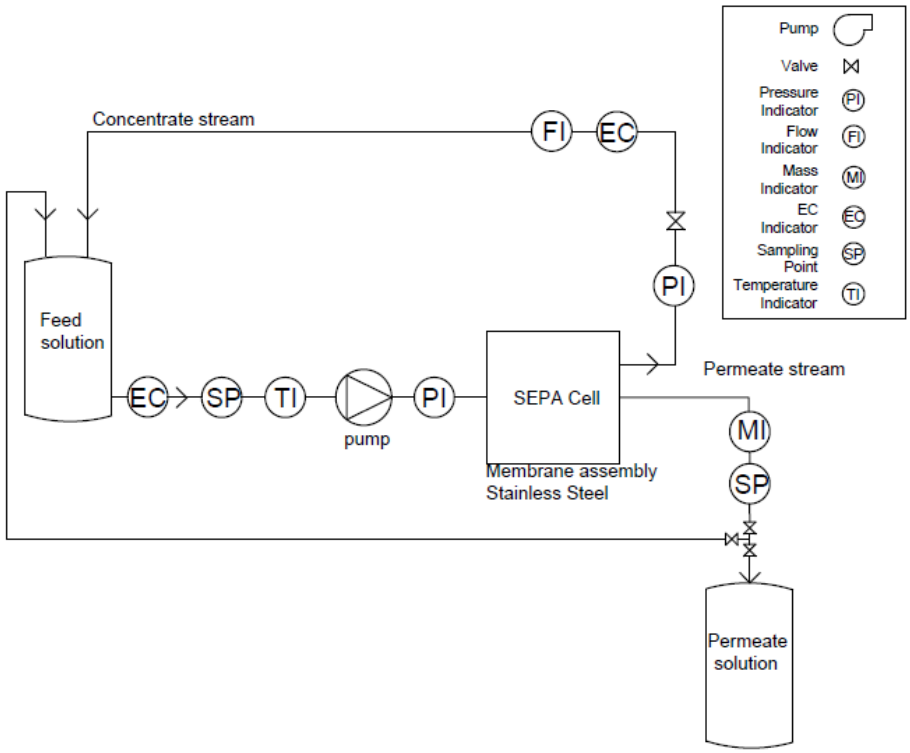

Figure 9: P&ID of the Sepa Cell unit

Table 6: Commercial nanofiltration and RO membranes

Model	Vendor	Polymer	MWCO (Da) According to provider	Max pressure (bar)	Max temperature (oC)	Avg. $MgSO_4$ Rejection (%)	Avg. NaCl rejection (%)
NFG	Synder	PA	600-800	41	50	50 (1)	10 (2)
NFW	Synder	PA	300-500	41	50	97 (1)	20 (2)
NF270	Dow	PA	200-400	41	45	>97 (1)	-
SR3D	Koch	PA	200	44.8	50	99 (3)	-
TS80	Trisep	PA	100-200	55	50	99.2	80-90 (2)
NF90	Dow	PA	120	41	45	>97 (5)	85-95 (4)
RO98pt	Alfa Laval	Polypropylene		55	60		98% (6)
LFC3-LD	Hydranautics	PA		41.4	45		99.7 (7)

1) Test conditions: 2000 ppm $MgSO_4$ solution at 110 psi (760kPa) operating pressure, 25°C
2) Test conditions: 2000 ppm NaCl solution at 110 psi (760kPa) operating pressure, 25°C
3) Test conditions: 5000 ppm $MgSO_4$ solution at 95 psi (650kPa) operating pressure, 25°C
4) Test conditions: 2000 ppm NaCl solution at 70 psi (483kPa) operating pressure, 25°C
5) Test conditions: 2000 ppm $MgSO_4$ solution at 70 psi (483kPa) operating pressure, 25°C
6) Test conditions: 2000 ppm NaCl solution at 232 psi (1600kPa) operating pressure, 25°C
7) Test conditions: 1500 ppm NaCl solution at 225 psi (1550kPa) operating pressure, 25°C

3.3.1 Permeability of the membranes

The membrane water permeability (K_w) is calculated by Equation 9. Demineralized water was filtered at different TMP, Equation 10, and a constant temperature of 20°C, and the membrane fluxes J_w were recorded. The osmotic pressure was zero during filtration with pure water. The membrane water permeability is dependent on the membrane's pores size (d_{pore}), the thickness (τ) and the porosity of

the membrane (p), Equation 11. The membrane water permeability remains constant over time and it is independent of the water quality.

Equation 9: Membrane permeability calculation [23]

$$K_w = J_w \frac{\mu}{TMP}$$

Equation 10: Transmembrane pressure calculation [23]

$$TMP = \Delta P - \Delta \pi = P_f - \frac{\Delta P_{hydr}}{2} - P_p - \Delta \pi$$

Equation 11: Membrane water permeability

$$K_W = \frac{p d_{pore}^2}{8 \tau l}$$

3.3.2 Concentration Polarization

Concentration polarization (CP) refers to a concentration gradient at the membrane/solution interface due to the solute retention by the membrane and accumulation at the membrane surface, Figure 10, when feed flow passes through the membrane layer. The increased concentration at the membrane wall causes high osmotic pressure difference and results in lower fluxes. The thickness of this layer depends on the cross-flow velocity. High cross-flow velocity will decrease the thickness of this layer and decrease the CP. The CP is calculated by the osmotic pressure of the solution near the membrane wall ($\pi_{membrane}$) divided by the osmotic pressure in the feed side (π_{feed}), Equation 14.

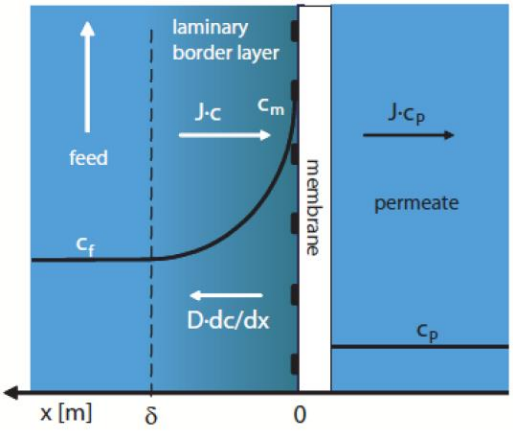

Figure 10: Concentration Polarization effect [23]

The CP was measured in the Sepa Cell unit to ensure that the lab tests will not be influenced by this phenomenon. For this experiment, 12 g/L of $MgSO_4 \cdot 7H_2O$ were composed and filtered through the membrane in the Sepa Cell unit at a TMP of 3 bars. The cross-flow velocity was high, constant and equaled 1.07 m/s to avoid high values of CP. The membrane flux J was recorded and as the membrane permeability coefficient is known from the experiment with demi water, the osmotic pressure difference was calculated, Equation 12. The osmotic pressure of the feed (π_{feed}) and the permeate solution ($\pi_{permeate}$) was calculated based on the measured EC of the solution. The osmotic pressure of the solution near the membrane wall was calculated by Equation 13.

Equation 12: Osmotic pressure difference calculation

$$J = K_w \frac{TMP}{\mu} = K_w \frac{\Delta P - \Delta \pi}{\mu} = K_w \frac{P_f - \frac{\Delta P_{hydr}}{2} - P_p - \Delta \pi}{\mu}$$

Equation 13: Osmotic pressure near the membrane wall calculation

$$\Delta \pi = \pi_{membrane} - \pi_{permeate}$$

Equation 14: Concentration Polarization equation

$$CP = \frac{\pi_{membrane}}{\pi_{feed}}$$

3.3.3 MWCO of the membranes

The MWCO of the NF membranes was measured. The MWCO is the molecular weight of a tracer molecule that is retained with 90% efficiency by the membrane [29]. For measuring the MWCO of the membranes, polyethylene glycols (PEGs) of molecular weights that range from 200 Da to 1000 Da and ethylene glycol of molecular weight of 62 Da were used.

PEG molecules are non-charged and therefore they are rejected only due to the steric effect [29]. Larger tracer molecules than the pore size of the membrane are rejected and the smaller pass through the membrane. A mixture of PEGs was composed with a concentration of 0.6 g/L of each. The membrane flux was constant and equal to 34 LMH. The feed pressure was manually adjusted. The temperature of the feed water was also constant and equal to 22^{O}C. The relationship between the molecular size of PEG tracer (d in nm) and the molecular weight (MW in Da) is given in Equation 15.

Equation 15: Relationship between molecular size and molecular weight of a tracer [30]

$$d = 0.065(\mathrm{MW})^{0.438}$$

3.4 Type of water tests

Artificial solutions were used as the feed water for the experiments. A high precision weighing scale was used to prepare the ion concentrations of the artificial feed water of the NF and RO membrane. The experiments can be separated in two parts: membranes comparison and feed water comparison.

3.4.1 Membranes comparison

In the first set of experiments, all the NF and RO membranes were tested with the same artificial feed water composition, Table 7. The ionic strength of the solution was 0.94 M and the molar ratio was 4.3. The solution was continuously concentrated during the lab test, and the ion rejection was also investigated in different CF.

Table 7: Feed water composition

Ion	mg/L	Ion	mg/L
Ca^{2+}	7590	**Cl^{-}**	23950
Mg^{2+}	1700	**Sr^{2+}**	24.5
Na^{+}	3266	**Ba^{2+}**	12
K^{+}	520		

3.4.2 Water type comparison

The most appropriate membrane that resulted in better ion separation of the IEX spent regenerant and gave high rejection of divalent ions, was further tested with two additional water types. The purpose was to research how the membrane performs with different ionic solutions. For further reduction of divalent ions in the permeate stream, a Double Pass NF was proposed, Figure 11. The membrane treated the permeate stream produced from the first pass. Finally, a lab test was performed where 300 mg/L of SO_4^{2-} were added to the feed solution.

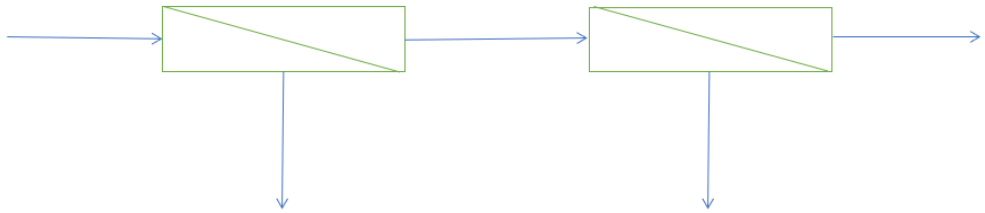

Figure 11: Double Pass NF

3.5 Chemicals

The following chemicals were dosed in the tank:

- $CaCl_2$ (calcium chloride)
- $MgCl_2$ (magnesium chloride)
- NaCl (sodium chloride)
- KCl (potassium chloride)
- $BaCl_2$ (Barium chloride)
- $SrCl_2$ (strontium chloride)
- $CaSO_4$ (calcium sulphate)
- PEGs (polyethylene glycols)
- Ethylene glycol

Each constituent chemical was measured separately on an electric balance with an accuracy of ±0.1 mg/L and dissolved in demi-water to make up 8 L of feed water. The prepared solution was stirred with a magnetic stirrer in a sealed beaker for a time period. The pH correction was done by dosing acid (HCl) or base (NaOH).

3.6 Analysis

The sample analysis was done by three different instruments. The ions were analyzed by ion chromatography (IC) and Inductively Coupled Plasma Mass Spectrometry (ICP-MS). The PEGs solutions were analyzed by high-performance liquid chromatography (HPLC).

For the IC analysis, the samples were diluted with Milli-Q water in the detection range of the IC instrument (0.1mg/L-100mg/L). For the ICP-Ms analysis, the samples were diluted with Milli-Q water and 1% HNO_3 in the detection range of the ICP-Ms instrument (1µg/L-10mg/L). Finally, for the HPLC analysis, the PEGs solutions were filtered by a 45µm filter.

4 *Results and Discussion*

4.1 CP Experiment

The CP was equal to 1.1. That means that the concentration gradient at the feed/membrane interface was prevented as the osmotic pressures of the feed solution and the solution near the membrane wall were almost equal. The calculations can be found in A.2. The aim of this test was to prove that the results of the lab tests will be representative.

4.2 Permeability and MWCO of the membranes

The membrane water permeability and the pore size (MWCO) of each membrane are depicted in Table 8. The results of the permeability test for each membrane are shown in appendix A.3. TS80 and NF270 membranes had a MWCO of 142 Da and 272 Da, respectively, because that was the molecular weight of the trace molecule that was retained by 90% by the membrane. The calculation of the MWCO of these two membranes is depicted in Figure 12 and Figure 13. The MWCO of the other membranes was calculated in the same way. Comparing NF90 and TS80, despite its smaller pore size, NF90 was more permeable than TS80. Based on equation 11, it is concluded that NF90 might have bigger porosity or smaller membrane thickness.

Table 8: Membrane water permeability and MWCO

Membrane name	Kw (m)	Pore size (Da)	Pore size (nm)
NFG	4.79E-14	508	0.996
NFW	1.81E-14	242	0.719
NF270	4.34E-14	272	0.757
SR3D	1.69E-14	200	0.66
TS80	1.93E-14	142	0.57
NF90	2.40E-14	115	0.519
RO98	8.53E-15		
LFC3J	9.03E-15		

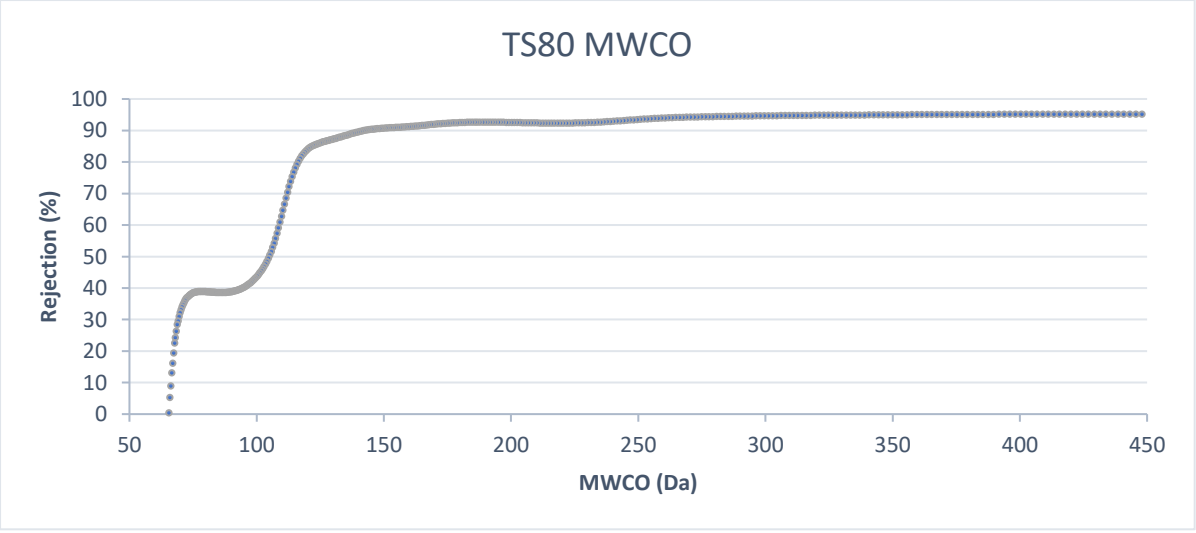

Figure 12: Calculation of the MWCO, TS80

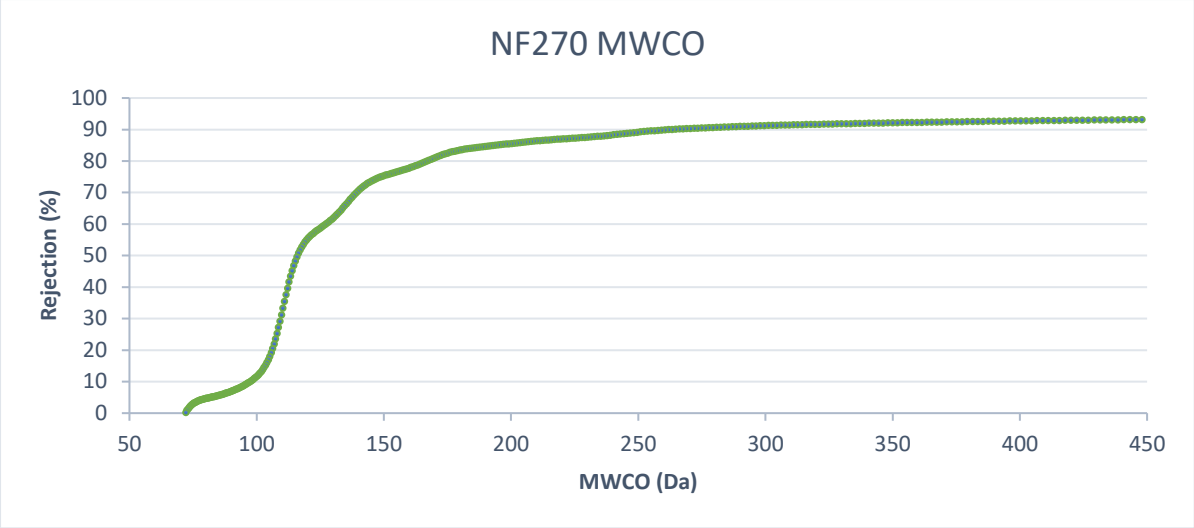

Figure 13: Calculation of the MWCO, NF270

4.3 Ion separation

Nano-filtration membrane separates the IEX spent regenerant into a sodium chloride and potassium chloride rich stream and a calcium chloride and magnesium chloride concentrate stream. The ion rejection was a result of the steric and dielectric exclusion. Separation depended on the MWCO of the membrane and the hydrated radius and the hydration energy of the ions. As it is depicted in Table 3, Na^+ and K^+, that have lower hydrated radius and lower hydration free energy, passed easier through the nanopores of the membrane resulting in lower rejection, Figure 14 and Figure 15. On the other hand, divalent cations that have higher hydrated radius and stronger hydration shell were more rejected, Figure 14 and Figure 15. Assumption 1 is proved, 2.2.3.1. The ion rejection increased with increasing permeate flux, as it can be seen in Figure 14 and Figure 13.

NF270 membrane (272 Da) is looser than TS80 membrane (142 Da) and the rejections of all ions found in the IEX spent regenerant were lower. Negative rejections of monovalent cations were also found. This behavior can be explained by the interaction between the different ions in the solution and is based on the electro migration transport mechanism. On the feed side, the cations were neutralized by the only anion in the mixture; Cl^-. Cl^- was found in high concentrations that exceeded Na^+ and K^+ concentration, Table 7. Driven by a gradient in electrochemical potential and since it was low rejected by the membrane, Cl^- anions were transported from the feed to the permeate side. Since the membrane was less permeable to Ca^{2+} and Mg^{2+} cations, the more mobile counter ions (Na^+ and K^+) neutralized the permeate solution (electro-neutrality condition) [8]. The Cl^- anions in the permeate side ''pulled in'' extra Na^+ and K^+ ions with them to satisfy the electroneutrality condition on both sides of the membrane.

In Figure 16, the rejection of ions in different CF and in constant membrane flux (30 LMH) is depicted. The rejection of divalent cations remained constant and the rejection of monovalent cations decreased when CF increases. Higher CF was attributed to higher concentrations of Ca^{2+} and Mg^{2+} on the feed side and resulted in more enhanced transportation of Na^+ and K^+ ions to the permeate side or even a negative rejection. NaCl permeability can be sharply increased by 25-50% when Ca^{2+} increases [5]. The molar ratio increased by 37% for a CF equal to 2.5, due to the increased Ca^{2+} concentration. Na^+ rejection decreased by 51.4%.

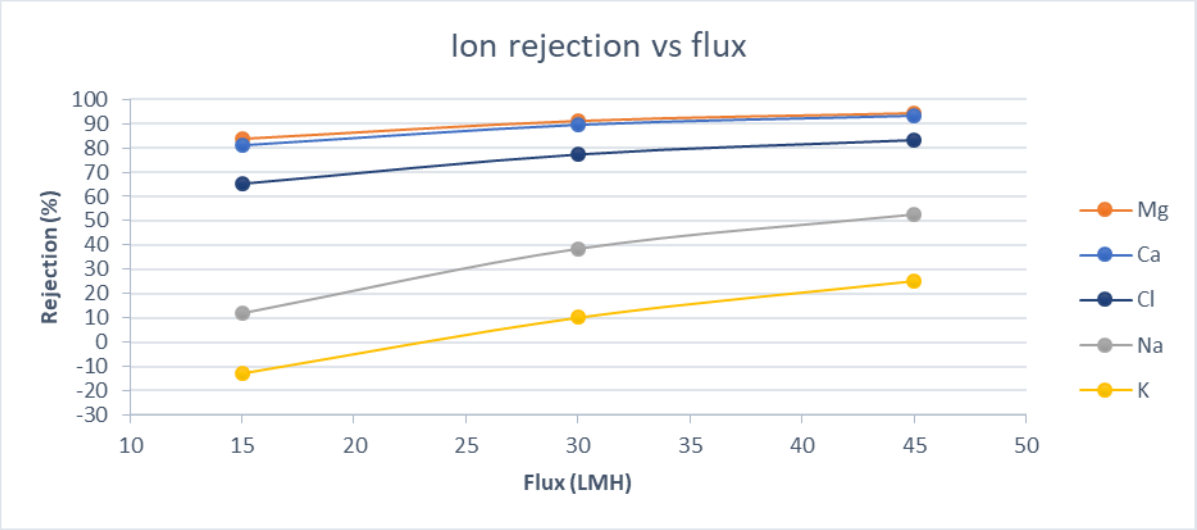

Figure 14: Monovalent and divalent ion separation, TS80 membrane

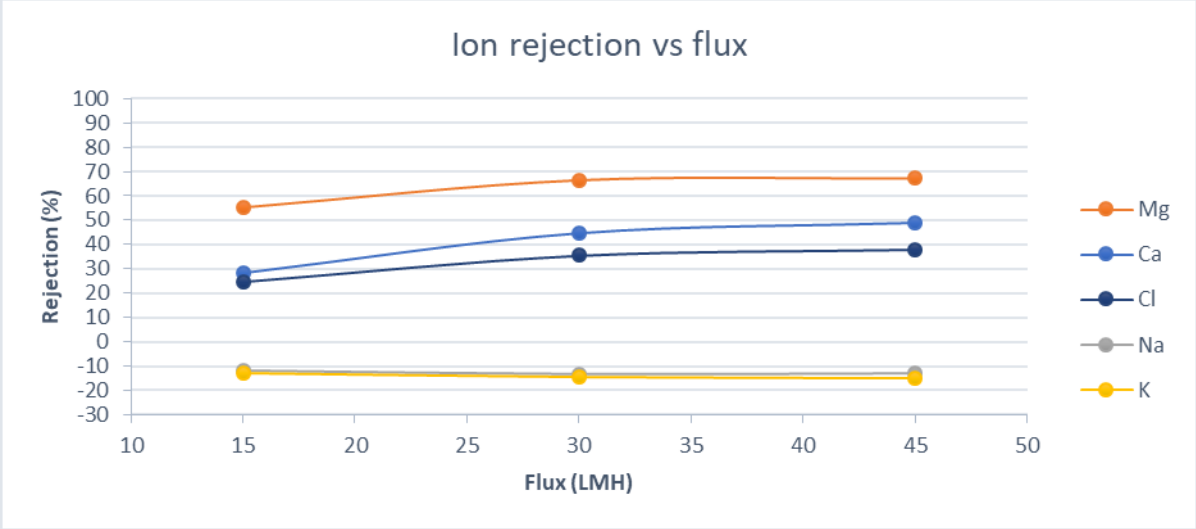

Figure 15: Monovalent and divalent ion separation, NF270 membrane

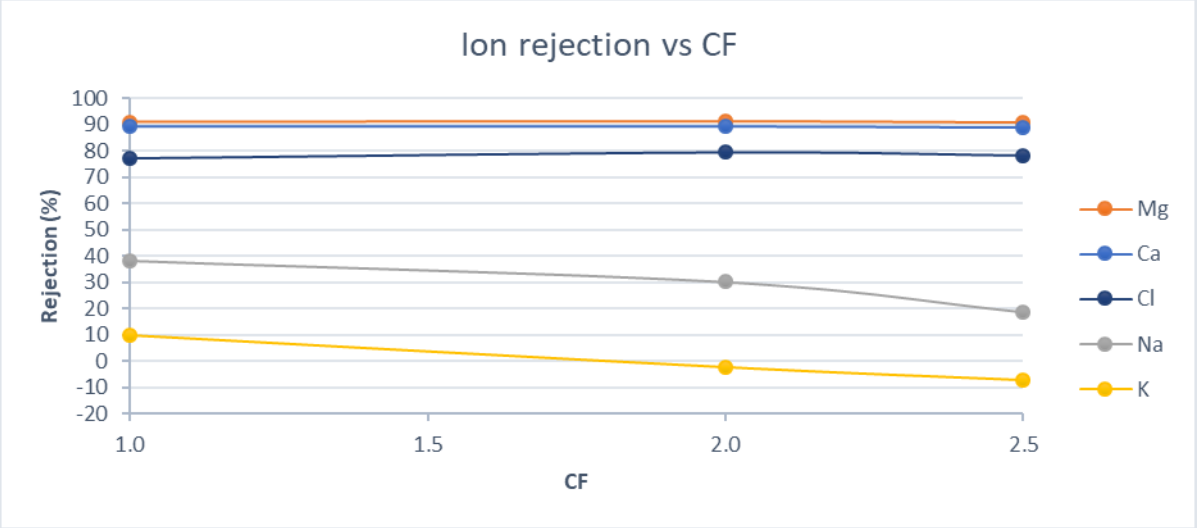

Figure 16: Ion rejection for different CF, TS80 membrane

4.4 Membrane comparison

This part contains results obtained by flat sheets tests using NF and RO membranes and at a constant feed water composition, Table 7. The aim was to assess how the MWCO of the membranes influences the ion rejection and choose the most appropriate membrane for the treatment of the IEX spent regenerant. In addition, figures that depict each ion rejection by different membranes were created, in order to illustrate how the permeate flux and the CF influence the ion rejection.

4.4.1 Ca^{2+} rejection

Figure 17 shows the calcium rejection by different NF and RO membranes in different permeate fluxes. As can be seen, Ca^{2+} rejection varied depending on the MWCO of the membrane. RO membranes and tight NF90 (114 Da) rejected more than 95% of Ca^{2+}. TS80 (141 Da) rejected 90% of Ca^{2+} when the permeate flux was 30 LMH. The looser membrane (NFG) rejected less than 10% of calcium while the remaining of the membranes rejected 30-60% of calcium, depending on the MWCO, when the membrane flux was 30 LMH. Ca^{2+} rejection remained constant when the CF increased for all the membranes, Figure 18. In figure 19, the relationship between the MWCO and the Ca^{2+} rejection is depicted.

4.4.2 Mg^{2+} rejection

Mg^{2+} rejection was also influenced by the MWCO of the membrane. RO and tight NF membranes rejected more than 90% of Mg^{2+}, Figure 20. The membranes SR3D, NF270 and NFW rejected similar percentage of Mg^{2+}. The looser membrane (NFG) rejected less than 10% of Mg^{2+}. The Mg^{2+} in different CF is depicted in Figure 34. The Mg^{2+} rejection remained constant in different CF, as it can be seen in section A4.

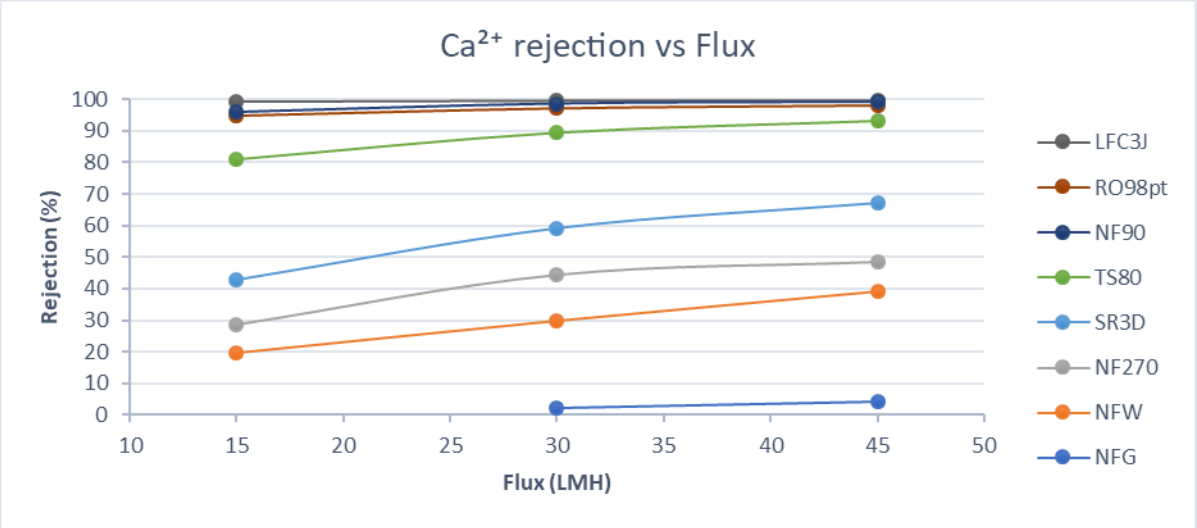

Figure 17: Ca^{2+} rejection for different fluxes

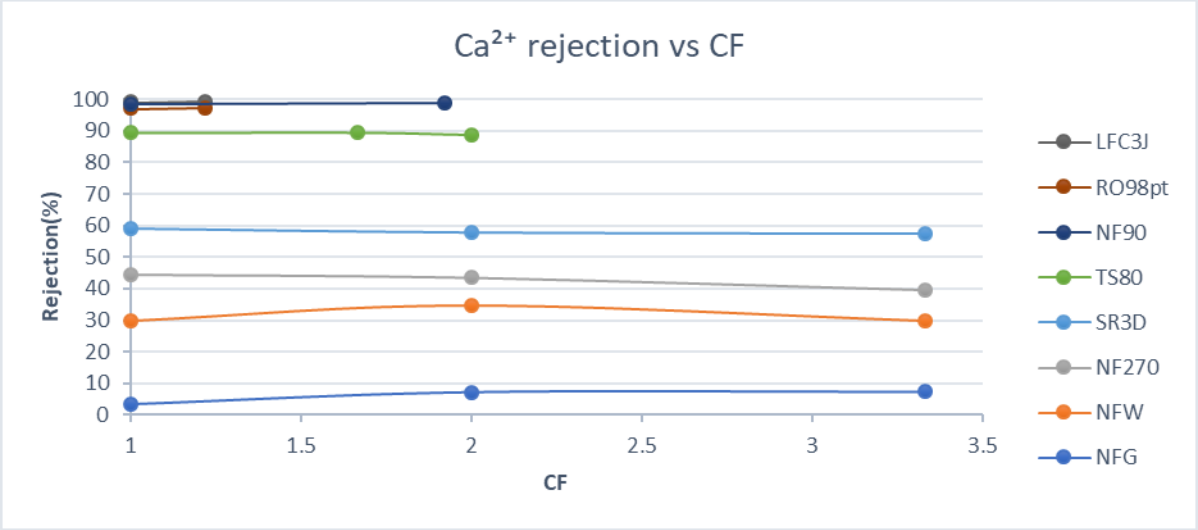

Figure 18: Ca^{2+} rejection for different CF

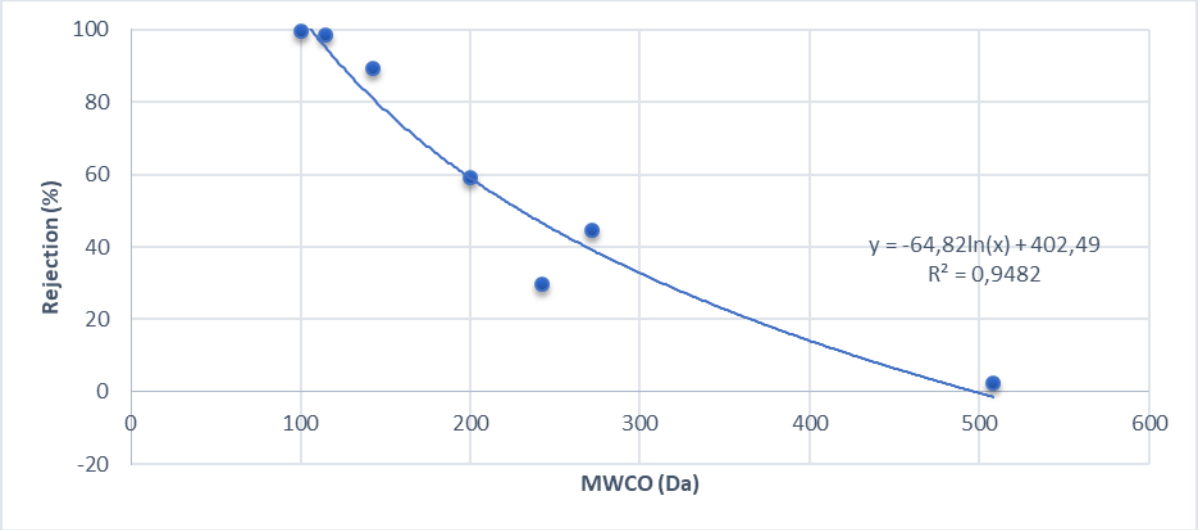

Figure 19: Ca^{2+} rejection vs MWCO

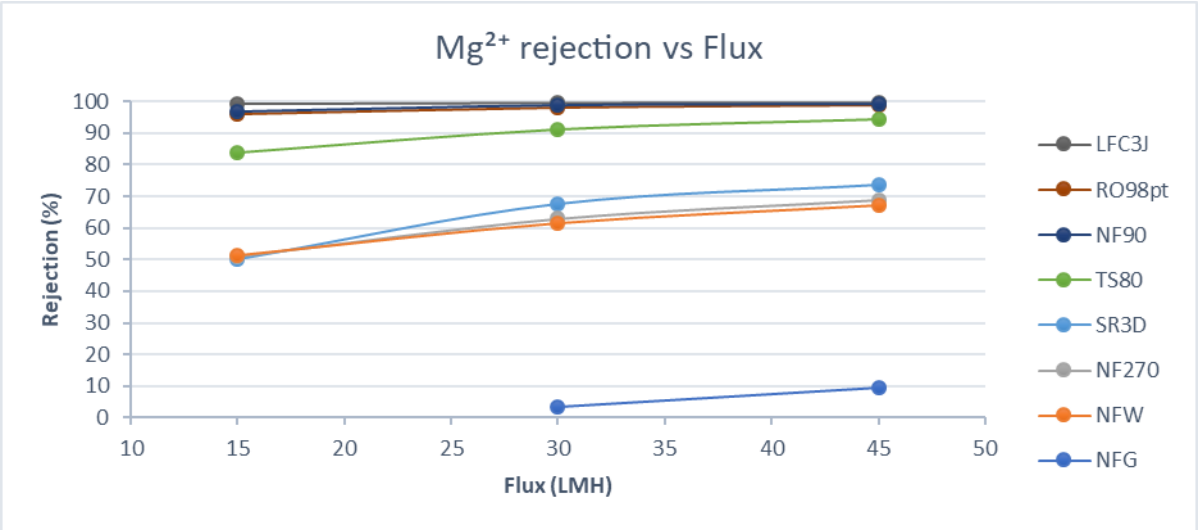

Figure 20: Mg^{2+} rejection for different fluxes

4.4.3 Na^+ rejection

Na^+ rejection in different fluxes is depicted in Figure 21. Na^+ was rejected more than 90% by the two RO membranes. The tightest NF membrane (NF90) rejected 80% of Na^+ for a permeate flux of 30 LMH, followed by TS80 membrane that rejected 40% of Na^+. Negative rejections were appeared for the looser membranes. Na^+ rejection decreased in higher CF, Figure 22, because of the presence of higher feed concentrations of Ca^{2+}, Mg^{2+} and Cl^- ions compared to Na^+ ions. The higher Cl^- flux through the membrane in higher CF, due to the concentration gradient, and the impermeability of divalent ions resulted in higher Na^+ flux through the membrane in order to keep the electroneutrality condition in the permeate side. Consequently, the rejection of Na^+ decreased in higher CF when the molar ratio of the solution was higher. Same trend was observed for the K^+ rejection, as it can be seen in section A4. It is also observed that the Na^+ rejection was more negative in tighter membranes such as NF270 than in looser membranes such as NFG. This can be explained by the fact that Cl^- permeation through NFG membrane resulted in both Ca^{2+} and Na^+ permeation. Ca^{2+} was not that impermeable to this membrane compared to NF270, where impermeability of divalent ions resulted in higher monovalent ion fluxes through the membrane, especially in higher CF.

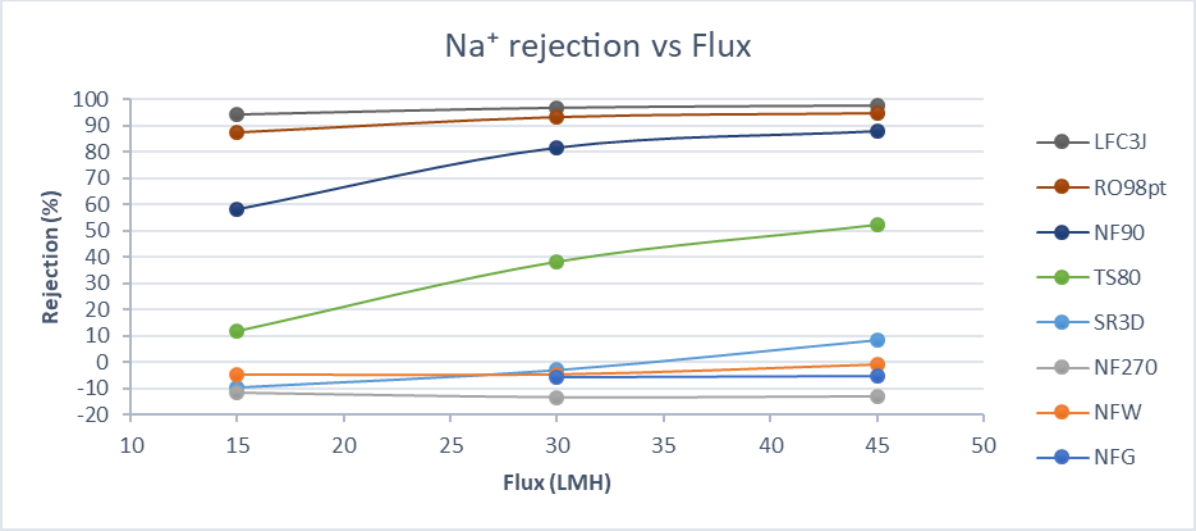

Figure 21: Na^+ rejection for different fluxes

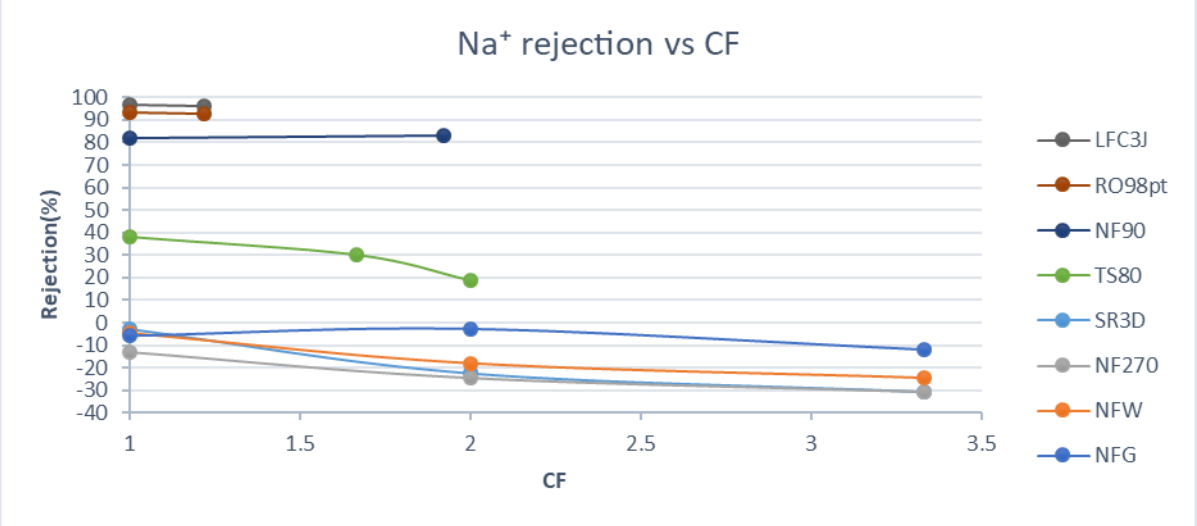

Figure 22: Na^+ rejection for different CF

4.4.4 Cl^- rejection

Cl^- rejection by different membranes is depicted in Figure 23. Tighter membranes rejected more Cl^- than looser membranes. This is explained by the high Ca^{2+} and Mg^{2+} rejections observed in tighter membranes. Cl^- was rejected to keep the electroneutrality on the feed side where divalent cations Ca^{2+} and Mg^{2+} were rejected. The Cl^- rejection in different CF is found in section A4.

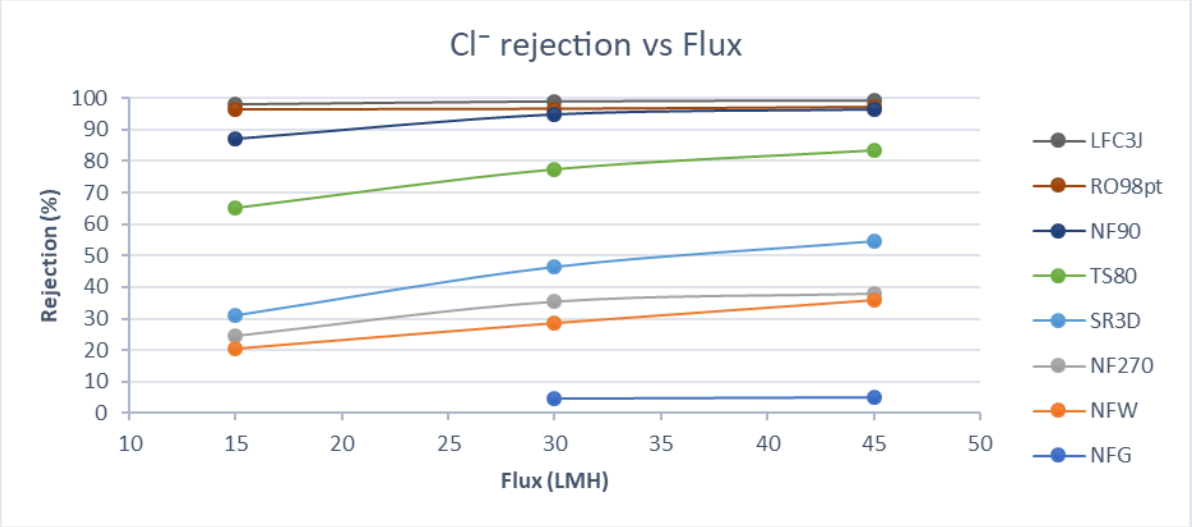

Figure 23: Cl^- rejection for different fluxes

4.4.5 Membrane selection

TS80 membrane performed better than the other tested membranes as it rejected 90% of Ca^{2+} and 40% of Na^+. The operating conditions are depicted in Figure 24. The permeate flux fluctuated from 28 LMH to 33 LMH. The applied feed pressure increased from 25.5 bars to 51.5 bars for a system recovery of 60%. The ion concentrations obtained in different concentration factors are depicted in Table 9. As it can be seen in Table 9, the permeate quality deteriorated with increasing CF. Diffusion transport mechanism became more dominant due to the higher concentration of the solute at the feed side when CF was increased.

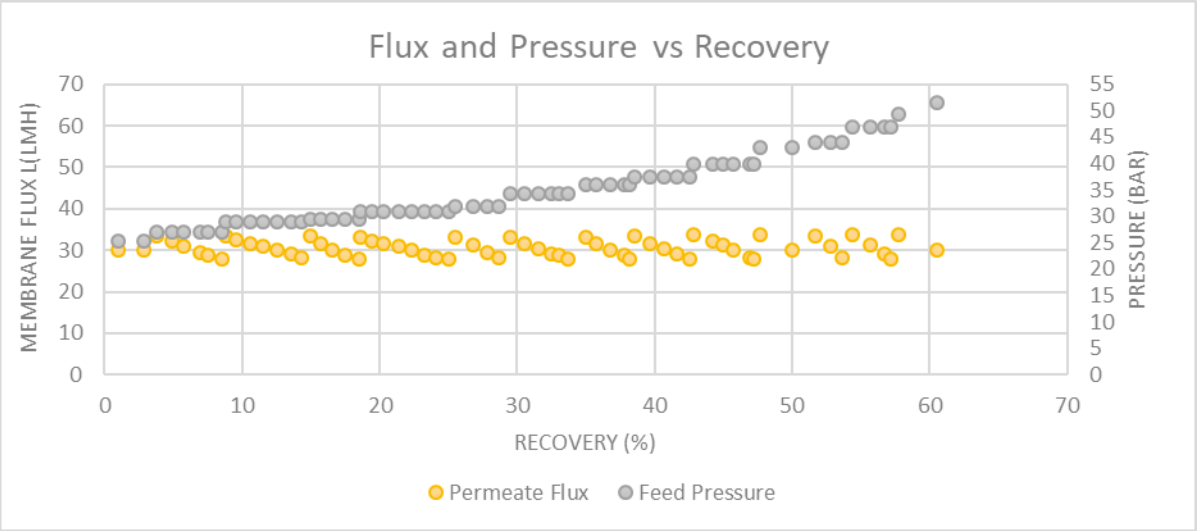

Figure 24: Membrane flux and feed pressure vs Recovery, TS80 membrane

Table 9: Rejections of different ions during TS80-lab test

Parameter	Unit	Feed water	Permeate mixture at				Concentrate
			CF 1	CF 1.43	CF 2	CF 2.5	CF 2.5
Calcium	mg/L	7800	829	1061	1206	1421	16705
Magnesium	mg/L	1693	150	197	218	261	3648
Sodium	mg/L	3266	2013	2126	2309	2675	4272
Chloride	mg/L	24278	5501	6179	6847	7800	47351

4.5 Water type comparison

4.5.1 Double pass NF

For the final aim of this study, NF permeate should be rich in NaCl but as poor as possible in Ca^{2+} and Mg^{2+} concentrations because divalent will compete with Na^{+} ions during the regeneration of the IEX resin. For this reason, a second pass NF was proposed to further treat the NF permeate of the first pass, Figure 25. The ion concentrations during the lab test are represented in Table 10. The flux was relatively constant and ranged between, 28 to 33 LMH and the feed pressure increased from 11.5 to 25 bars, Figure 26.

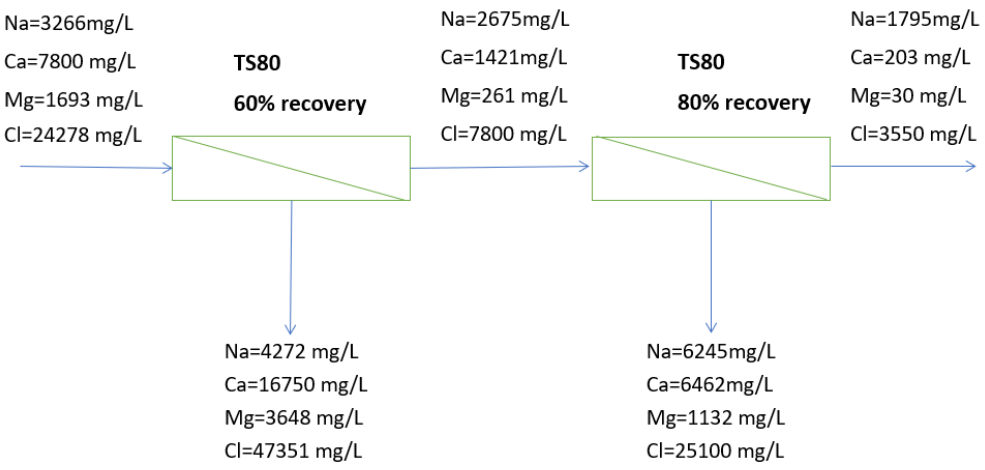

Figure 25: Double Pass NF, TS80 membrane

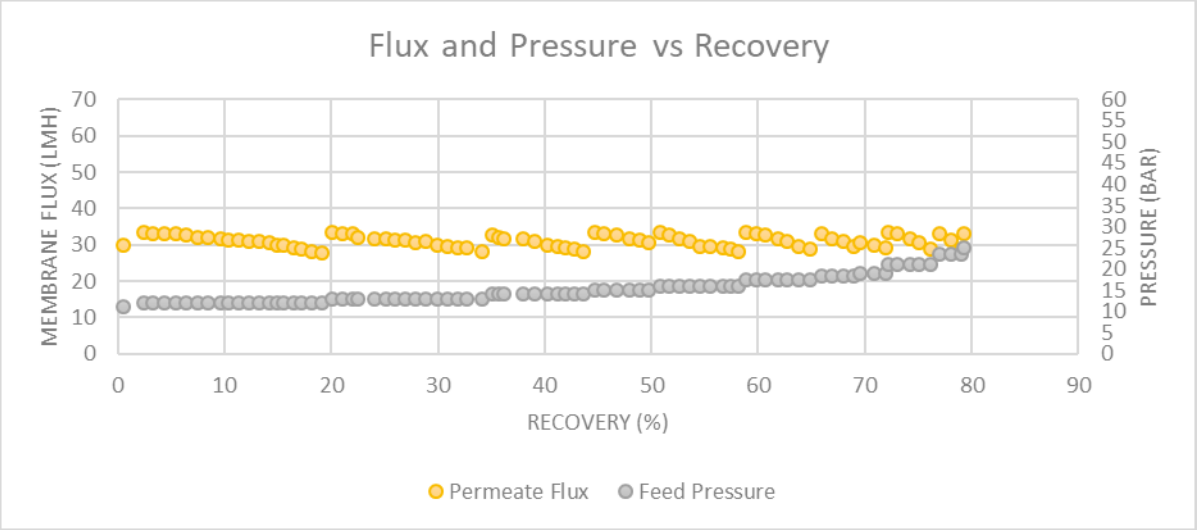

Figure 26: Membrane flux and feed pressure vs Recovery of the Second Pass NF, TS80 membrane

Table 10: Rejections of different ions during second pass TS80-lab test

Parameter	Unit	Feed water	Permeate mixture at				Concentrate
			CF 1	CF 2	CF 3.33	CF 5	FC 5
Calcium	mg/L	1421	143	160	185	203	6462
Magnesium	mg/L	261	23	25	28	30	1132
Sodium	mg/L	2675	1375	1514	1725	1795	6245
Chloride	mg/L	7800	2700	3000	3400	3550	25100

The rejections of the divalent cations of the second pass TS80 membrane were the same as the first pass TS80 membrane, Figure 27. However, the rejections of the monovalent cations were increased. Na^+ rejection increased by 27%. The molar ratio of this solution was 60% lower than the molar ratio of the initial solution. Lower Ca^{2+} and Mg^{2+} concentrations compared to Na^+ concentration explain the decrease in Na^+ rejection. In addition, Cl^- rejection was decreased by 15% due to the lower concentrations of Ca^{2+} in the feed side and therefore to the less need of Cl^- anions to keep the electroneutrality in the feed side.

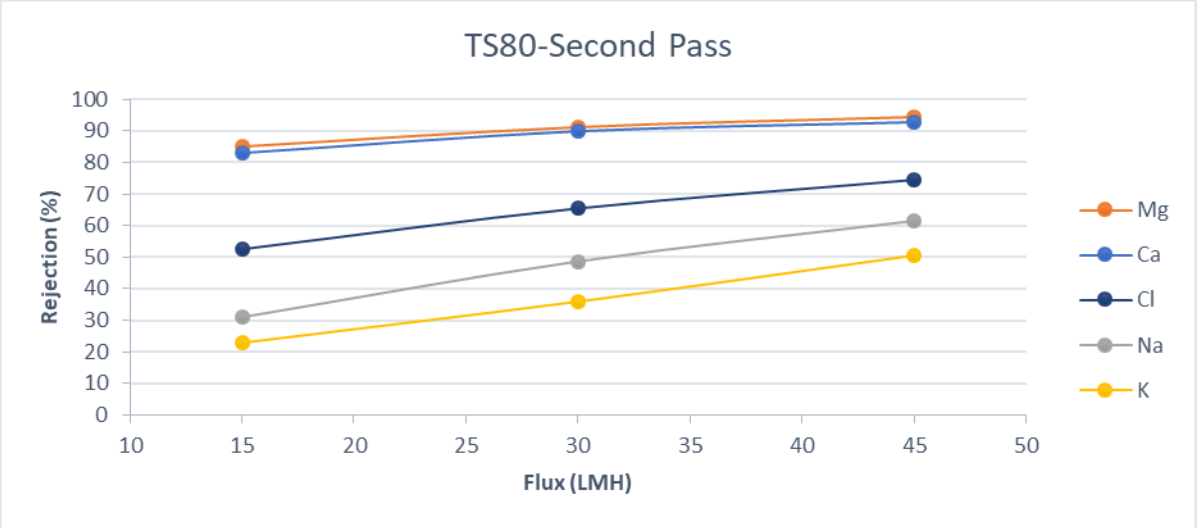

Figure 27: Ion rejection for different fluxes of the Second Pass NF, TS80

4.5.2 SO_4^{2-} addition

A small increase in the Ca^{2+} and Mg^{2+} rejection was observed when SO_4^{2-} was added, Figure 28. This can be explained by three factors. Firstly, another coupon of the flat sheet was used, and it might be that the MWCO of the membranes slightly differed. Assuming the MWCO of both membranes were the same, if SO_4^{2-} was present besides Cl^- in the feed phase, both ions were competing as counterions in the transport of the cations. Since SO_4^{2-} is larger compared to Cl^-, this resulted in a lower transport and thus a higher rejection. This behavior can be also explained by the presence of ion pairing of Ca^{2+} and SO_4^{2-} and thus to higher rejection due to the steric effect. It should be noted that $CaSO_4$ did not precipitate as the saturation index was not exceeded.

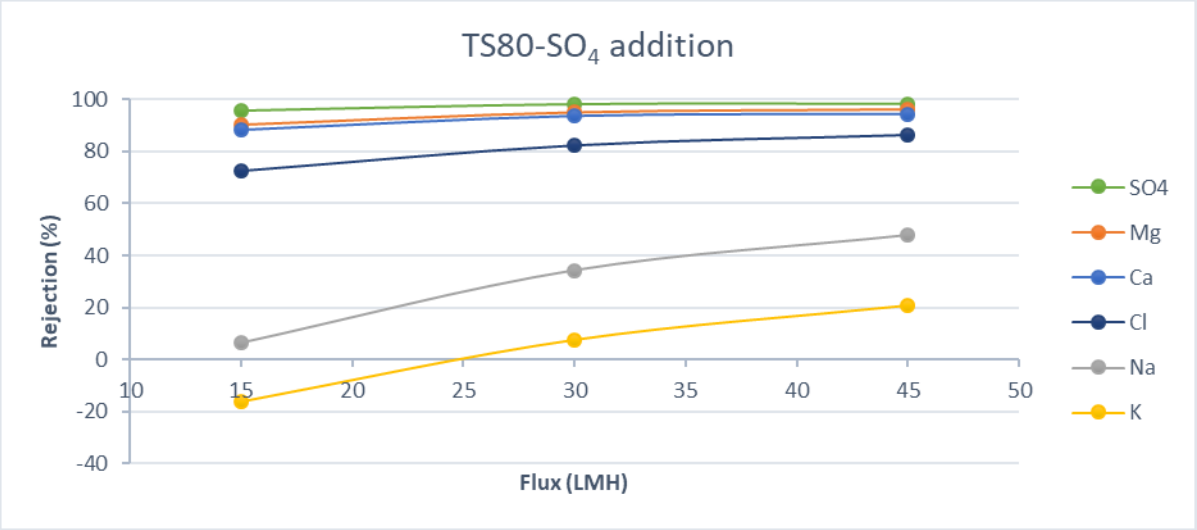

Figure 28: Ion rejection for different fluxes, TS80-SO_4 addition

4.6 Effect of Temperature on rejection

It is already demonstrated that the pore size of the membrane increases with an increase in temperature, [25]. In figure 29, the rejection of Ca^{2+}, Mg^{2+} and SO_4^{2-} in different temperatures is depicted. The CF was increased by a factor of 2. Based on the previous experiments, the rejection of divalent ions was expected to be constant in different CF, when the temperature was constant. Increased temperature resulted in lower rejections of Ca^{2+}, Mg^{2+} and SO_4^{2-}. Particularly, 5 degrees difference reduced the Ca^{2+} and Mg^{2+} rejection by 19%, Figure 29. Assumption 5 is proved.

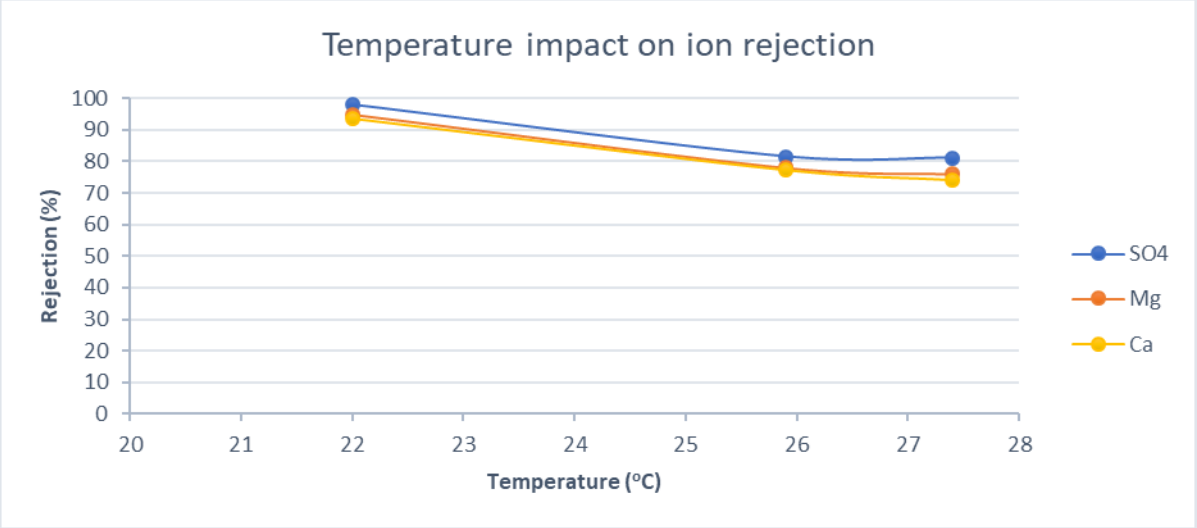

Figure 29: Temperature impact on ion rejection, TS80 membrane

5 *Conclusions*

The aim of this study was to investigate how ion rejection of the IEX spent regenerant is influenced by different membrane characteristics, by different operating parameters and by different ionic mixtures. It was concluded that the ion rejection of the IEX spent regenerant was mainly affected by the pore size of the membranes. Due to the high ionic strength of this stream, the Donnan exclusion mechanism did not influence the ion rejection. The steric and dielectric exclusion were the major rejection mechanisms. The ions found in the IEX spent regeneration stream were rejected due to their hydrated radius and their hydration free energy.

Loose membranes with MWCO greater than 500 Da rejected less than 10% of Ca^{2+} and Na^{+}. Membranes with pore size from 200 Da to 300 Da rejected 30-60% of Ca^{2+} and contributed to negative rejections of Na^{+}. NF membranes with MWCO of approximately 150 Da, rejected 90% of Ca^{2+} and 40% of Na^{+}. Tighter NF membranes with a pore size of 120 Da rejected 95% of Ca^{2+} and 80% of Na^{+}. Finally, RO membranes rejected more than 95% of both Na^{+} and Ca^{2+}.

The rejection of the divalent ion remained constant in different ionic strengths and molar ratios. Contrary, the rejection of monovalent cations was greatly influenced by the molar ratio of the solution due to the presence of predominant amounts of ion of higher charge of the same sign and the need of the ions to maintain electroneutrality. Higher molar ratio resulted in lower rejection of monovalent cations. Due to the high fluctuations of the ion composition in the IEX spent regeneant, it is predicted that the divalent cation rejection will remain approximately constant while the rejection of monovalent ions will fluctuate depending on the molar ratio of the solution.

The permeate flux also had a great effect on ion rejections. Higher fluxes resulted in higher ion rejection and different ion separation. Temperature also had a big effect on the ion rejection; higher temperature resulted in lower ion rejections. Since the pore size of the membrane was the dominant factor in the ion rejection of the IEX spent regenerant, it is concluded that temperature was also very crucial factor as a 5^{o}C increase of the temperature decreased the rejection of the divalent cations by 19%.

TS80 membrane performed better than other membranes as it rejected 90% of Ca^{2+} and 40% of Na^{+}. Double Pass NF with TS80 membrane was proposed as the first treatment step of the IEX spent regenerant stream as it resulted in 97% Ca^{2+} and 45% Na^{+} rejection.

6 *Recommendations*

Some relevant conclusions are made in this study regarding the ion separation of the IEX spent regenerant by Nanofiltration. However, still a few questions are raised leading to the following recommendations for further research.

- The zeta potential of the membranes should be measured to demonstrate that it is close to zero.
- Lab tests under different pH should be done to confirm that pH does not have a big impact on the ion rejection of the spent IEX regeneration stream.
- More lab tests with different membranes, under varying temperature are needed. For example, NF90 membrane in higher temperature can perform much better as the pore size will be bigger and reject much less Na^+. Through company networking, it is known that 95% rejection of bivalent ions (based on SO_4^{2-} removal) and 5% rejection of monovalent ions was achieved. RO and tight NF membranes were used and operated at very high temperatures (70-80 ^oC).
- The permeate stream that was produced after the NF Double Pass should be tested if it can regenerate the IEX resin, after the concentration step.
- Membrane filtration with a flux of 15 LMH is proposed as the TS80 First Pass as this offers better separation; 81% of Ca^{2+} and 12% of Na^+ rejection. The second pass could be with NF90 membrane that offers 96% Ca^{2+} rejection.
- A pilot unit is necessary to test the performance of spiral membranes due to the variations in temperature and ion composition.

7 *References*

[1] E. Vaudevire and E. Koreman, "Ion exchange brine treatment: closing the loop of NaCl use and reducing disposal towards a zero liquid discharge," 2014.

[2] M. Bevacqua, A. Cipollina, A. Tamburini, A. Brucato and G. Micale, "Magnesium recovery from exhausted brine," 2015.

[3] L. Wang, J. Chen, Y.-T. Hung and N. Shammas, Membrane and Desalination Technologies vol 13, 2011.

[4] M. Telzhensky, L. Birnhack, O. Lehmann, E. Windler and O. Lahav, "Selective separation of seawater Mg ions for use in downstream water treatment process," *Chemical Engineering Journal 175,* pp. 136-143, 2011.

[5] N. Fridman-Bishop, K. A. Tankus and V. Freger, "Permeation mechanism and interplay between ions in nanofiltration," *Journal of Membrane Science 548,* pp. 449-458, 2018.

[6] J. V. Nicolini, C. P. Borges and H. C. Ferraz, "Selective rejection of ions and correlation with surface properties of nanofiltration membranes," *Searation and Purification Technology 171,* pp. 238-247, 2016.

[7] S. Deon, A. Escoda, P. Fievet, P. Dutournie and P. Bourseau, "How to use a multi-ionic transport model to fully predict rejection of mineral salts by nanofiltration membranes," *Chemical engineering 189,* pp. 24-31, 2012.

[8] O. Labban, C. Liu, T. H. Chong and J. H. Lienhard V, "Fundamentals of low-pressure nanofiltration: Membrane characterization, modeling, and understanding the multi-ionic interactions in water softening," *Journal of Membrane Science 521,* pp. 18-32, 2017.

[9] W. R. Bowen and H. Mukhtar, "Charactarisation and prediction of separation performance of nanofiltration membranes," *Journal of Membrane Science 112,* pp. 263-274, 1996.

[10] W. Bowen and J. Welfoot, "Modelling the performance of membrane nanofiltration-critical assessment and model developement," *Chemica Engineering Science 57,* pp. 1121-1137, 2002.

[11] V. Geraldes and A. Alves, "Computer program for simulation of mass transport in nanofiltration membranes," *Journal of Membrane Science ,* pp. 172-182, 2008.

[12] V. Silva, V. Geraldes, A. B. Alves, L. Palacio, P. Pradanos and A. Hernandez, "Multi-ionic nanofiltration of highly concentrated salt mixtures in the seawater range," *Dealination 277,* pp. 29-39, 2011.

[13] J. Luo and Y. Wan, "Effects on pH and salt on nanofiltration-a critical review," *Journa of Membrane Science 438,* pp. 18-28, 2013.

[14] Y. Roy, M. Sharqawy and J. Lienhard V, "Modeling flat-sheet and spiral-wound nanofiltration configurations and its application in seawater nanofiltration," *Journal of Membrane Science 493,* pp. 360-372, 2015.

[15] R. Yagnasemi, D. M. Warsinger and J. H. Lienhard, "Effect of temperature on ion transport in nanofiltration membranes: Diffusion, convection and electromigration," *Desalination 420,* pp. 241-257, 2017.

[16] B. Tansel, J. Sager, T. Rector, J. Garland, R. Strayer, L. Levine, M. Roberts, M. Hummerick and J. Bauer, "Significance of hydrated radius and hydration shells on ionic permeability during nanofiltration in dead end and cross flow modes," *Separation and Purification Technology 51,* pp. 40-47, 2006.

[17] M. R. Teixera, M. J. Rosa and M. Nystrom, "The role of membrane charge on nanofiltration performance," *Journal of Membrane Science 265,* pp. 160-166, 2005.

[18] J. Havel and E. Hogfeldt, "Evaluation of water sorption equillibrium data on Dowex ion exchanger using WSLET-MINUIT program," *Sript Fac. Sci. Nat. Masaryk. Brun., Chem. 25,* pp. 73-84, 1995.

[19] A. Volkov , S. Paula and D. Deamer, "Two mechanisms of permeation of small neutral molecules and hydrates ions across phospholipid bilayers," *Bioelectrochem Bionerg 42 ,* pp. 153-160, 1997.

[20] H. Binder and O. Zschorning , "The effect of metal cations on the phase behavior and hydration characteristics of phosholipid membranes," *Chem. Phys. Lipids 115,* pp. 39-61, 2002.

[21] A. Escoda, Y. Lanteri, P. Fievet, S. Deon and A. Szymczyk, "Determining the Dielectric constant inside Pores of Nanofiltration Membranes from Membrane Potential Meausrements," *LANGMUIR,* pp. 14628-14635, 2010.

[22] S. Bason, Y. Oren and V. Freger, "Ion transport in the polyamide layer of RO membranes: Composite membranes and free-standing films," *Journal of Membrane Science,* no. 367, 2011.

[23] Sanitary Engineering Departement, TU Delft, Drinking water treatment, Delft: TU Delft, 2009.

[24] T. Luxbacher, B. Coday and T. Cath, "Does the surface zeta potential approach zero at high salinity?," in *Advances in Civil, Environmental, and Materials Research (ACEM14)*, 2014.

[25] N. B. Amar, H. Saidani, A. Deratani and J. Palmeri, "Effect of temperature on the transport of water and neutral solutes across nanofiltration membranes," *Langmuir 2007,* pp. 2937-2952, 2006.

[26] H. Chen and E. Ruckenstein, "Hydrated ions: From Individual Ions to Ion Pairs to Ion clusters," *The journal of Physical chemistry,* 2015.

[27] L. Fumagalli, A. Esfandiar, R. Fabregas, S. Hu, P. Ares, A. Janardanan, Q. Yang, . B. Radha, . T. Taniguchi, K. Watanabe, G. Gomila, K. S. Novoselov and A. K. Geim, "Anomalously low dielectric constant of confined water," *Science 360, 1339-1342,* 2018.

[28] B. Averill and P. Eldredge, General Chemisty: Principles, Patterns, and Applications, Boston: FlatWord, 2011.

[29] R. Shang, A. Goulas, C. Y. Tang, F. S. Xavier, L. C. Rietveld and S. G. Heijman, "Atmospheric pressure atomic layer deposition for tight ceramic nanofiltration membranes: Synthesis and application in water purification," *Journal of Membrane Science 528,* pp. 163-170, 2017.

[30] B. V. Bruggen and C. Vandecasteele, "Modelling of the retention of uncharged molecules with nanofiltration," *Water Research 36,* pp. 1360-1368, 2002.

[31] T. Jiricek, W. De Schepper, T. Lederer, P. Cauwenberg and I. Genne, "Recovery of salts from ion-exchange regeneration streams by a coupled nanofiltration-membrane distillation process," *Water Science & Technology,* 2015.

[32] M. Reig, S. Casas, O. Gibert, C. Valderrama and J. Cortina, "Integration of nanofiltration and bipolar electrodialysis for valorization of seawater desalination brines: Production of drinking and waste water treatment chemicals," *Desalination 382,* pp. 13-20, 2016.

[33] W. Bowen and J. Welfoot, "Modelling of membrane nanofiltration-pore size distribution effects," *Chemical Engineering Science 57,* pp. 1381-1407, 2002.

[34] A. Szymczyk, M. Sbai, P. Fievet and A. Vidonne, "Transport properties and electrokinetic characterization of an amphoteric nanofliter," *Langmuir 22,* pp. 3910-3919, 2006.

[35] S. Bandini and D. Vezzani, "Nanofiltration modeling: the role of dielectric exlusion in membrane characterization," *Chemical Engineering Science 58,* pp. 3303-3326, 2003.

[36] N. Hilal, H. Al-Zoubi, N. A. Darwish and A. W. Mohammad, "Performance of Nanofiltration Membranes in the Treatment of Synthetic and Real Seawater," *Separation Science and Technology 42,* pp. 493-515, 2007.

[37] J. Liu, J. Yuan, Z. Ji, B. Wang, Y. Hao and X. Guo, "Concnetration brine from seawater desalination process by nanofiltration-electrodialysis integrated membrane technology," *Desalination,* pp. 53-61, 2016.

[38] V. Freger, "Sweling and morphology of the skin layer of polyamide composite membranes: an atomic force microscopy study," *Envrironment Science Technology 38,* pp. 3168-3175, 2004.

[39] J. Tanninen, M. Manttari and M. Nystrom, "Effect of salt mixture concentration on fractionation with NF membranes," *Journal of Membranes Science 283,* pp. 57-64, 2006.

[40] M. Elimelech, W. Chen and J. Waypa, "Measuring the zeta (electrokinetic) potential of reverse osmosis membranes by a streaming potential analyzer," *Desalination 95,* pp. 269-286, 1994.

[41] S. Deon, A. Escoda, P. Fievet and R. Salut, "Prediction of single salt rejection by NF membranes: An experimental methodology to assess physical parameters from membrane and streaming potentials," *Desalination 315,* pp. 37-45, 2013.

[42] Q. Nan, P. Li and B. Cao, "Fabrication of positively charged nanofiltation membrane via the layer-by-layer assembly of graphene oxide and polyethylenimine for desalination," *Applided Surface Science 387,* pp. 521-528, 2016.

[43] S. Cheng, D. L. Oatley, P. M. Williams and C. J. Wright, "Positively charged nanofiltration membranes: Review of current fabrication methods and introduction of a novel approach," *Advances in Colloid and Interface Science 164,* pp. 12-20, 2011.

[44] S. Deon, P. Dutournie, L. Limousy and P. Bourseau, "Transport of salt mixtures through nanofiltration membranes: numerical identification of electric and dielectric contributions," *Separation Purificion and Technology 69,* pp. 225-233, 2009.

[45] M. Manttari, A. Pihlajamaki and M. Nystrom, "Effect of pH on hydrophilicity and charge and their effect on the filtration efficiency of NF membranes at different pH," *Journal of Membrane Science 280,* pp. 311-320, 2006.

[46] S. Szoke, G. Patzay and L. Weiser, "Characteristics of thin-film nanofiltratin membranes at various pH-values," *Desalination 151,* pp. 123-129, 2002.

[47] J. Ceulemans, P. Cauwenberg, J. Dijkstra, H. Weijdema and B. Oostvogels, "Reuse of NaCl for regneration of softening resin by combining nanonfiltration and membrane distilation," *1st IWA Resource Recovery Conference,* 2015.

[48] M. Saifuzzaman, "Water for pharmaceutical use," Water Purification Engineering, 2014. [Online]. Available: http://slideplayer.com/slide/1678319/. [Accessed 8 10 2018].

A. Appendix

The appendix is divided in six parts. The first part includes the description of the IEX principle and the sampling process during IEX regeneration. The second part includes the concentration polarization experiment. The third part contains the pure water permeability test of the different membranes. The fourth part contains the comparison of ion rejection by different membranes. The fifth part contains the Sepa Cell experiments for each membrane. For each membrane the ion rejection in different fluxes and concentration factors (CF) is depicted. In addition, the ion concentration in the permeate and the concentrate stream is reported. Finally, the operating conditions such as the applied feed pressure and the recorded flux and feed EC for each system recovery are described. The last part of the appendix includes the HPLC results for the measurement of the MWCO of the membranes.

A.1 Ion exchange

Ion exchange principle

Ion exchange is the displacement of one ion by another. Ion exchange columns are used in industries as treatment steps to produce drinking or industrial process water. Cation and anion exchange resin is used as exchange material. Ion exchange resins constitute insoluble granular substances and have in their molecular structure acid or basic radicals, Figure 30. Positive or negative ions fixed on these radicals are replaced by ions with the same sign that are found in the solution that is in contact with the resin. Na^+ or H^+ ions are used in case of cationic exchange resin and Cl^- or OH^- are used in case of anionic exchange resin.

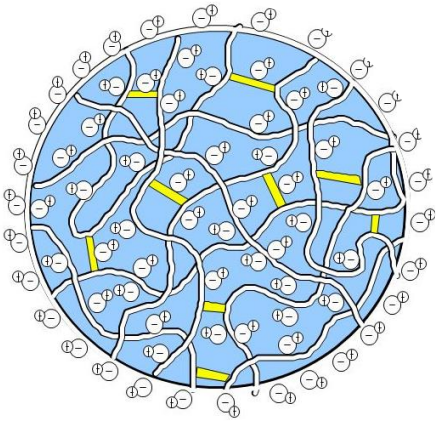

Figure 30: Ion exchange resin [48]

Regeneration of cation exchange column

When the capacity of the cationic exchange resin is exhausted, the exchanger should be regenerated by the reverse reaction so that the Na^+ ions will replace again the divalent cations (Mg^{2+}, Ca^{2+}, Ba^{2+} etc.) that have occupied the acidic radicals. The resin found in EVIDES site is regenerated by NaCl. During the regeneration process a highly concentrated stream of Na^+, Ca^{2+}, Mg^{2+}, Cl^- ions is produced.

Sample collection

High fluctuations of the ion compositions are observed during regeneration. For this reason, several samples are necessary to be taken during different steps of the IEX regeneration, to better characterize the IEX spent regenerant. The steps during the regeneration cycle of EVIDES IEX reactors

are showed in Figure 31. During the injection step, softened water with 9% NaCl is injected with an upward flow of 100 m^3/h for 12 min. Afterwards, softened water washes out the resin with an upward flow of 160 m^3/h for 23 min. Finally, the flow is reversed and for 15 minutes softened water is rinsing the IEX resin until the EC of the water is lower than 750 µS/cm. The IEX regeneration curve is depicted in Figure 32.

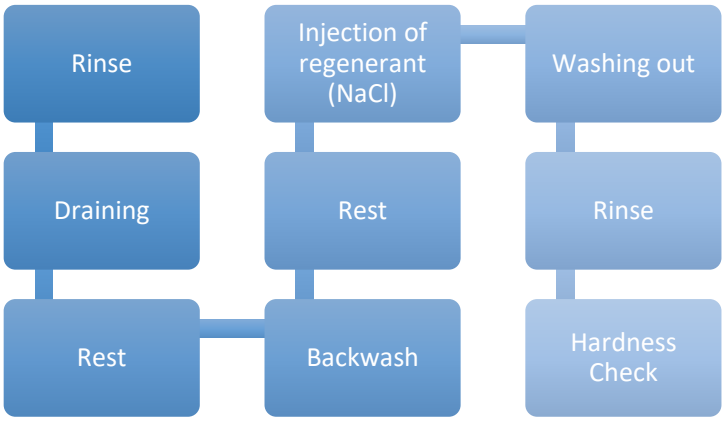

Figure 31: Regeneration cycle

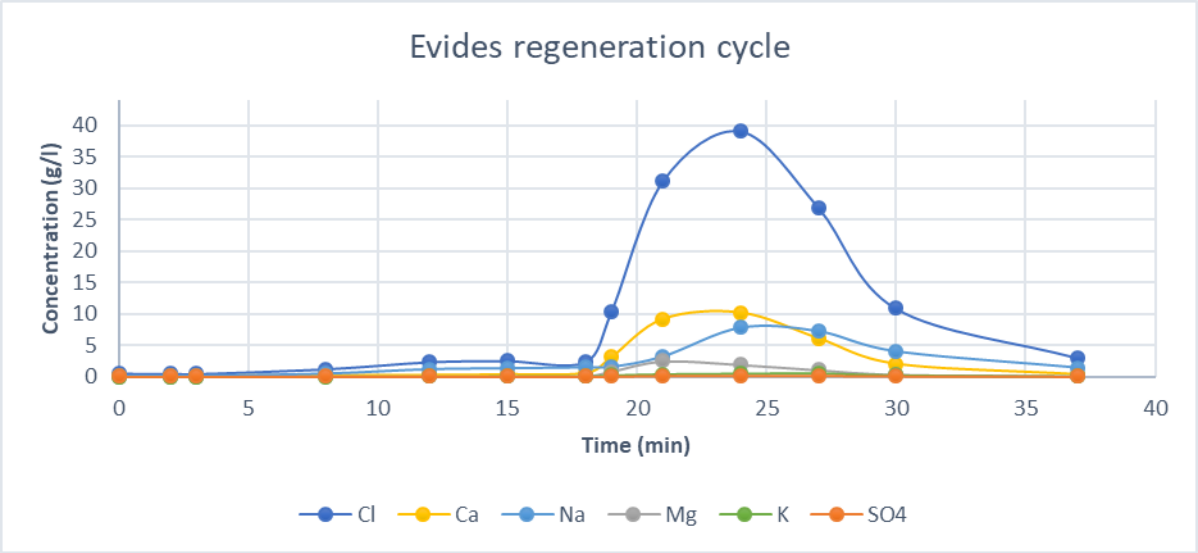

Figure 32: IEX regeneration cycle

Currently, softened water is used to regenerate the IEX resin. SO_4^{2-} that is found in the softened water in a concentration of almost 60 mg/L ends up in the IEX spent regenerant. During nanofiltration $CaSO_4$ and $BaSO_4$ can scale the membranes and reduce the recovery. In addition, SO_4^{2-}, that will be retained by the NF membrane and will end to the concentrate stream, will interfere with the $Ca(OH)_2$ and $Mg(OH)_2$ recovery. For these reasons, it is decided that the regeneration of the IEX will be done with demi water. For the filtration of the IEX spent regeneration stream by nano-membranes, the most concentrated part is better to be treated; time step 18 min to time step 35 min.

A.2 CP experiment

Table 11: CP experiment results

	Test with demi water	**Test with MgSO4**
Feed pressure (bar)	3	3
Concentrate pressure (bar)	3	3
TMP (Pascal)	300000	300000
Flow (L/h)	0.51	0.3
Flux (m/s)	1.0119E-05	5.95238E-06
μ	0.001005857	-
kw	**3.39277E-14**	-
Δπ (bar)	-	1.24
EC feed water (μS/cm)	-	5210.00
EC permeate (μS/cm)	-	1642.00
πfeed (bar)	-	1.55
πpermeate (bar)	-	0.49
πmembrane (bar)	-	1.72
CP	-	**1.11**

A.3 Permeability of the membranes

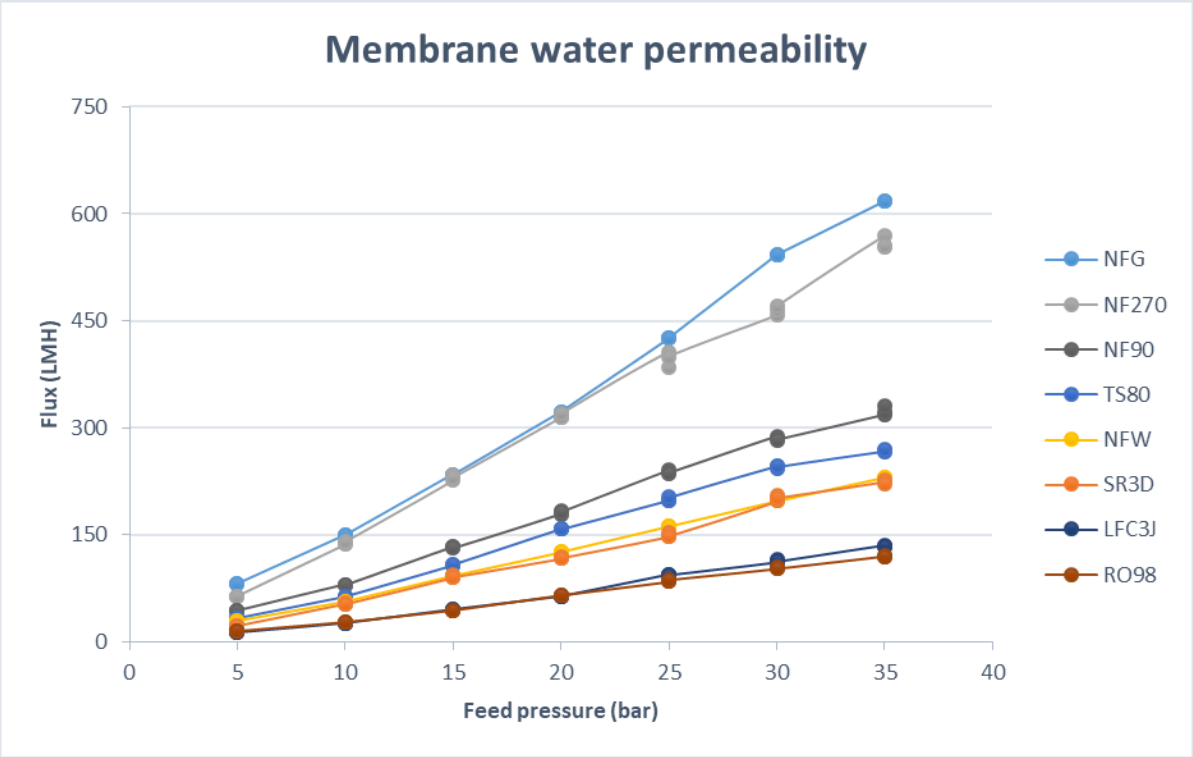

Figure 33: Pure water permeability of different membranes

A.4 Ion rejection by different membranes

Mg^{2+} rejection

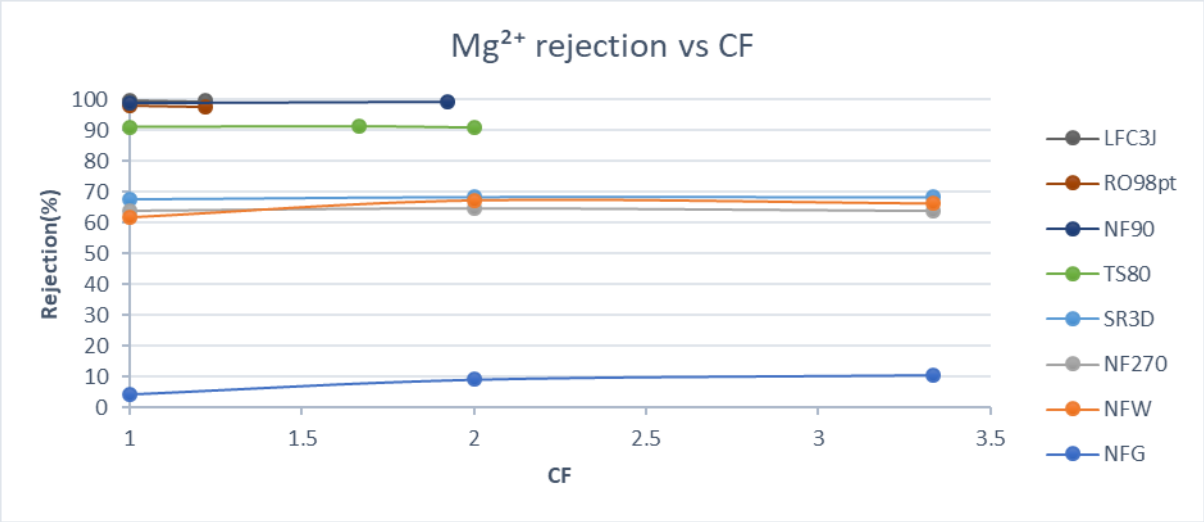

Figure 34: Mg rejection for different CF

Cl^- rejection

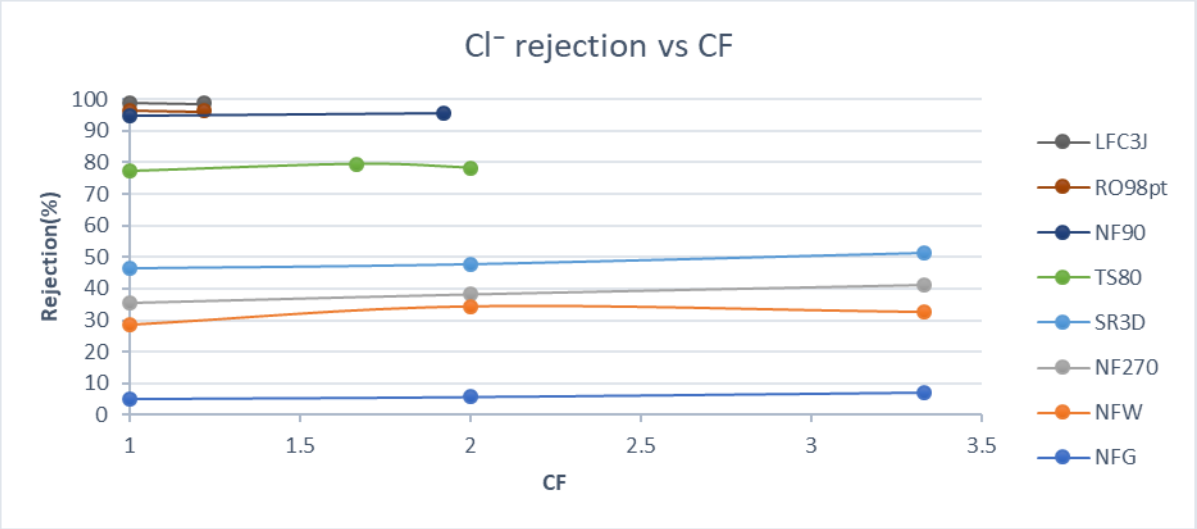

Figure 35: Cl rejection for different CF

K^+ rejection

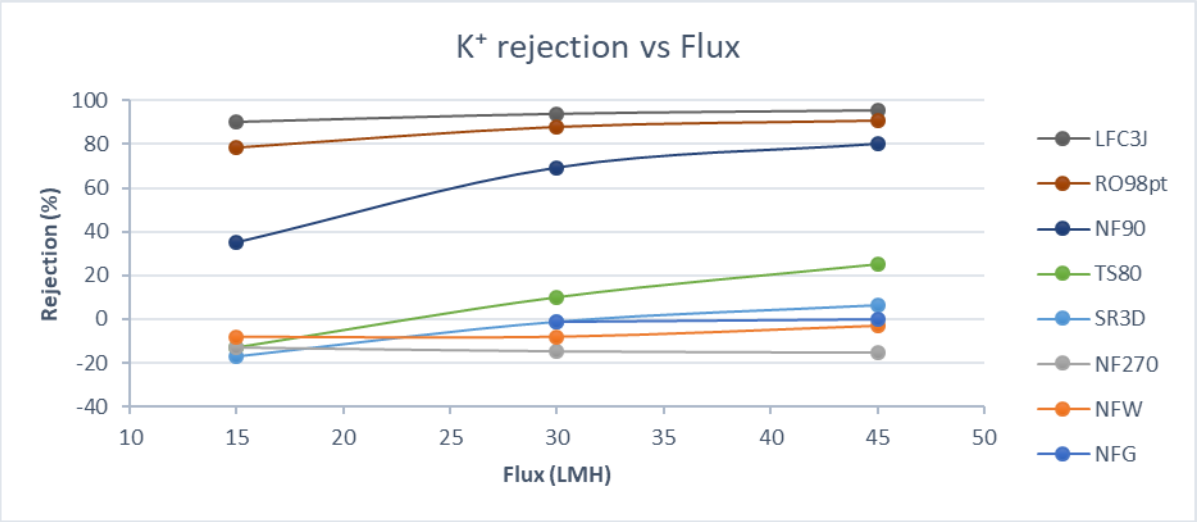

Figure 36: K rejection for different fluxes

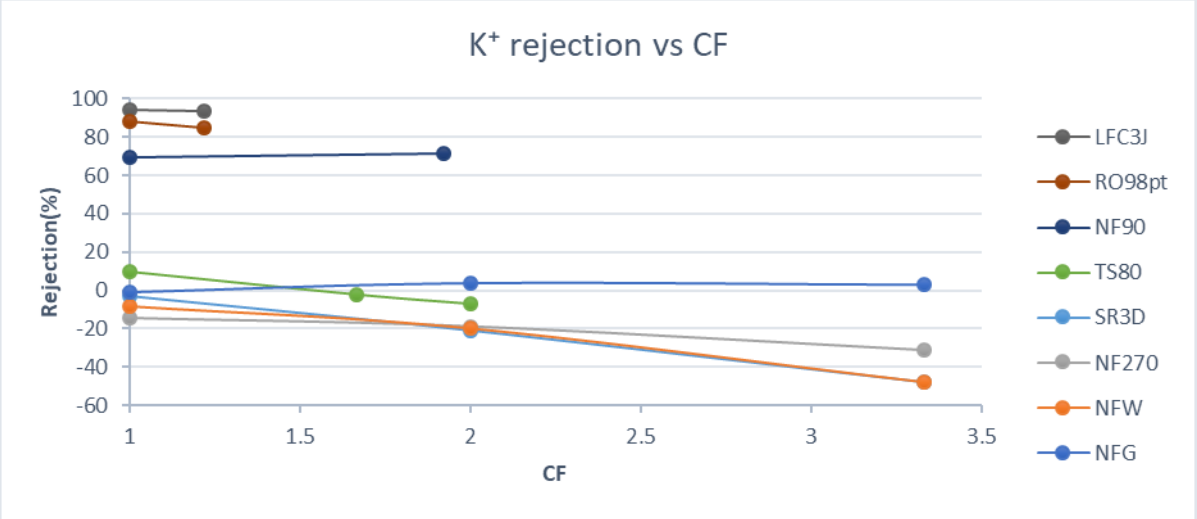

Figure 37: K rejection for different CF

Ba^{2+} rejection

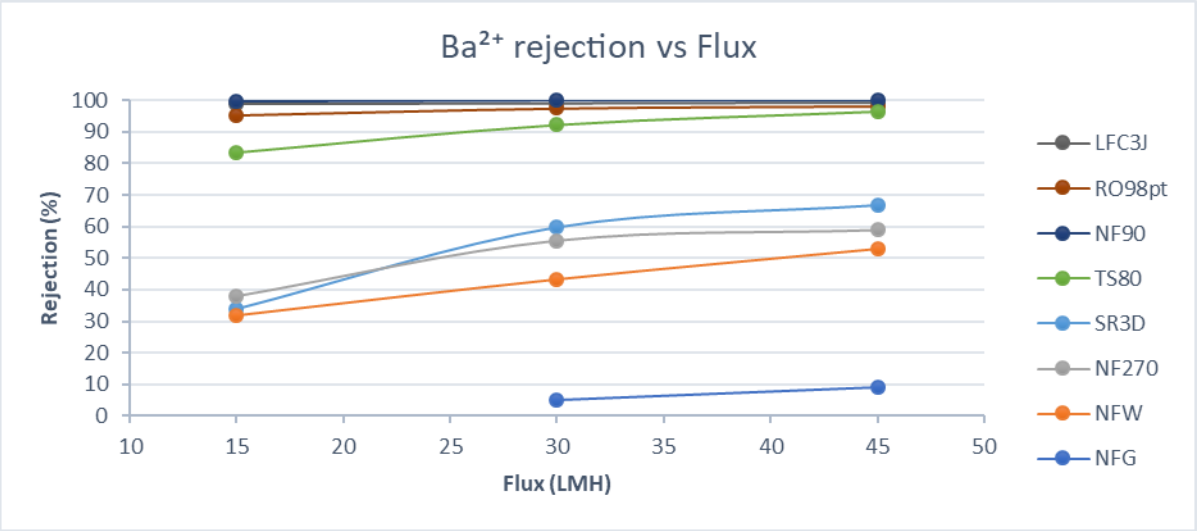

Figure 38: Ba rejection for different fluxes

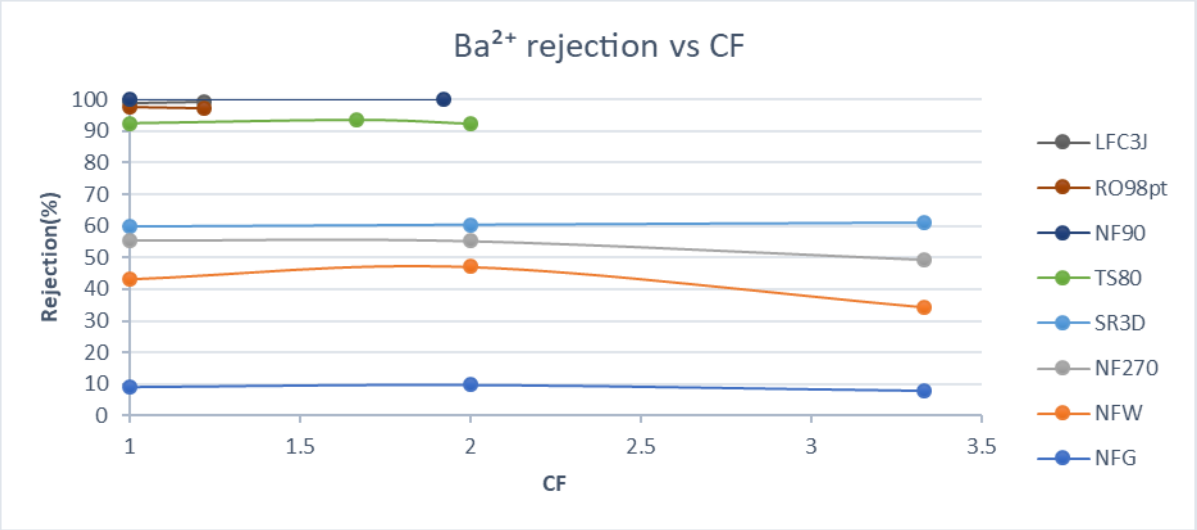

Figure 39: Ba rejection for different CF

Sr^{2+} rejection

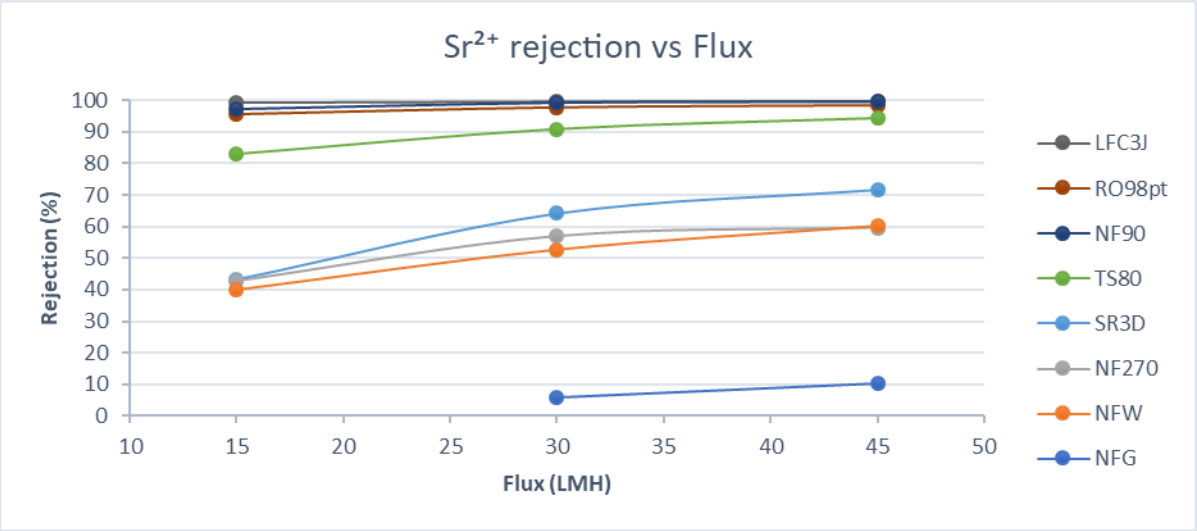

Figure 40: Sr rejection for different fluxes

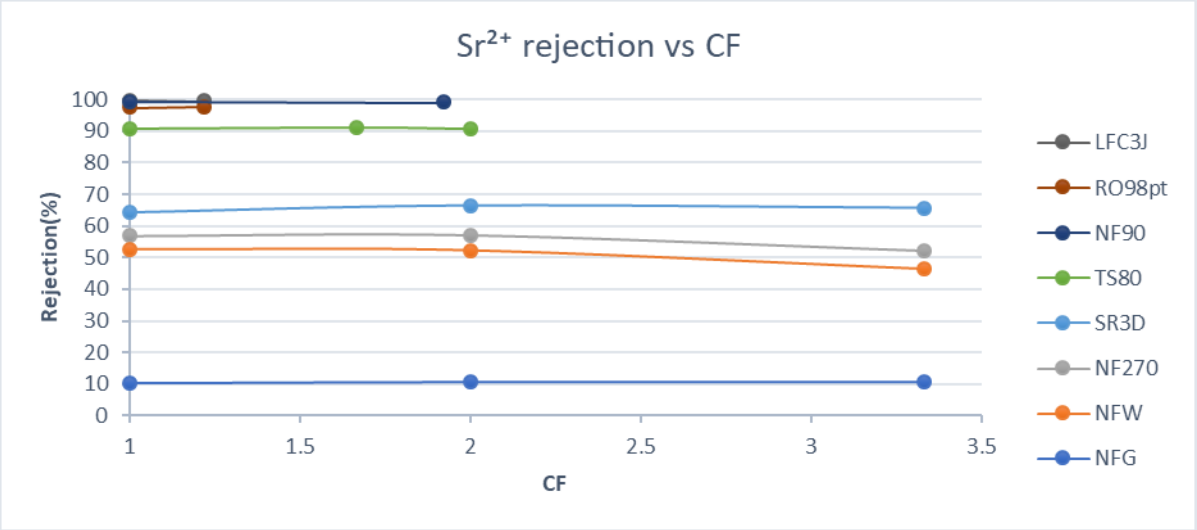

Figure 41: Sr rejection for different CF

A.5 Sepa Cell Experiments

NFG Membrane

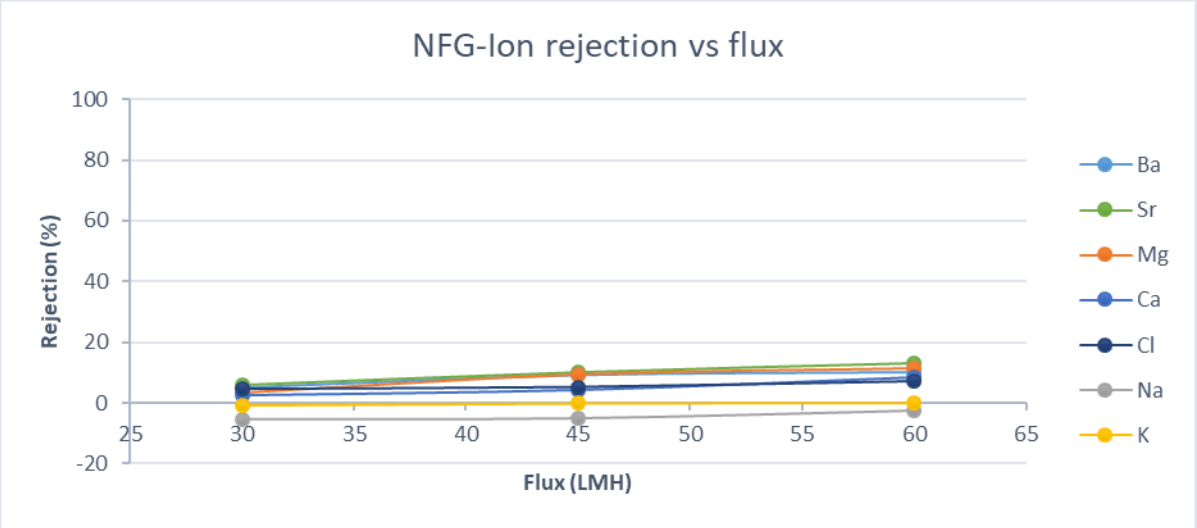

Figure 42: NFG-Ion rejection vs flux

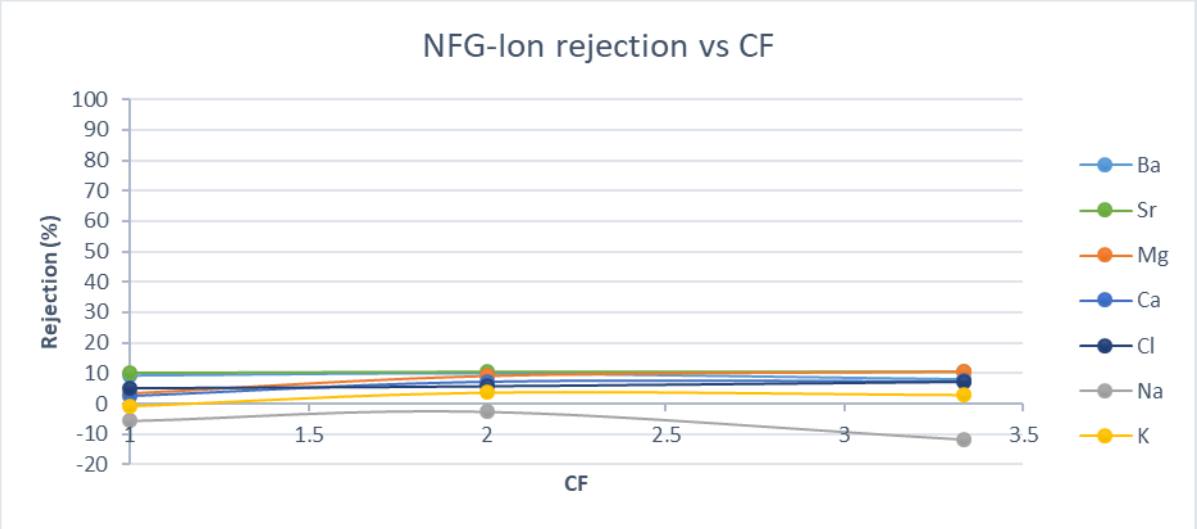

Figure 43: NFG-Ion rejection vs CF

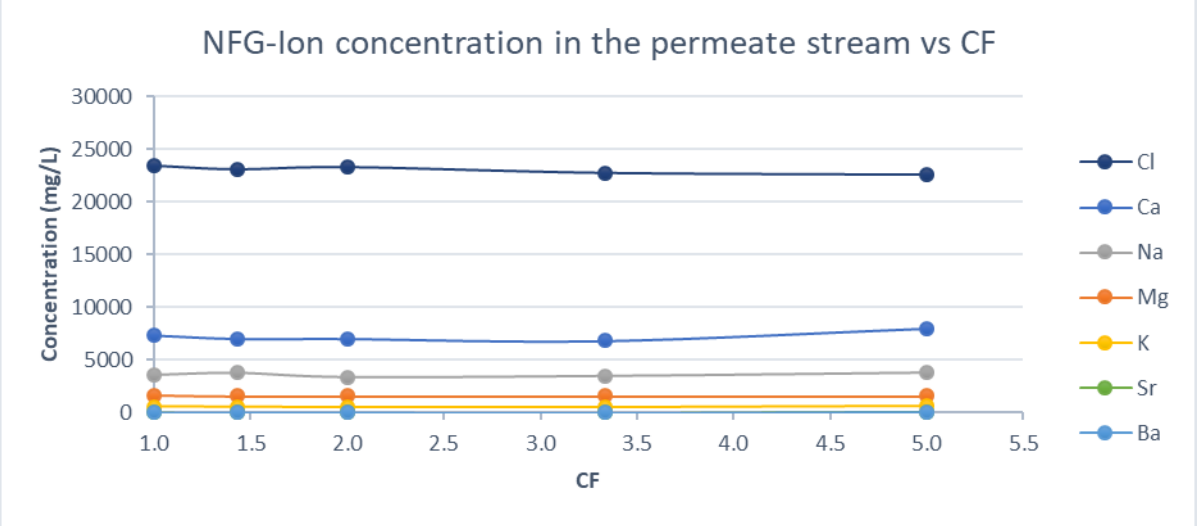

Figure 44: NFG-Ion concentration in the permeate stream vs CF

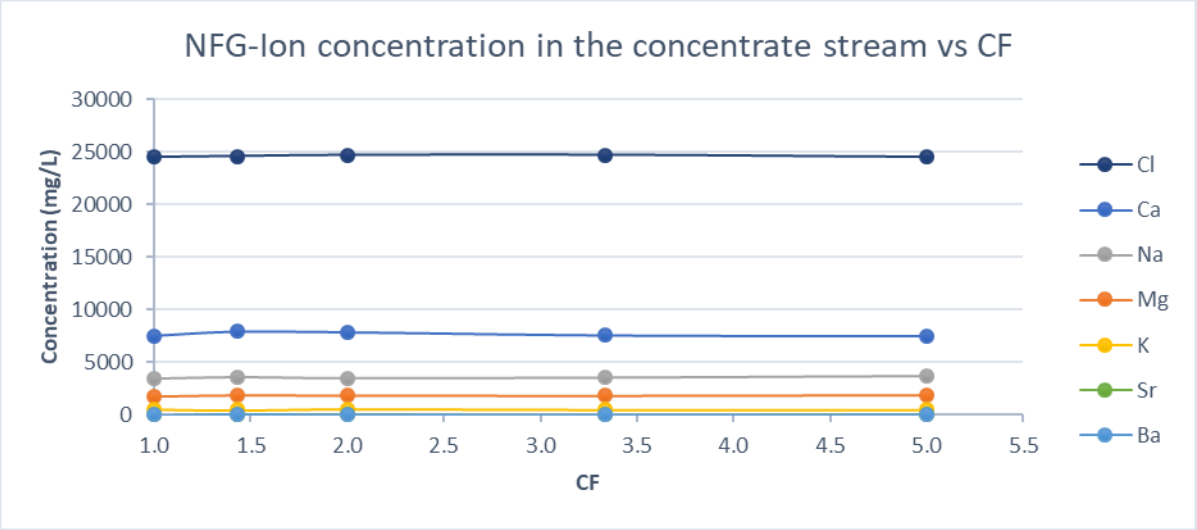

Figure 45: NFG-Ion concentration in the concentrate stream vs CF

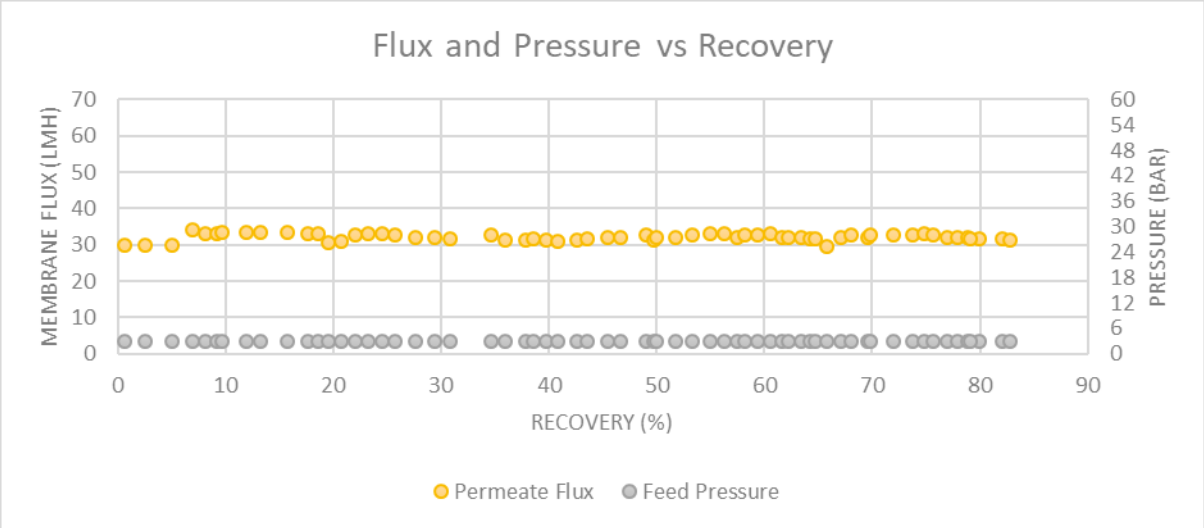

Figure 46: NFG- Flux and pressure vs recovery

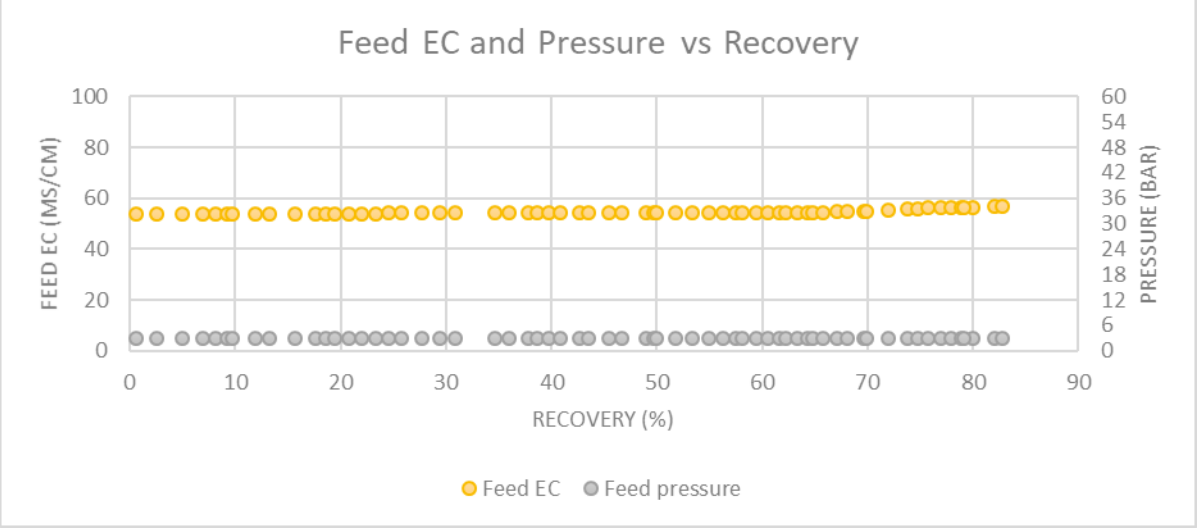

Figure 47: NFG-Feed EC and pressure vs Recovery

NFW Membrane

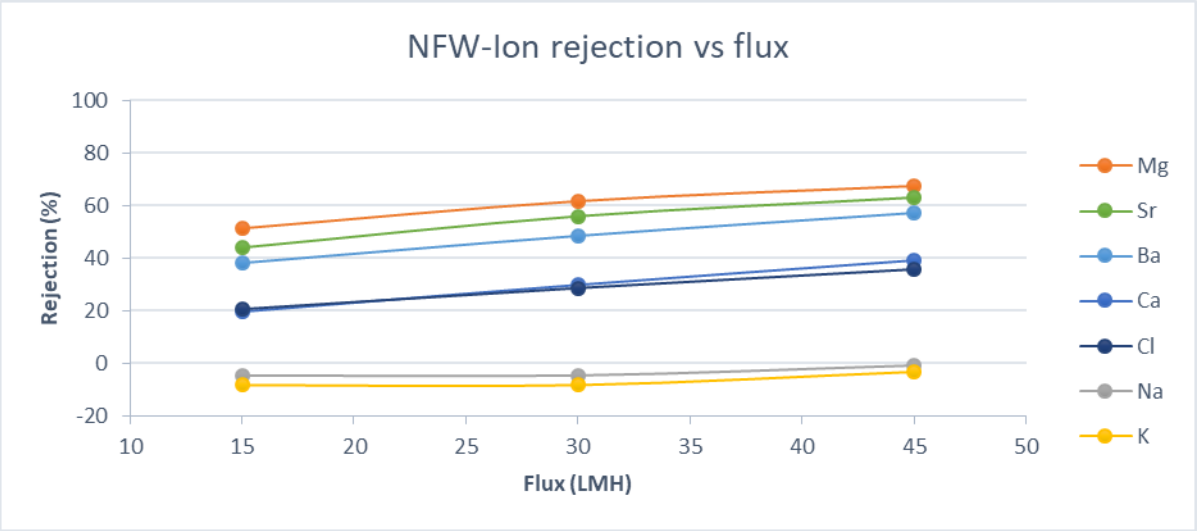

Figure 48: NFW-Ion rejection vs flux

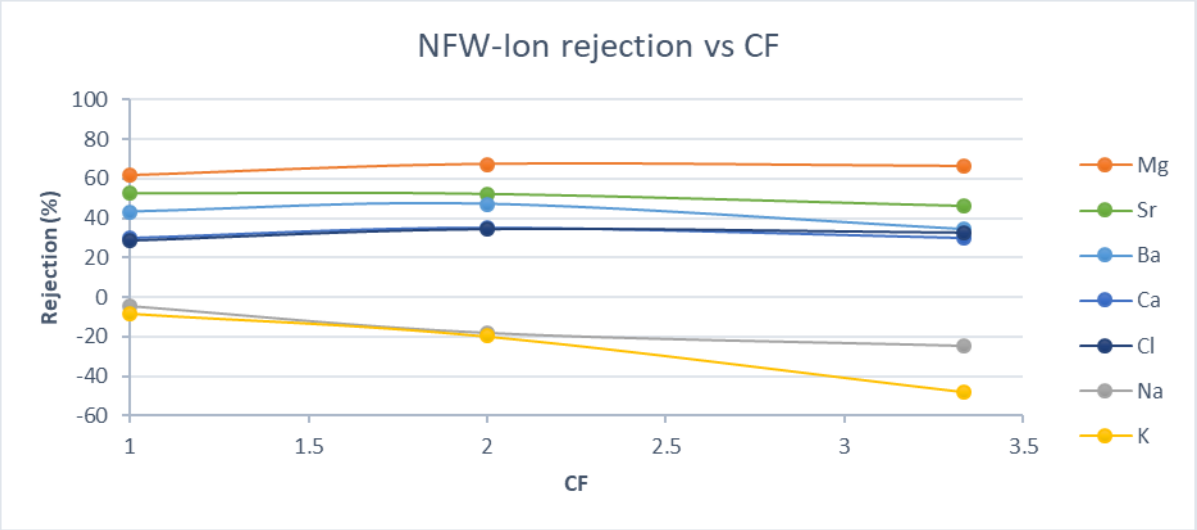

Figure 49: NFW-Ion rejection vs CF

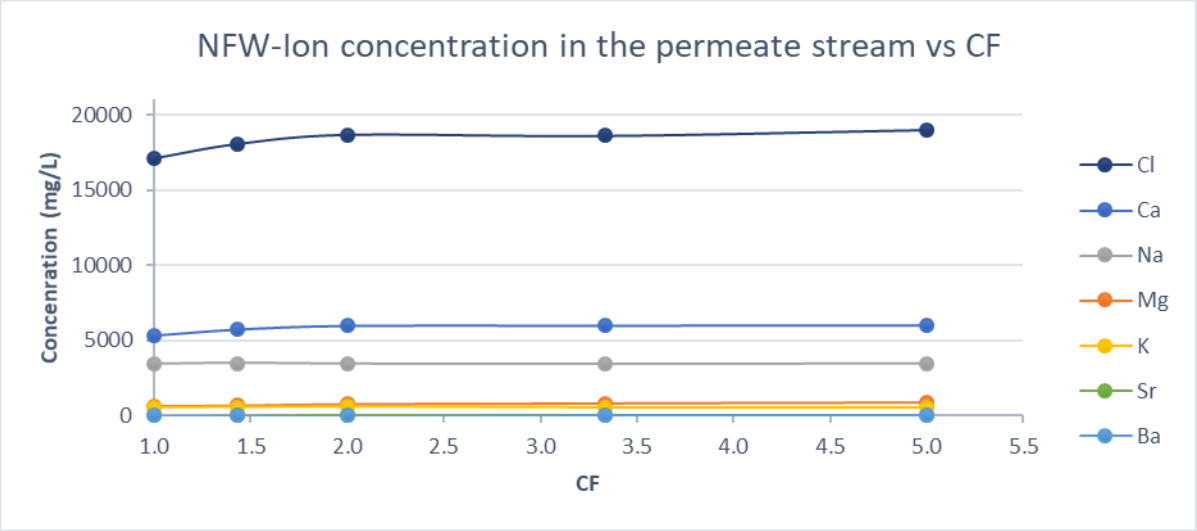

Figure 50: NFW-Ion concentration in the permeate stream vs CF

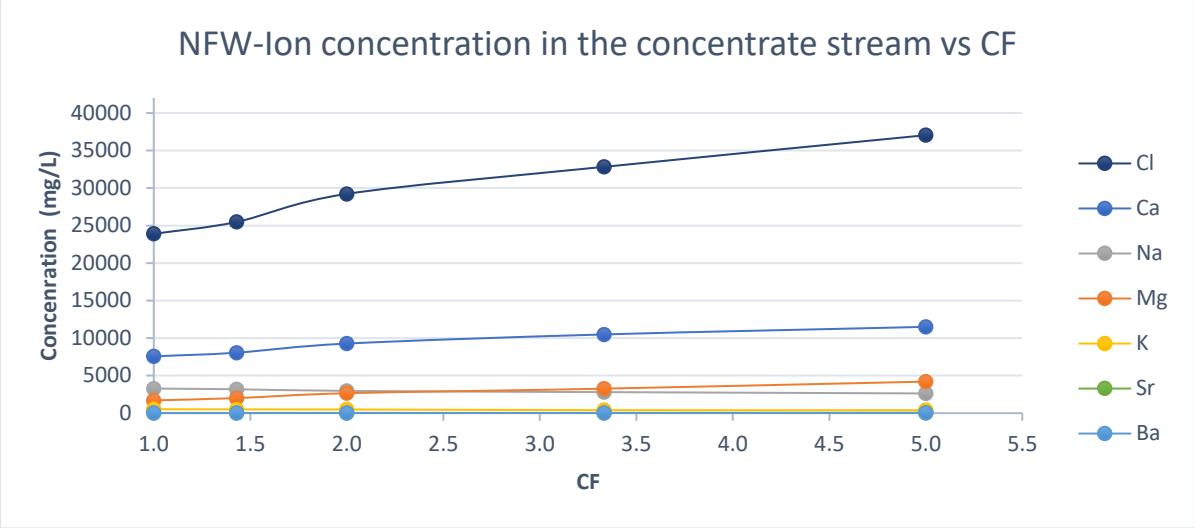

Figure 51: NFW-Ion concentration in the concentrate steam vs CF

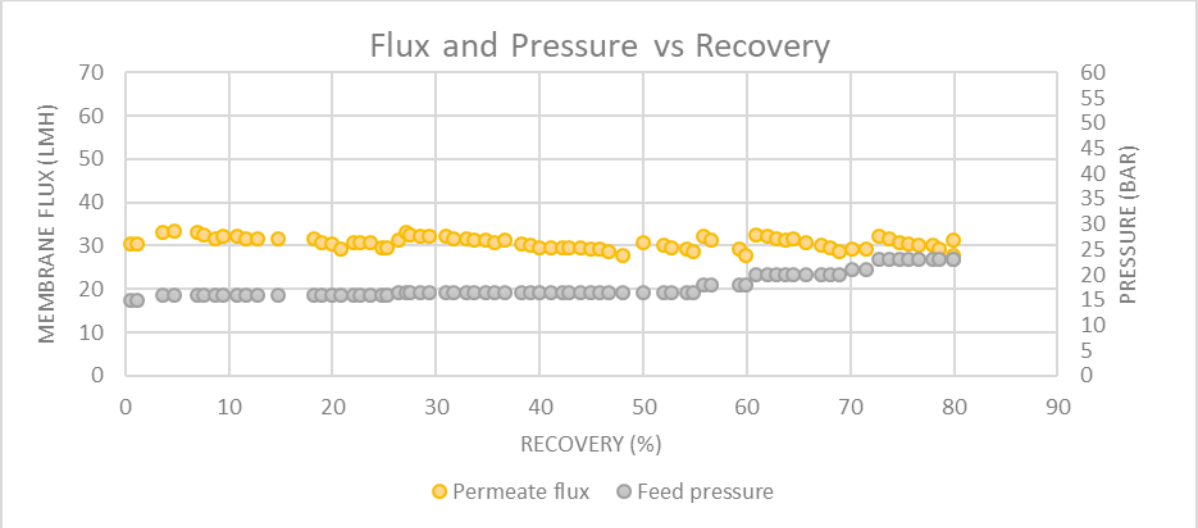

Figure 52: NFW-Flux and Pressure vs Recovery

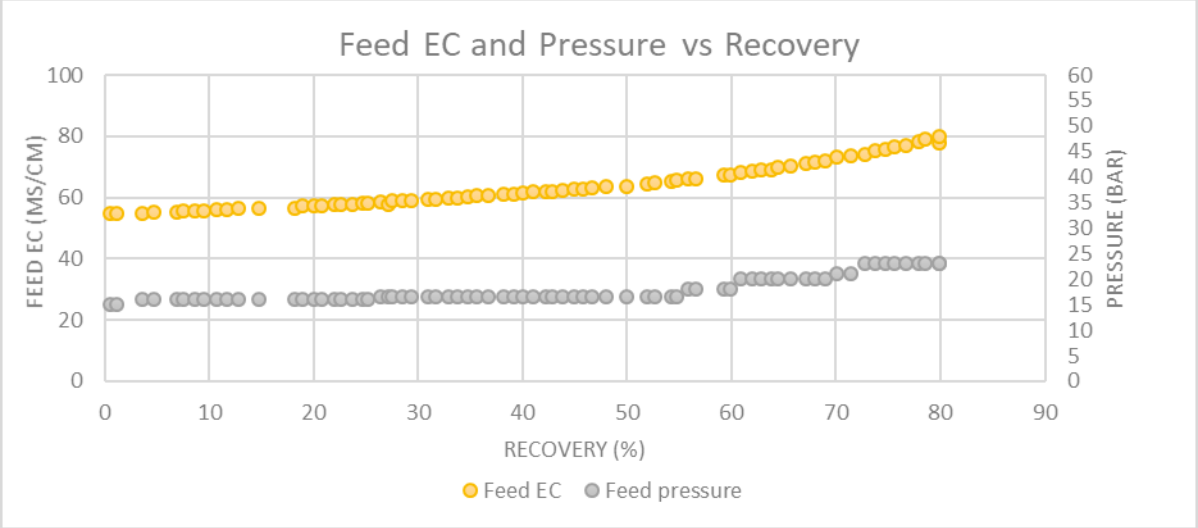

Figure 53: NFW-Feed EC and Pressure vs Recovery

NF270 Membrane

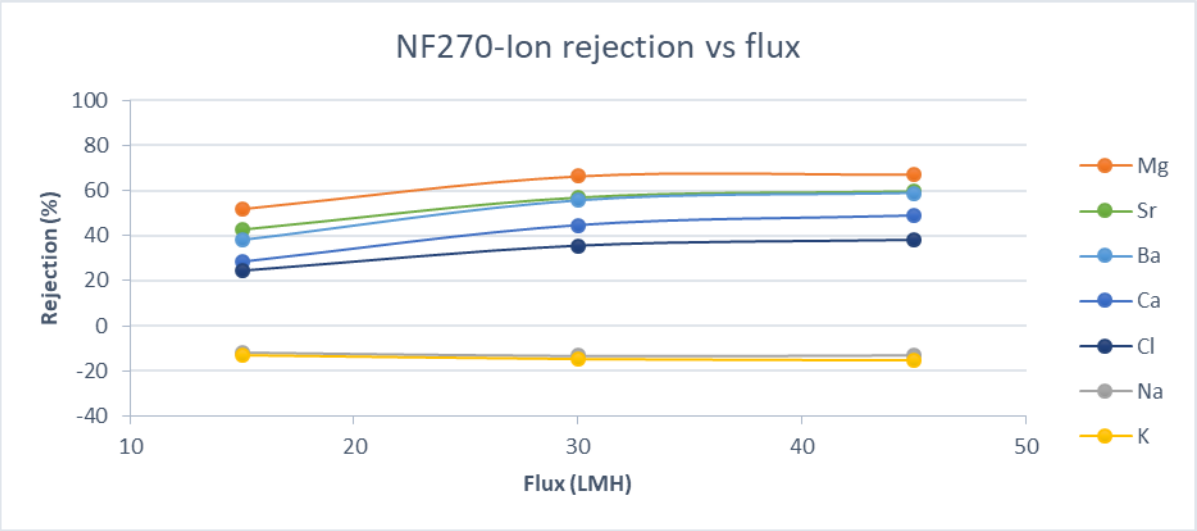

Figure 54: NF270-Ion rejection vs flux

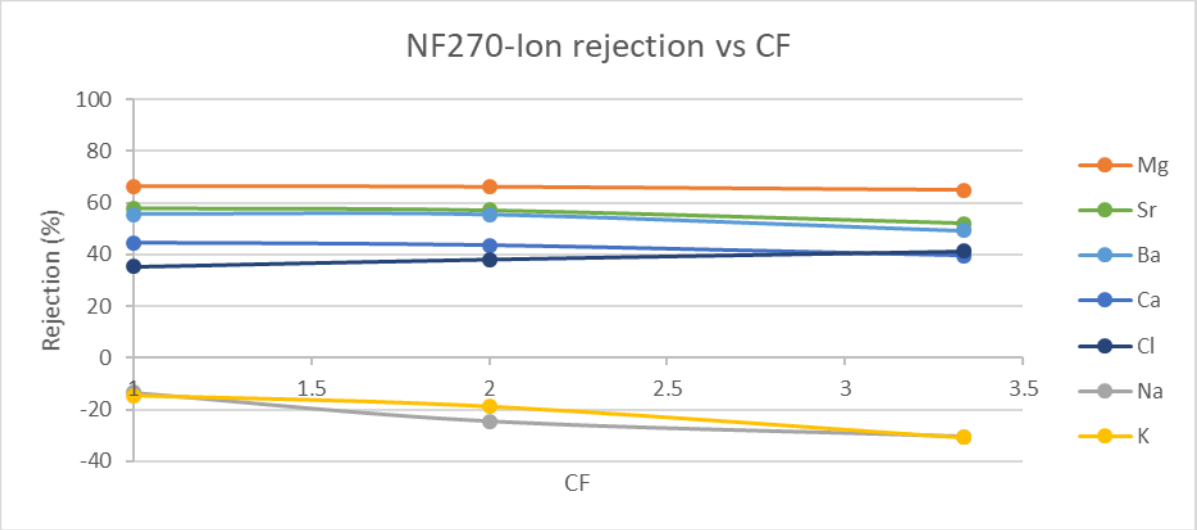

Figure 55: NF270-Ion rejection vs CF

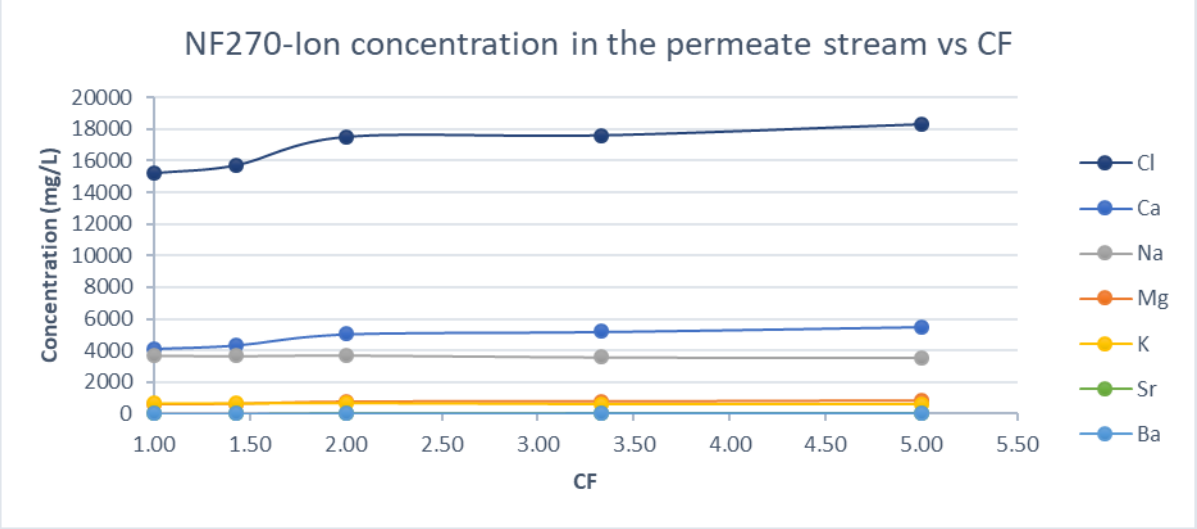

Figure 56: NF270-Ion concentration in the permeate stream vs CF

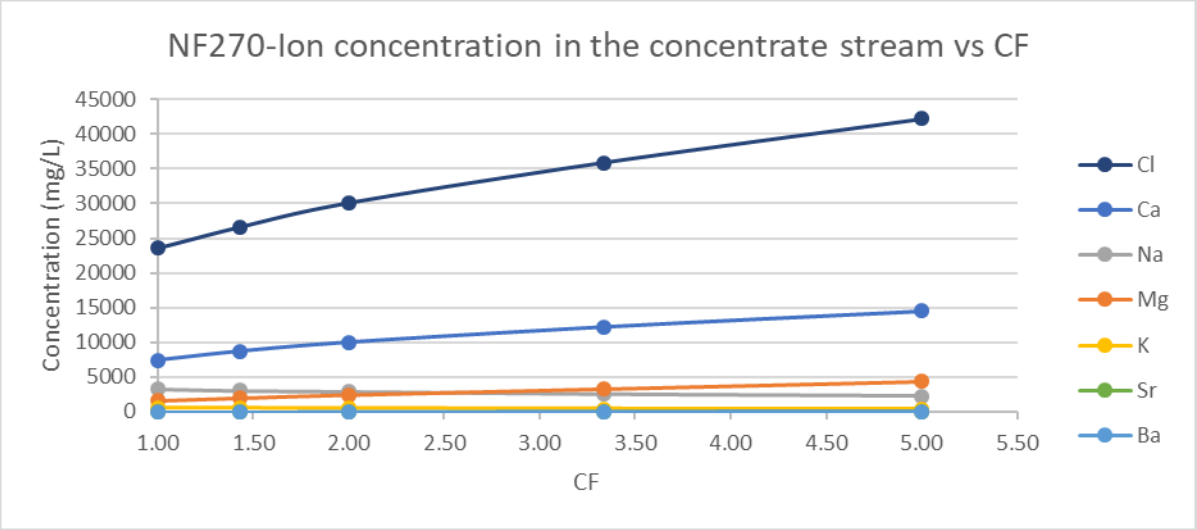

Figure 57: NF270-Ion concentration in the concentrate stream vs CF

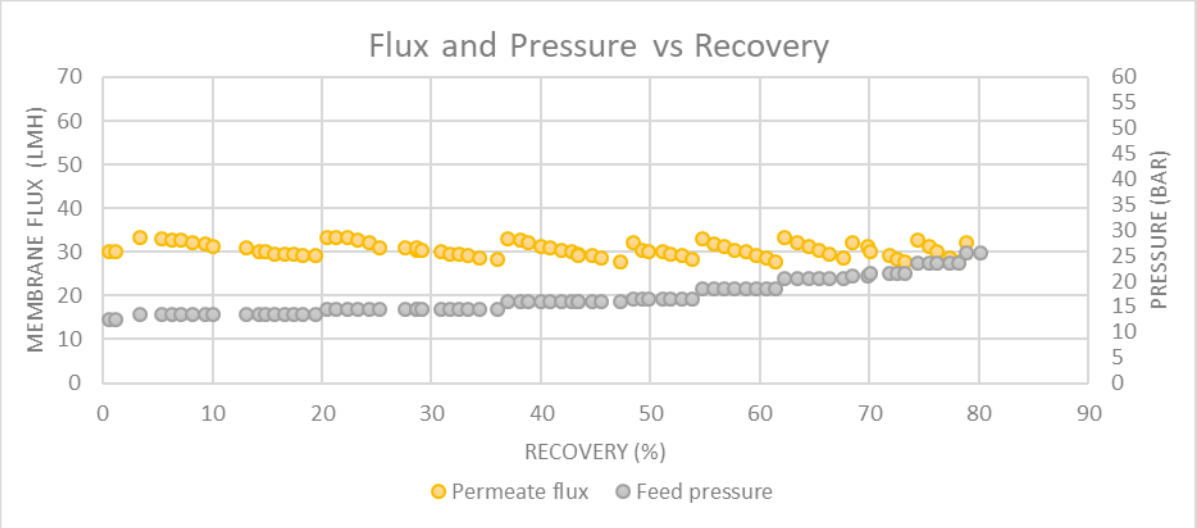

Figure 58: NF270- Flux and Pressure vs Recovery

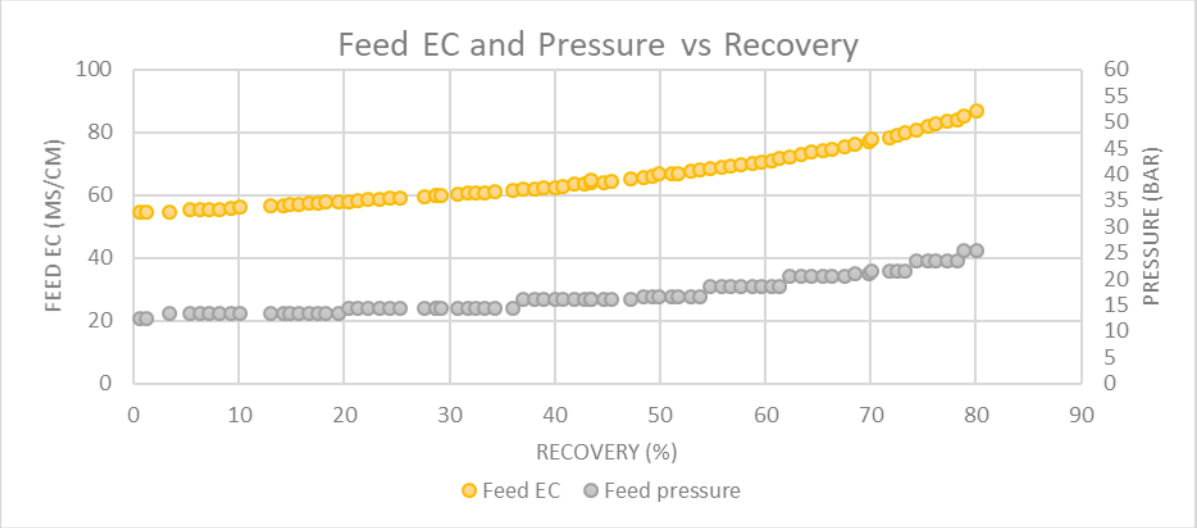

Figure 59: NF270-Feed EC and Pressure vs Recovery

SR3D Membrane

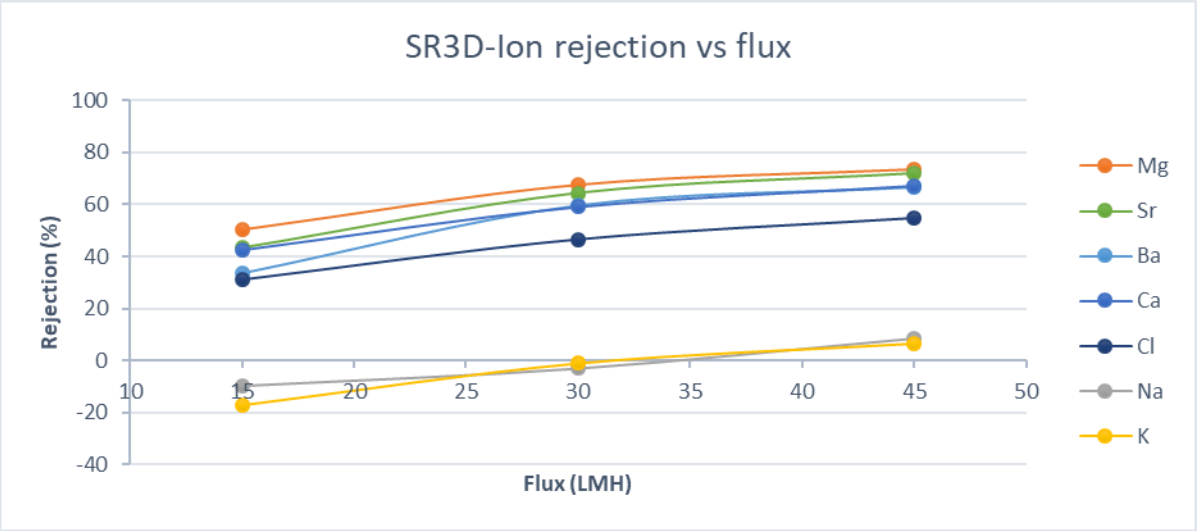

Figure 60: SR3D-Ion rejection vs flux

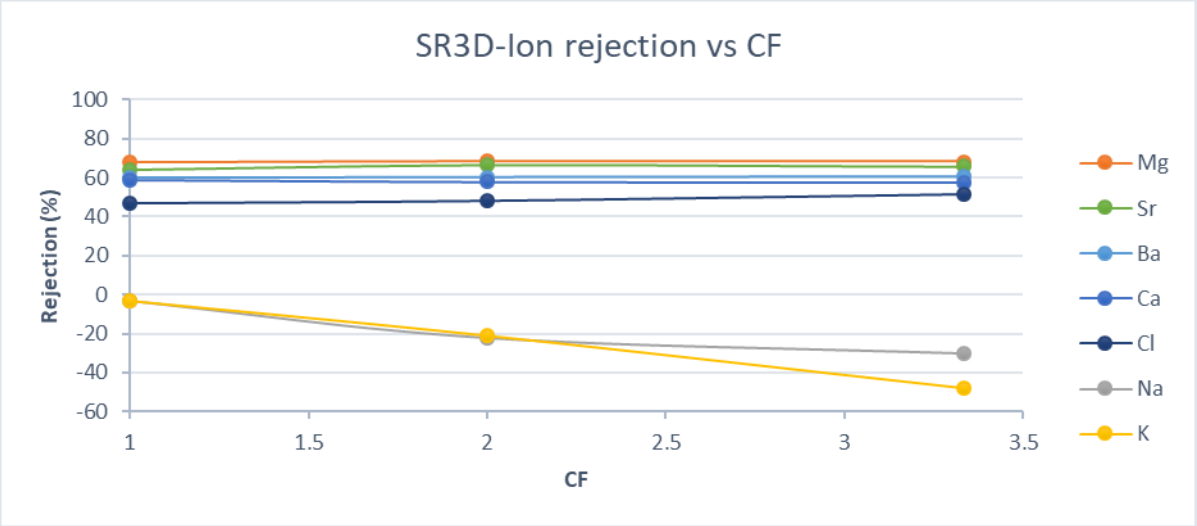

Figure 61: SR3D-Ion rejection vs CF

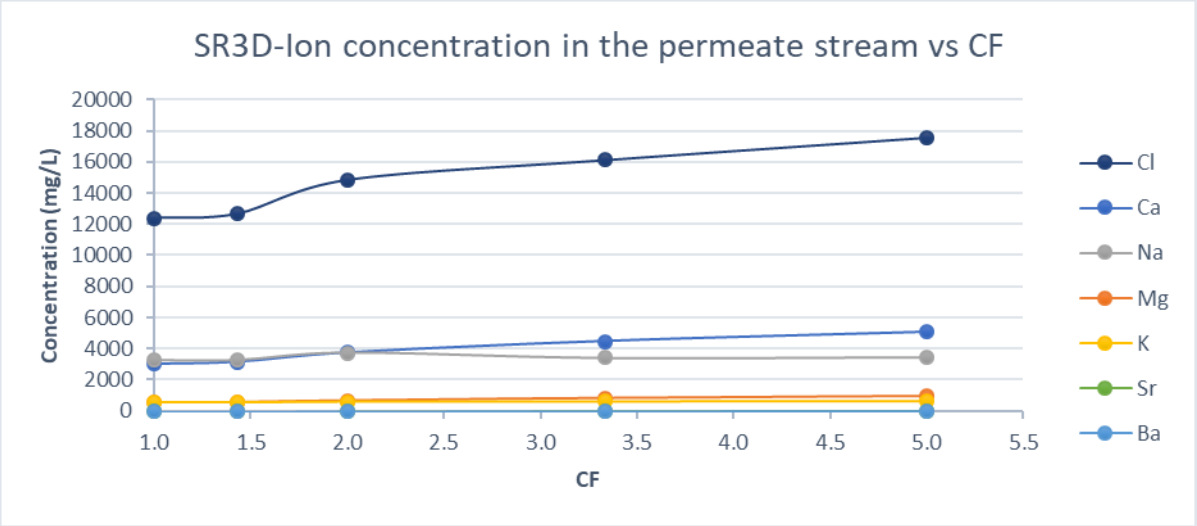

Figure 62: SR3D-Ion concentration in the permeate stream vs CF

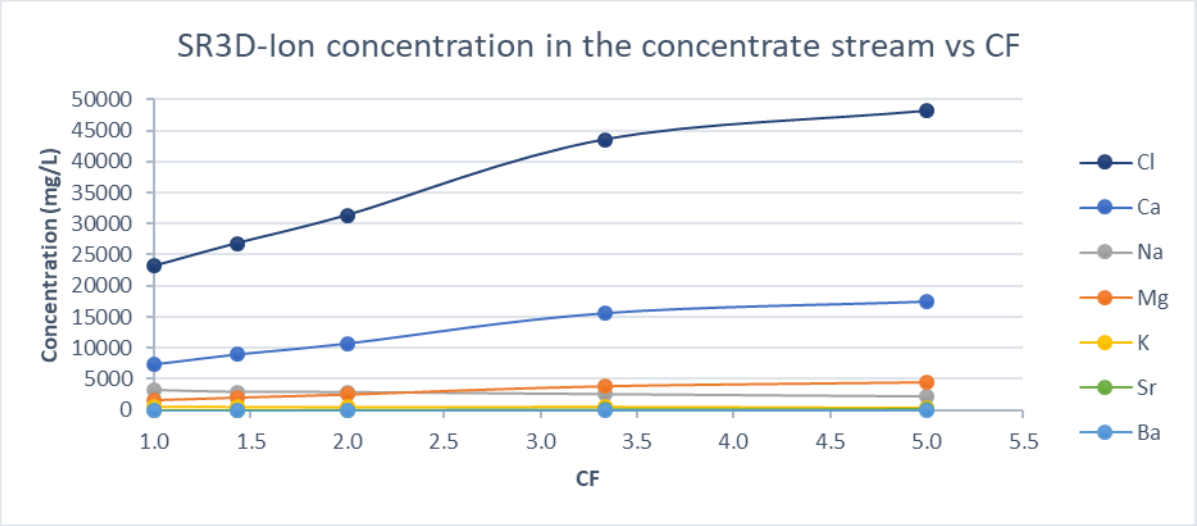

Figure 63: SR3D-Ion concentration in the concentrate stream vs CF

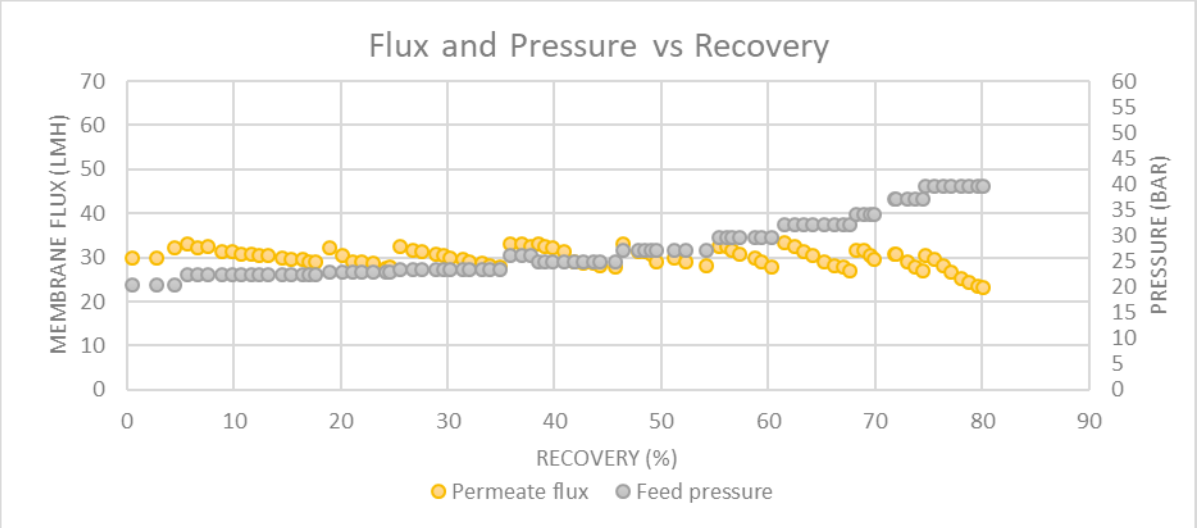

Figure 64: SR3D-Flux and pressure vs Recovery

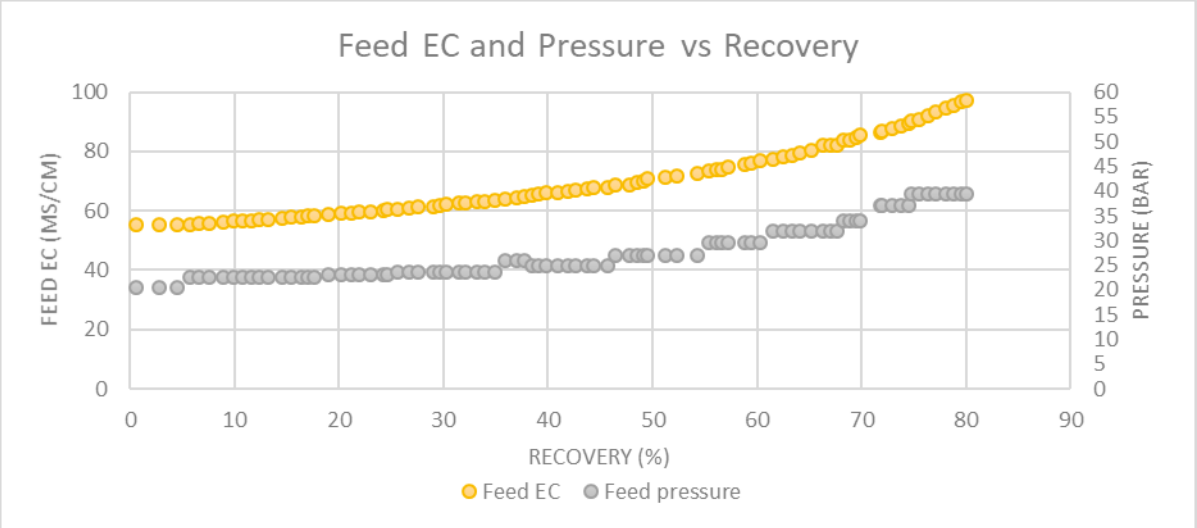

Figure 65: SR3D-Feed EC and Pressure vs Recovery

TS80 Membrane

TS80 First pass

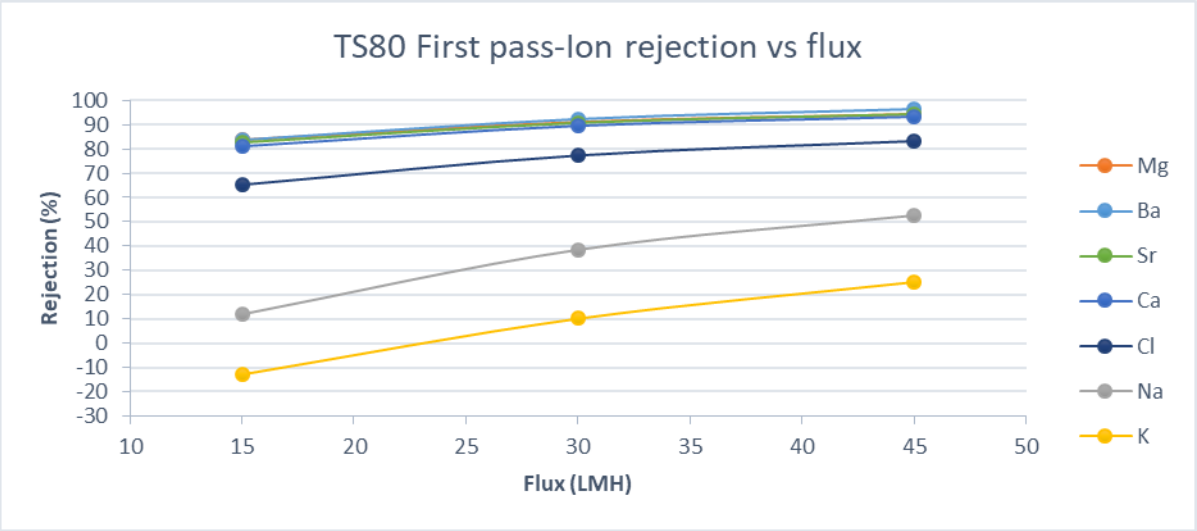

Figure 66: TS80 First Pass-Ion rejection vs flux

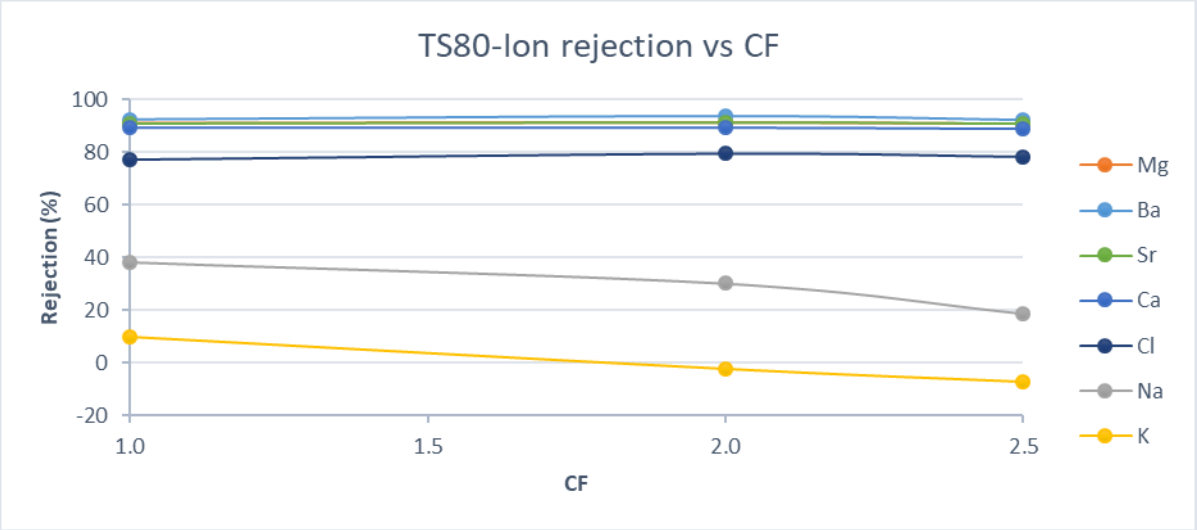

Figure 67: TS80 First Pass-Ion rejection vs CF

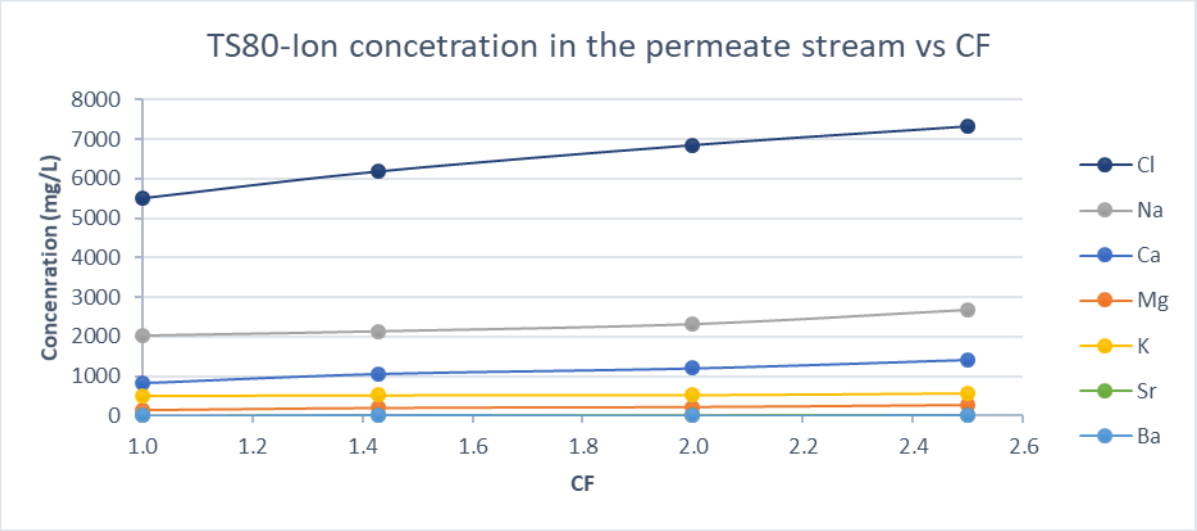

Figure 68: TS80 First Pass- Ion concentration in the permeate stream vs CF

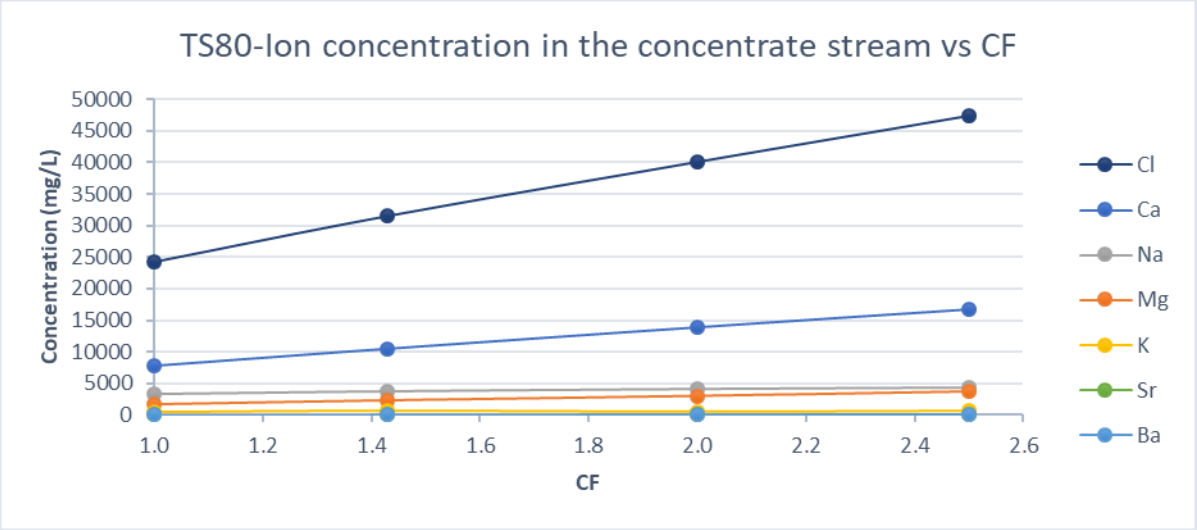

Figure 69: TS80 First Pass- Ion concentration in the concentrate stream vs CF

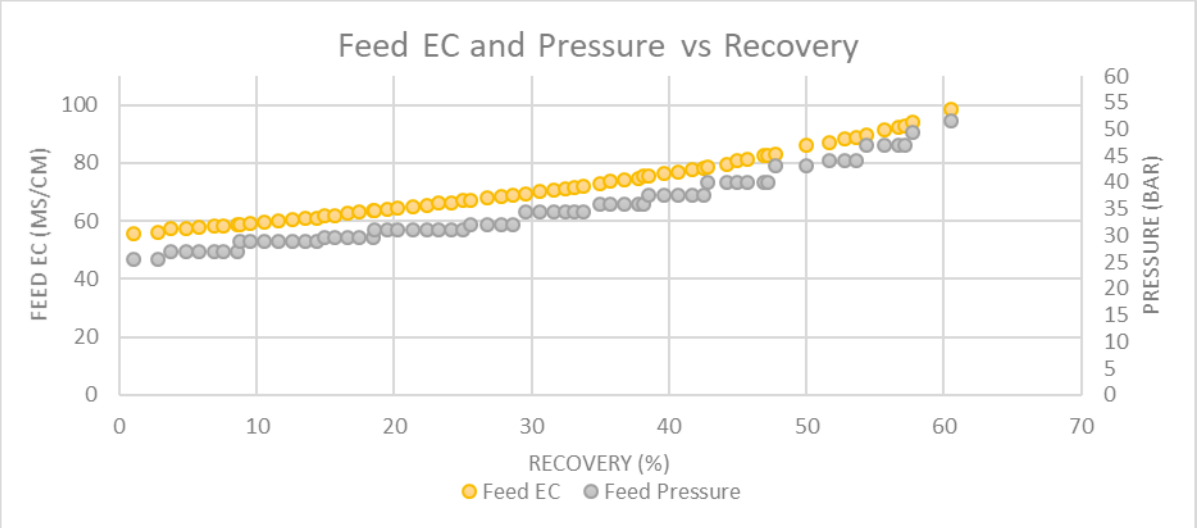

Figure 70: TS80 First Pass- Feed EC and pressure vs recovery

TS80 Second pass

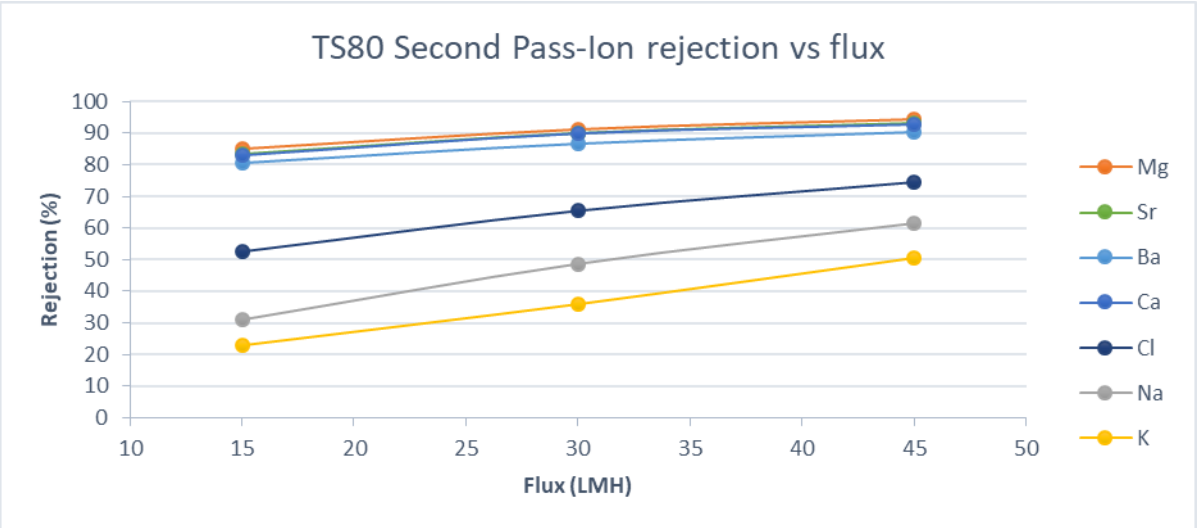

Figure 71: TS80 Second Pass-Ion rejection vs flux

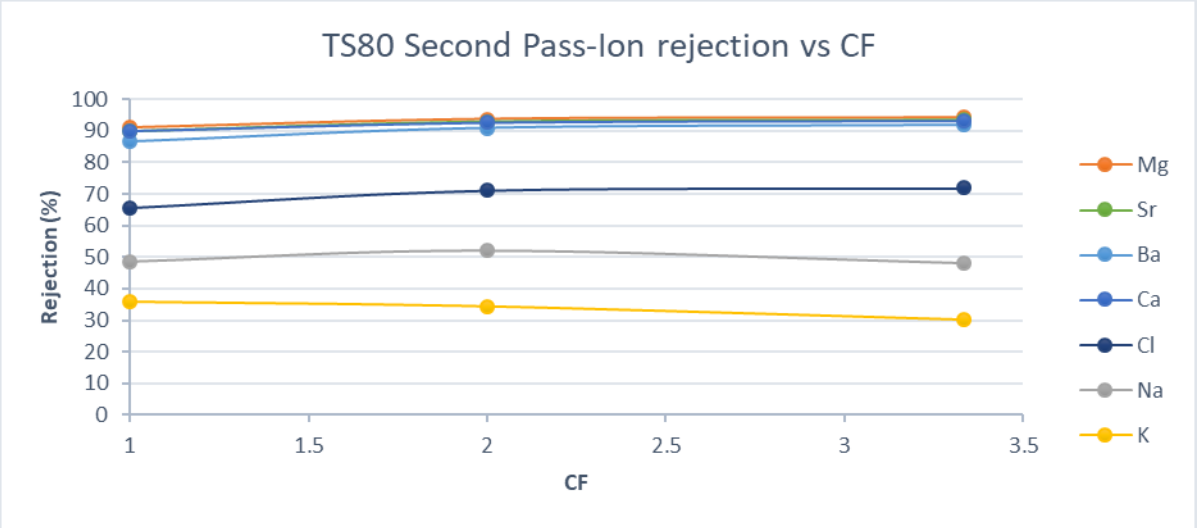

Figure 72: TS80 Second Pass-Ion rejection vs CF

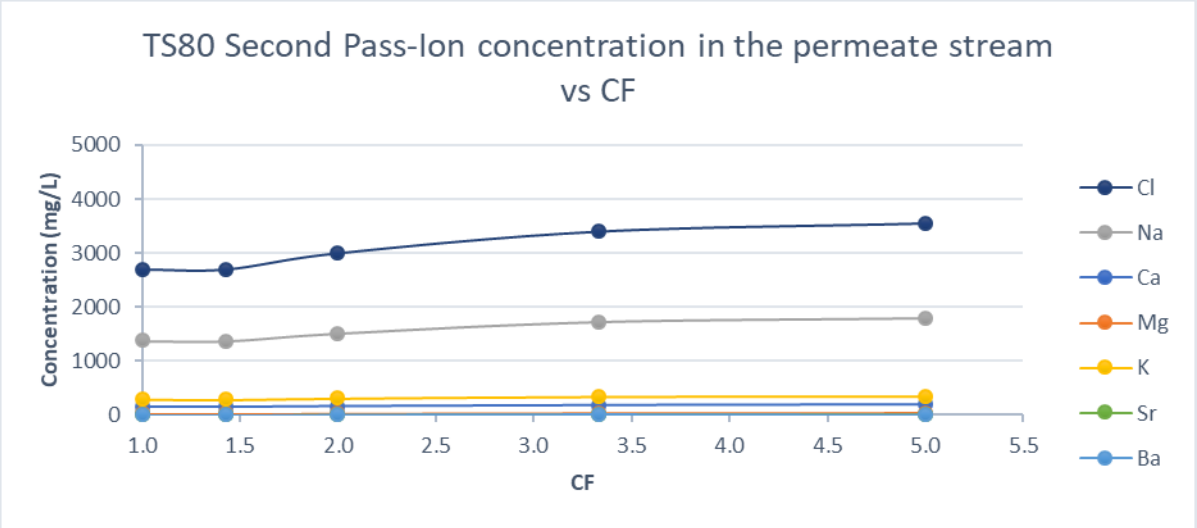

Figure 73: TS80 Second Pass-Ion concentration in the permeate stream vs CF

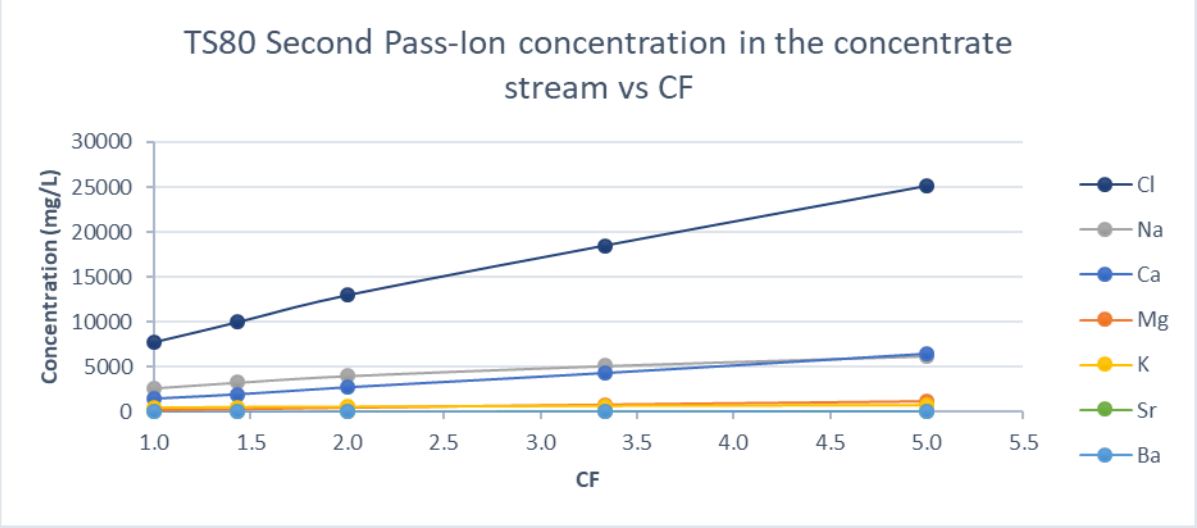

Figure 74: TS80 Second Pass-Ion concentration in the concentrate stream vs CF

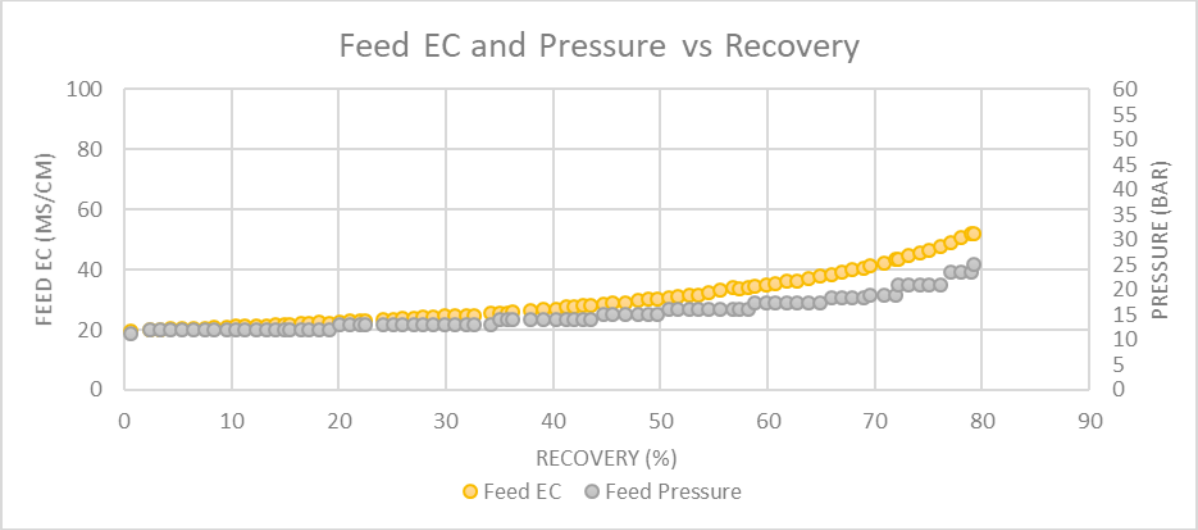

Figure 75: TS80- Feed EC and Pressure vs Recovery

NF90 Membrane

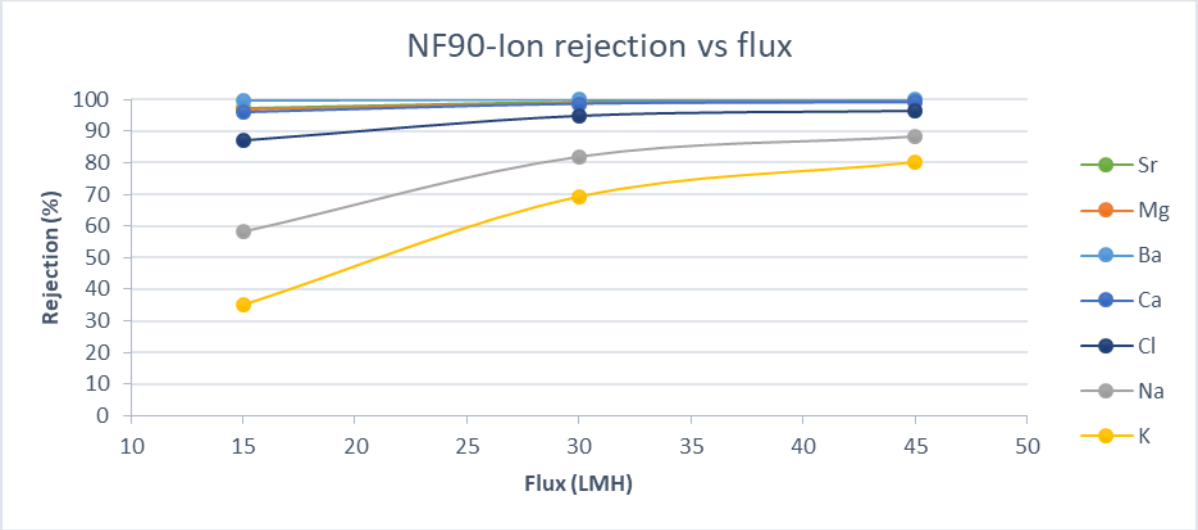

Figure 76: NF90-Ion rejection vs Flux

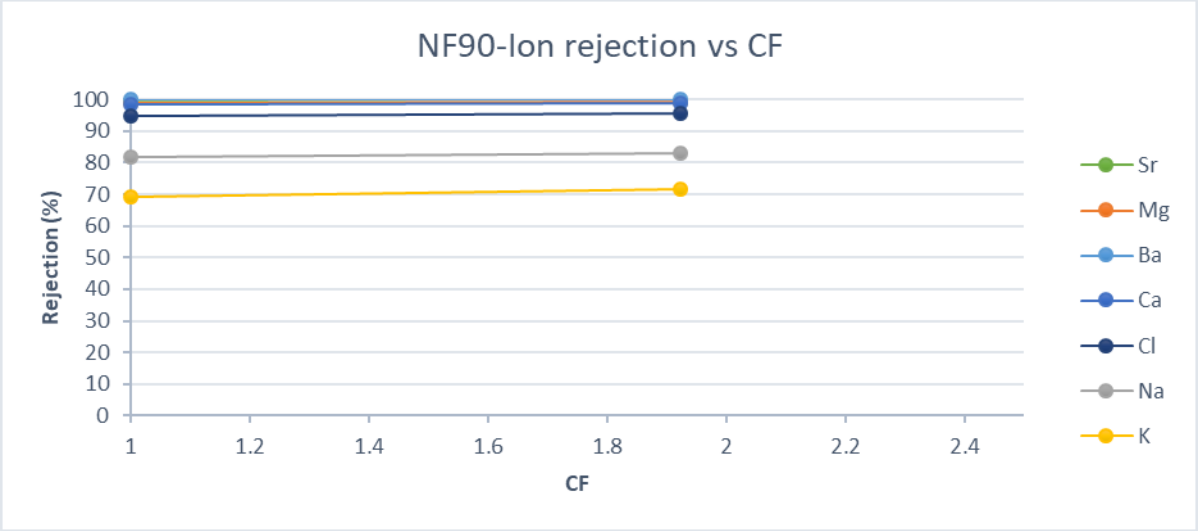

Figure 77: NF90-Ion rejection vs CF

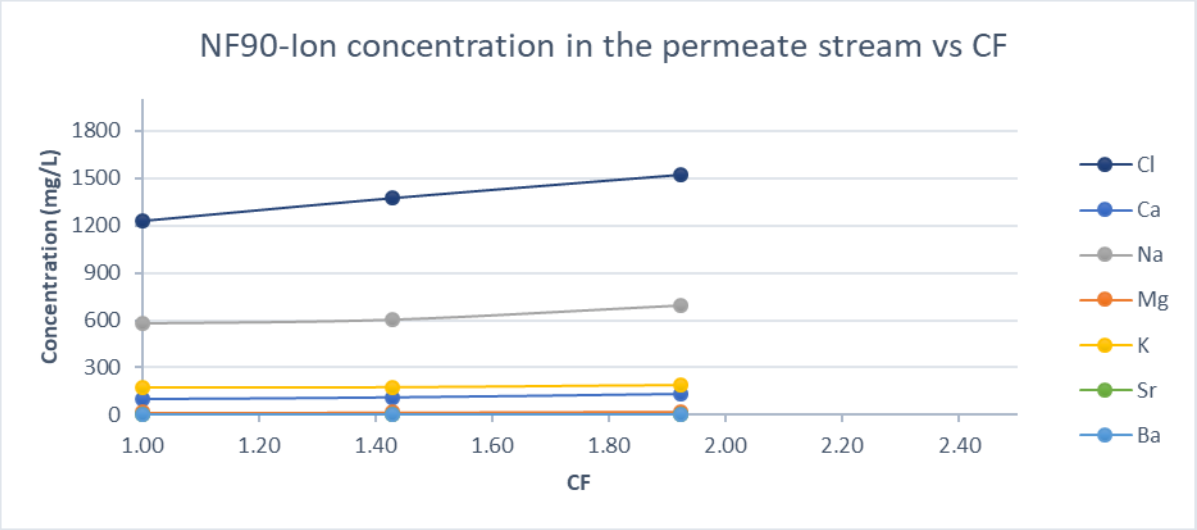

Figure 78: NF90- Ion concentration in the permeate stream vs CF

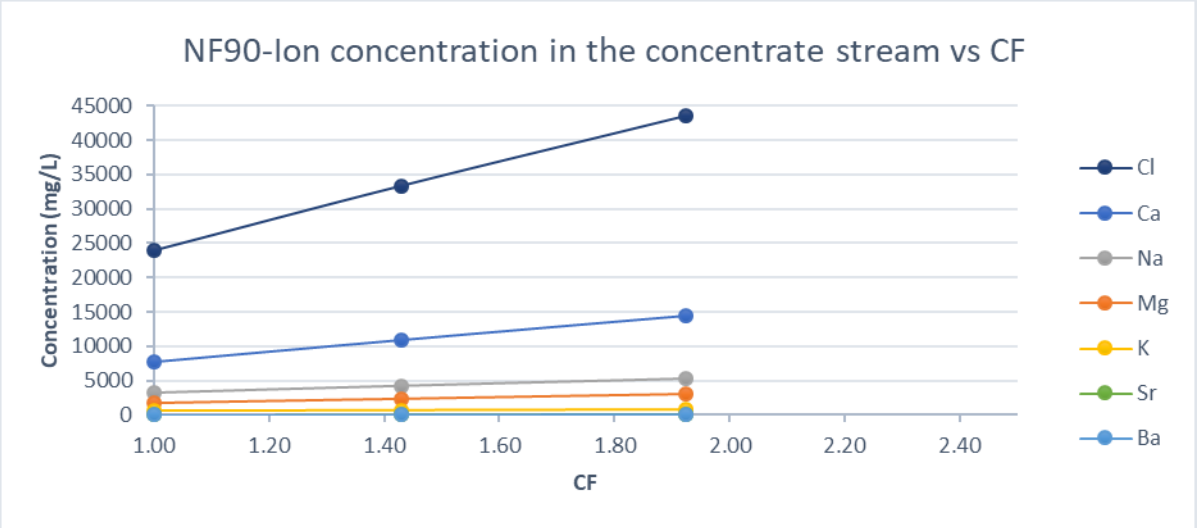

Figure 79: NF90- Ion concentration in the concentrate stream vs CF

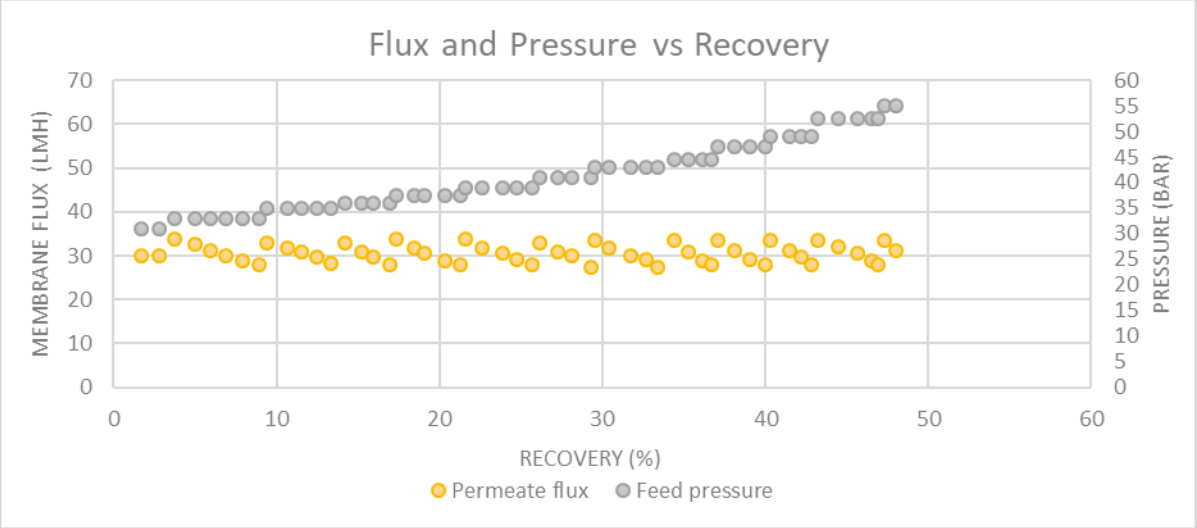

Figure 80: NF90-Flux and Pressure vs Recovery

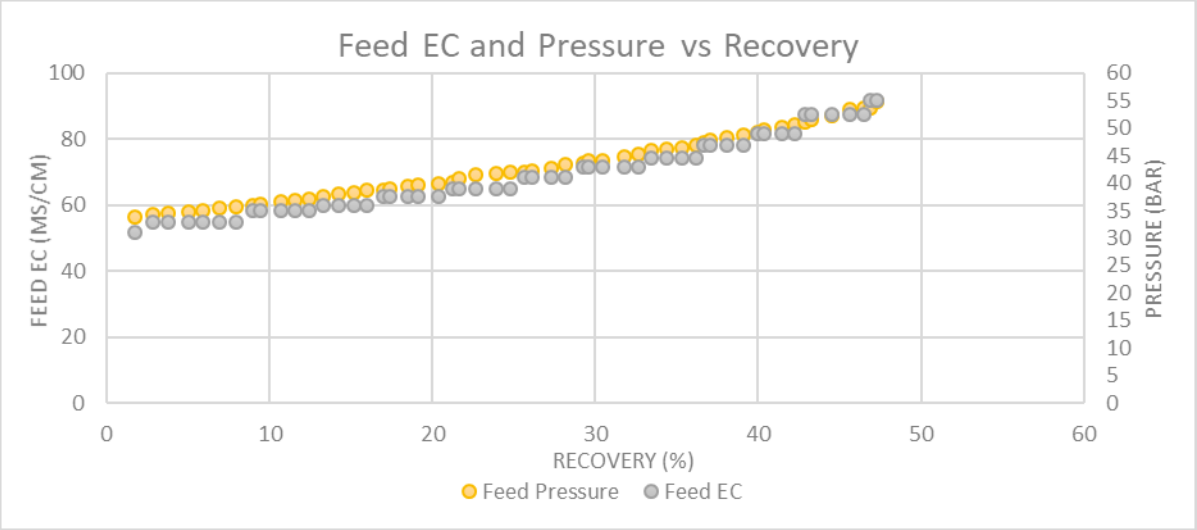

Figure 81: NF90- Feed EC and Pressure vs Recovery

RO98pt Membrane

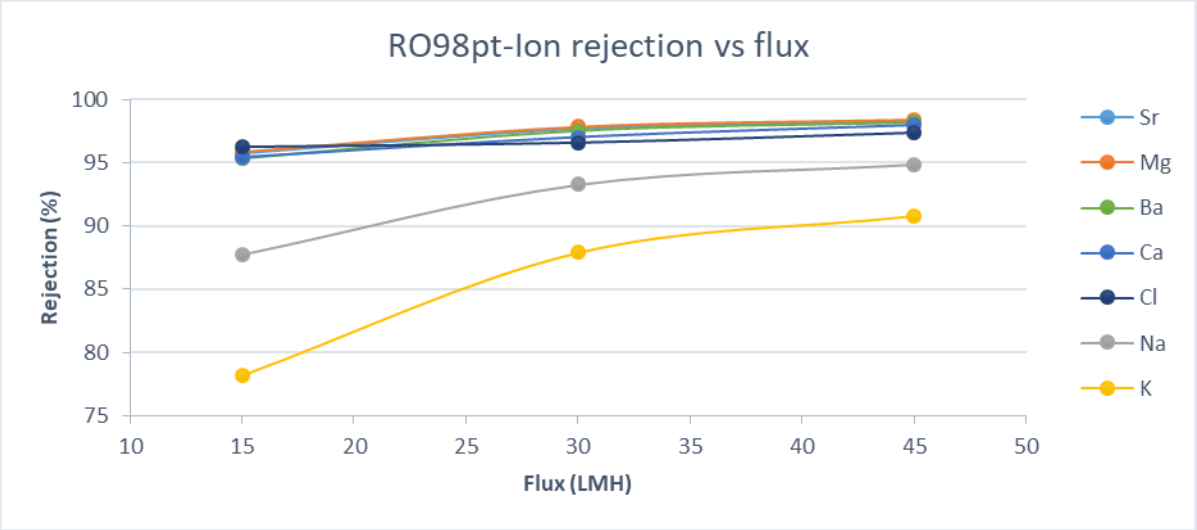

Figure 82: RO98pt-Ion rejection vs Flux

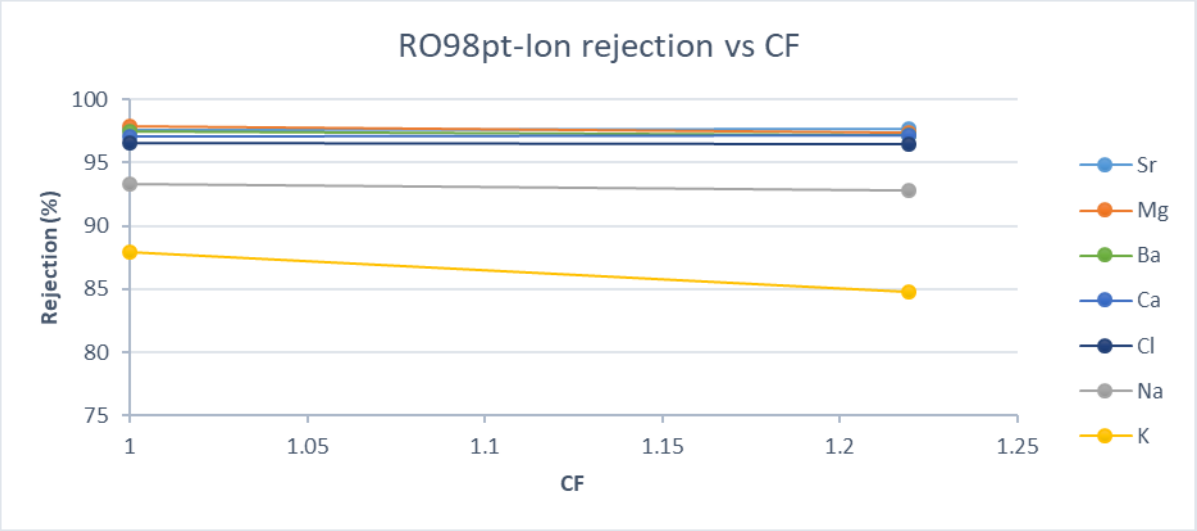

Figure 83: RO98pt-Ion rejection vs CF

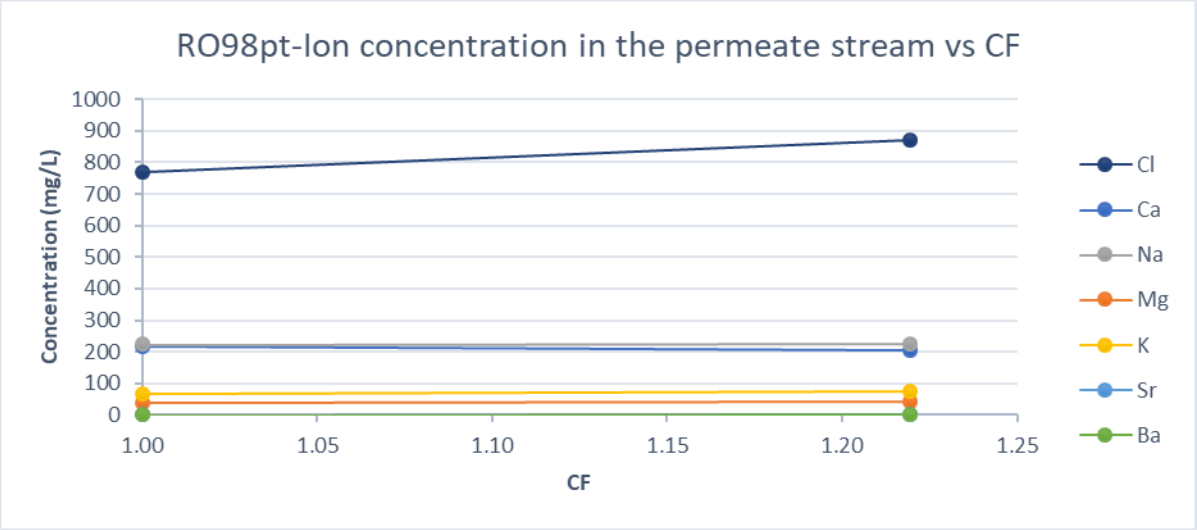

Figure 84: RO98pt-Ion concentration in the permeate stream vs CF

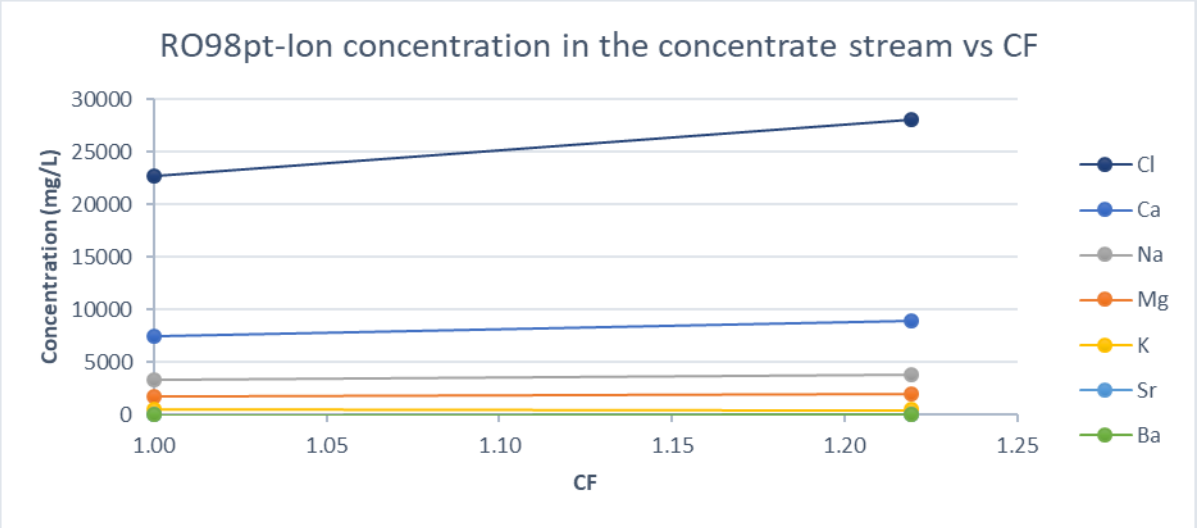

Figure 85: RO98pt-Ion concentration in the concentrate stream vs CF

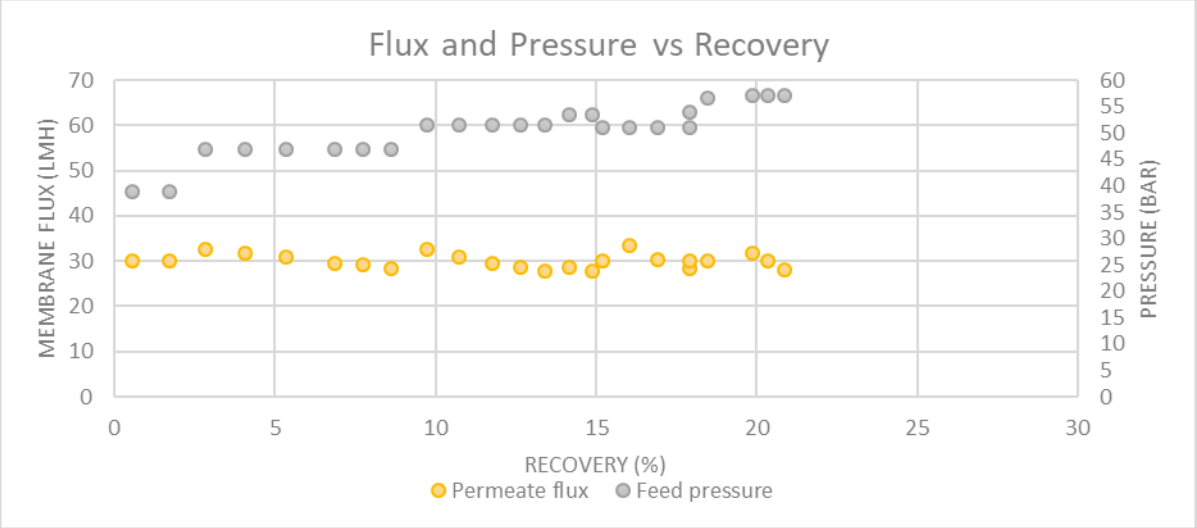

Figure 86: RO98pt- Flux and Pressure vs Recovery

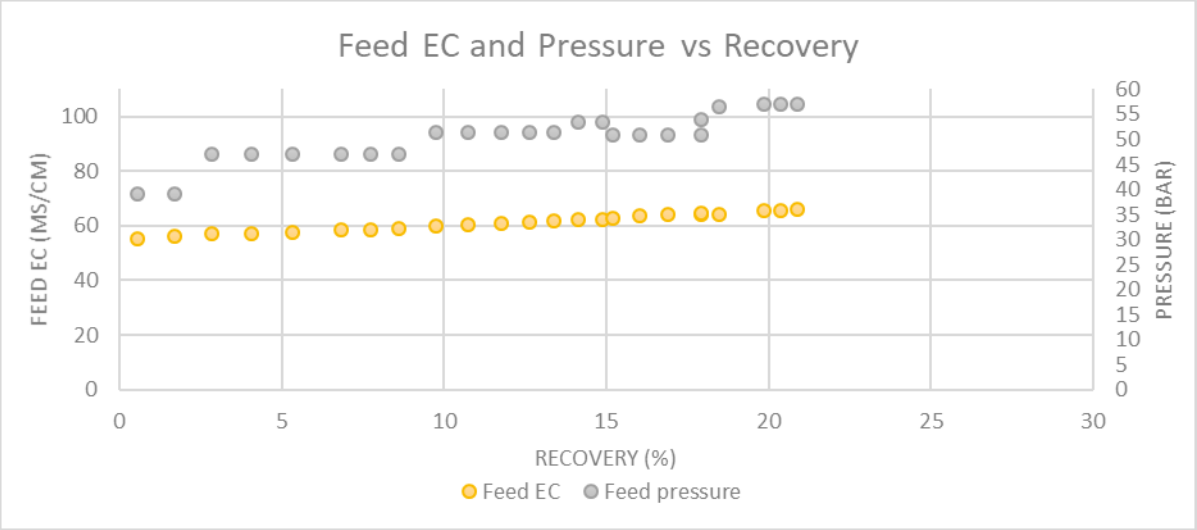

Figure 87: RO98pt- Feed EC and Pressure vs Recovery

LFC3J Membrane

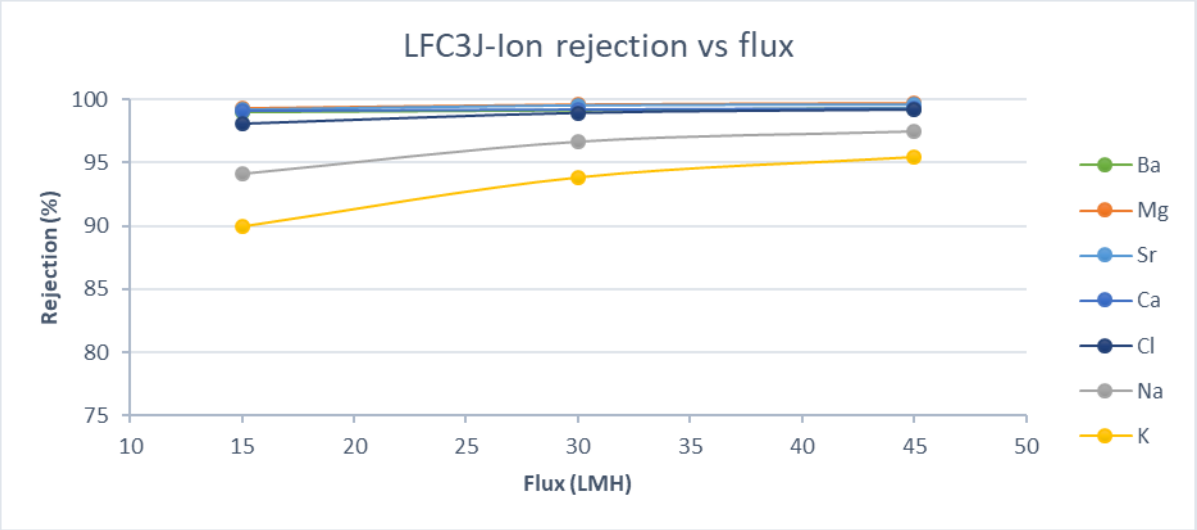

Figure 88: LFC3J-Ion rejection vs flux

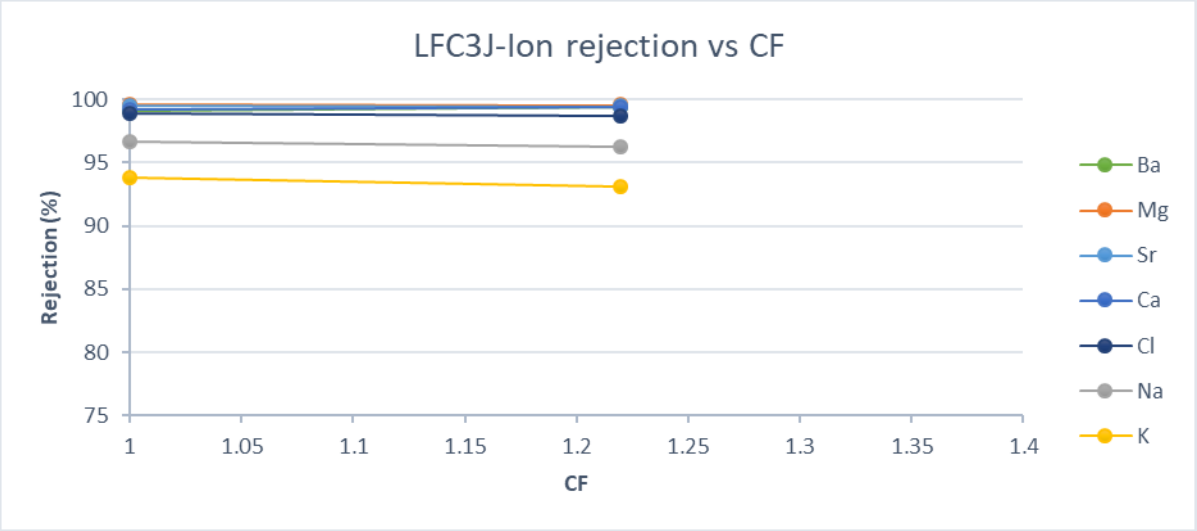

Figure 89: LFC3J-Ion rejection vs CF

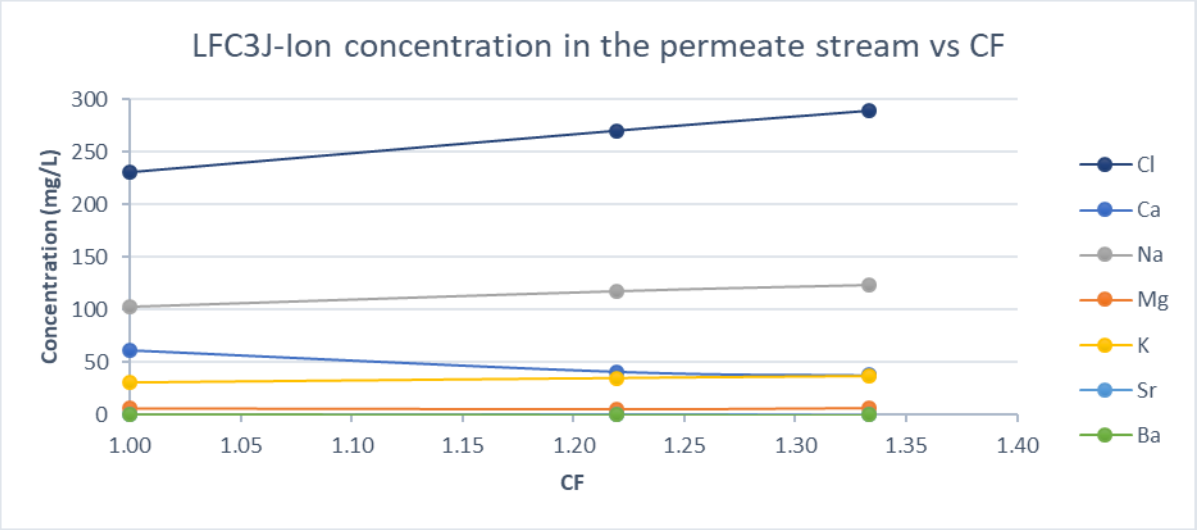

Figure 90: LFC3J-Ion concentration in the permeate stream vs CF

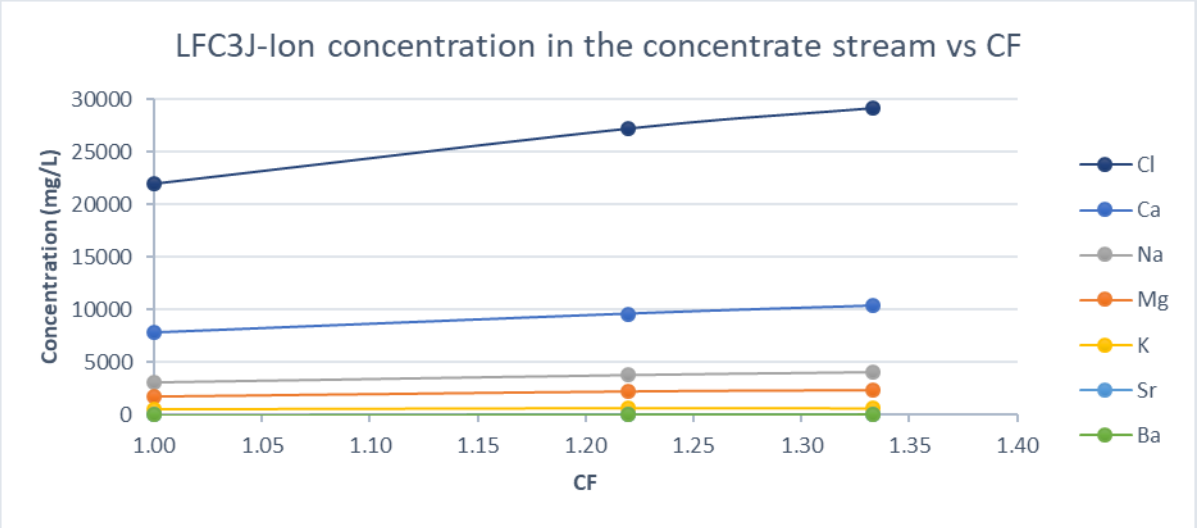

Figure 91: LFC3J-Ion concentration in the concentrate stream vs CF

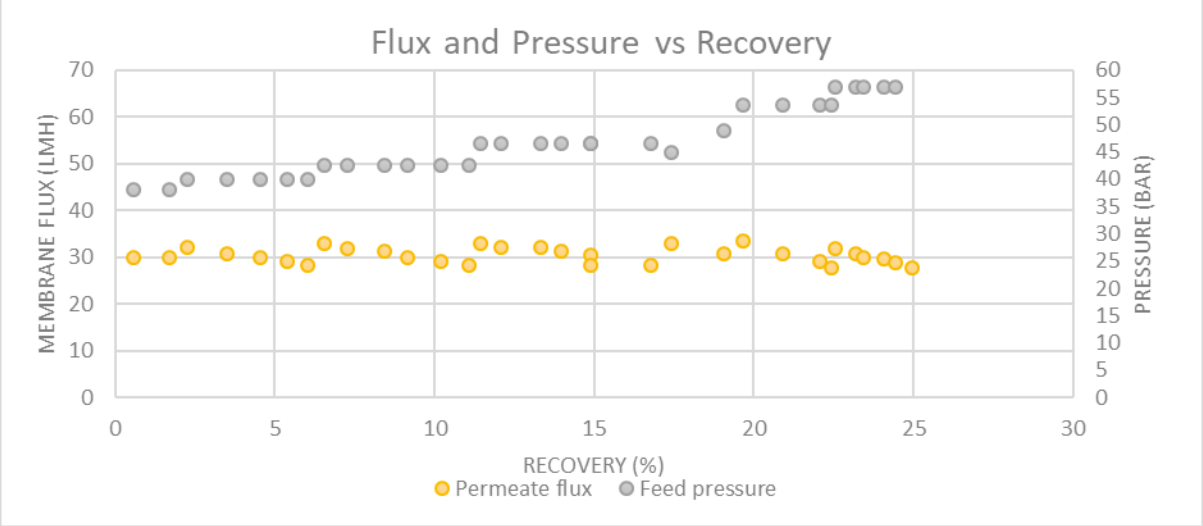

Figure 92: LFC3J- Flux and Pressure vs Pressure

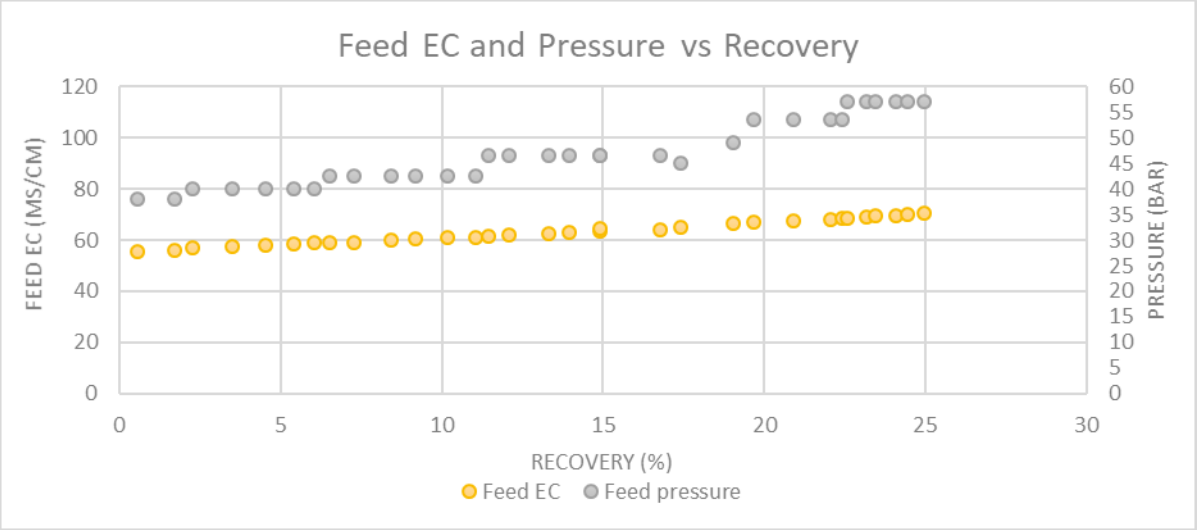

Figure 93: LFC3J- Feed EC and Pressure vs Recovery

A.6 MWCO Experiment

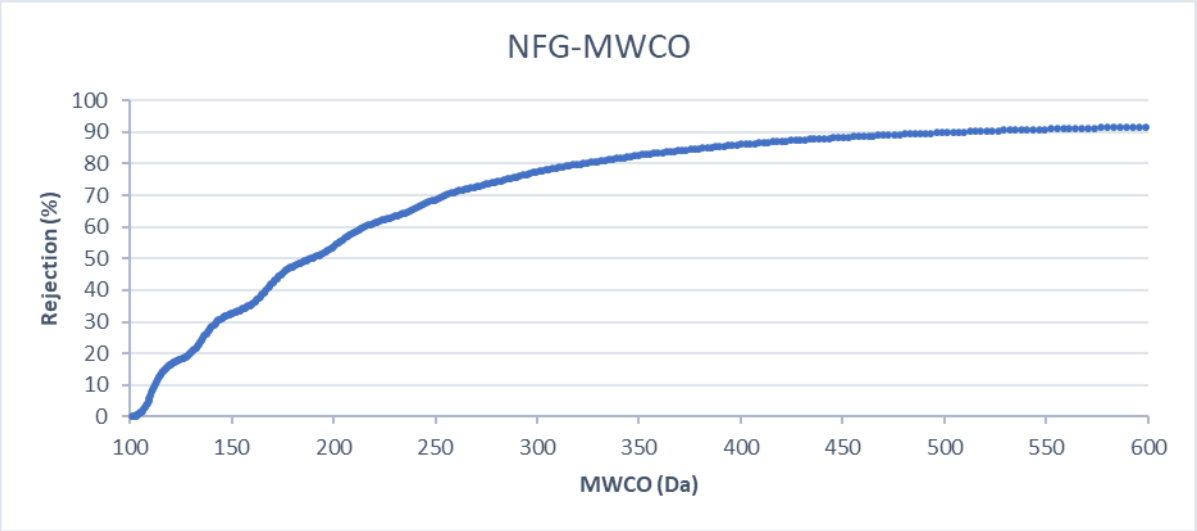

Figure 94: NFG MWCO

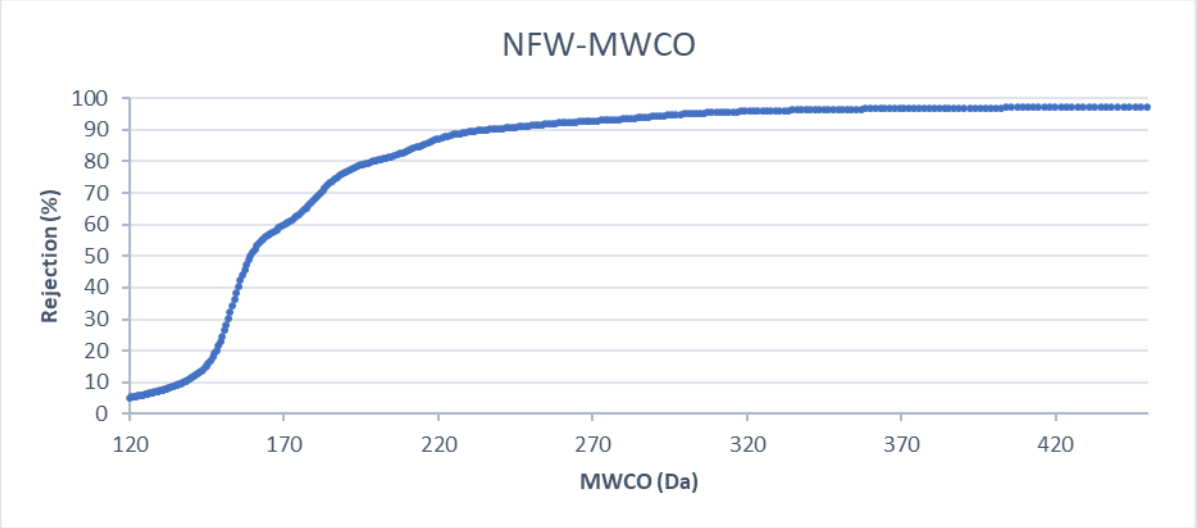

Figure 95: NFW MWCO

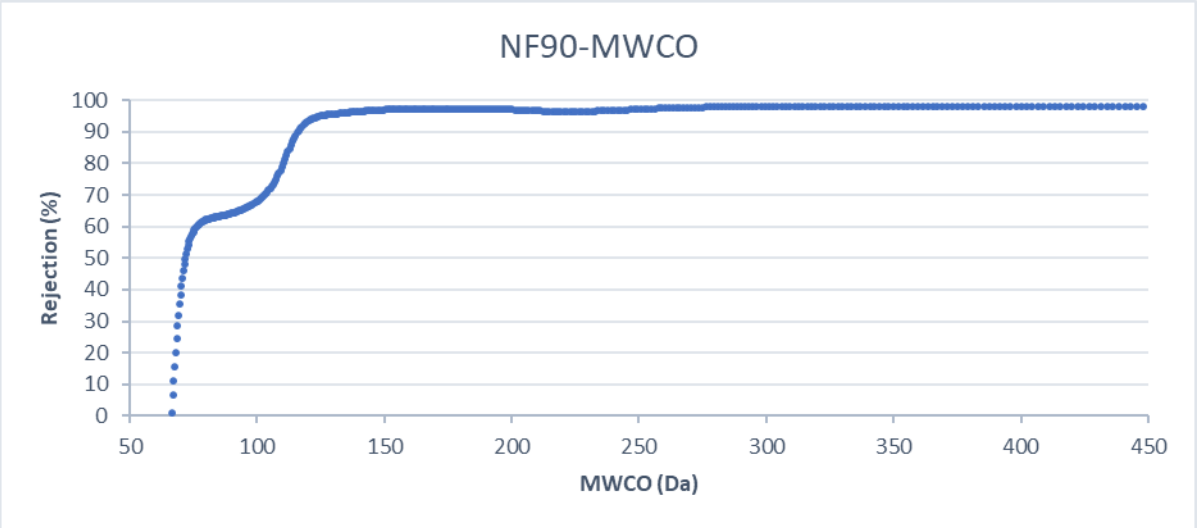

Figure 96: NF90 MWCO